Please include this report under the following descriptors :
SOUND VELOCITY STRUCTURE
NORTH ATLANTIC OCEAN
MEDITERRANEAN INTERMEDIATE WATER

IR NO. 71-13

AD 733990

INFORMAL REPORT

THE SOUND VELOCITY STRUCTURE
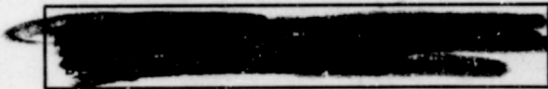# OF THE NORTH ATLANTIC OCEAN

NOVEMBER 1971

D D C
RECEIVED
DEC 16 1971
B

NAVAL OCEANOGRAPHIC OFFICE
WASHINGTON, D.C. 20390

ABSTRACT

All available sound velocity data in the North Atlantic Ocean between 15° and 65° N. latitude and east of 65° W. longitude (excluding the Labrador Sea) have been analyzed in terms of the seasonal areal extent and average axial depth of the upper sound channel, the annual areal extent and average depth of the subsurface sound velocity maximum, and the annual average depth of the deep sound channel axis. The vertical extent of these and other sound velocity structures are shown on nine north-south and nine east-west sound velocity cross-sections that extend to a maximum depth of 5000 meters. These cross-sections include four winter/summer pairs along the same meridian and three winter/summer pairs along the same parallel. In addition, sound velocity/temperature-salinity comparisons for winter and summer are given for 50 locations throughout the North Atlantic Ocean. Sound velocity structures are interpreted in terms of warm and cold water surface circulation patterns; "18° Water" in the Sargasso Sea; intrusions of Mediterranean, Arctic, and Antarctic Intermediate Waters; and various Norwegian Sea overflows.

DON F. FENNER
PAUL J. BUCCA

Undersea Surveillance Oceanographic Project
Ocean Science Department
Science and Engineering Center

iii

BLANK PAGE

TABLE OF CONTENTS

FIGURES

FIGURES (CONTINUED)

FIGURES (CONTINUED)

FIGURES (CONTINUED)

FIGURES (CONTINUED)

INTRODUCTION

The Naval Oceanographic Office (NAVOCEANO) has prepared a partial summary of sound veloc.ty and bottom characteristics for the North Atlantic Ocean (Fenner, et al., Jun 1971) at the request of the Chief of Naval Research (Code 102-OS). This report supplements the above partial summary utilizing sound velocity cross-sections and sound velocity/temperature-salinity (T-S) comparisons as well as areal contour charts of various sound velocity parameters. This report also explains the occurrence of an upper sound channel, subsurface sound velocity maximum, deep sound channel, and other sound velocity structures in terms of water mass analysis and existing circulation patterns. For purposes of this study, deep axial depth is defined as the deepest sound velocity minimum (usually absolute minimum). Names of physical features used in the report are given on Figure 1. Locations of sound velocity cross-sections cited herein are shown on Figure A-1. Locations of sound velocity/T-S comparisons are given on Figure B-2.

SOURCES AND TREATMENT OF DATA

Sound velocity data from the archives of the National Oceanographic Data Center (NODC), from the NAVOCEANO Marine Geophysical Survey (MGS) Program, from the archives of the Woods Hole Oceanographic Institution and Lamont-Doherty Geophysical Observatory, and from various other sources were analyzed in preparation of this report. A complete listing of these data is given by Fenner, et al., Jun 1971. Nansen cast and salinity-temperature-depth (STD) recorder data were converted into sound velocity profiles using the equation of Wilson, 1960.

These data were analyzed for the depth of the upper sound channel axis, depth of the subsurface sound velocity maximum, and depth of the deep sound channel axis and compiled by one-degree square and season. One-degree square compilations were averaged by two-degree square (i.e., four one-degree squares) on a seasonal basis for upper axial depth and on an annual basis for subsurface sound velocity maxima and deep axial depth. The two-degree square averages of these parameters then were contoured on an areal basis. Data coverage for the areal figures is shown as an insert in the upper right-hand corner of each figure. Regions where upper sound channels and subsurface sound velocity maxima are present more than 80% of the time, 20-80% of the time, and less than 20% of the time also were derived on a two-degree square basis and generalized on an areal basis. Throughout the remainder of this report, the first type of region above will be referred to as having a PERMANENT upper sound channel or subsurface sound velocity maximum, the second as TRANSITORY. In the third region, upper sound channels or subsurface sound
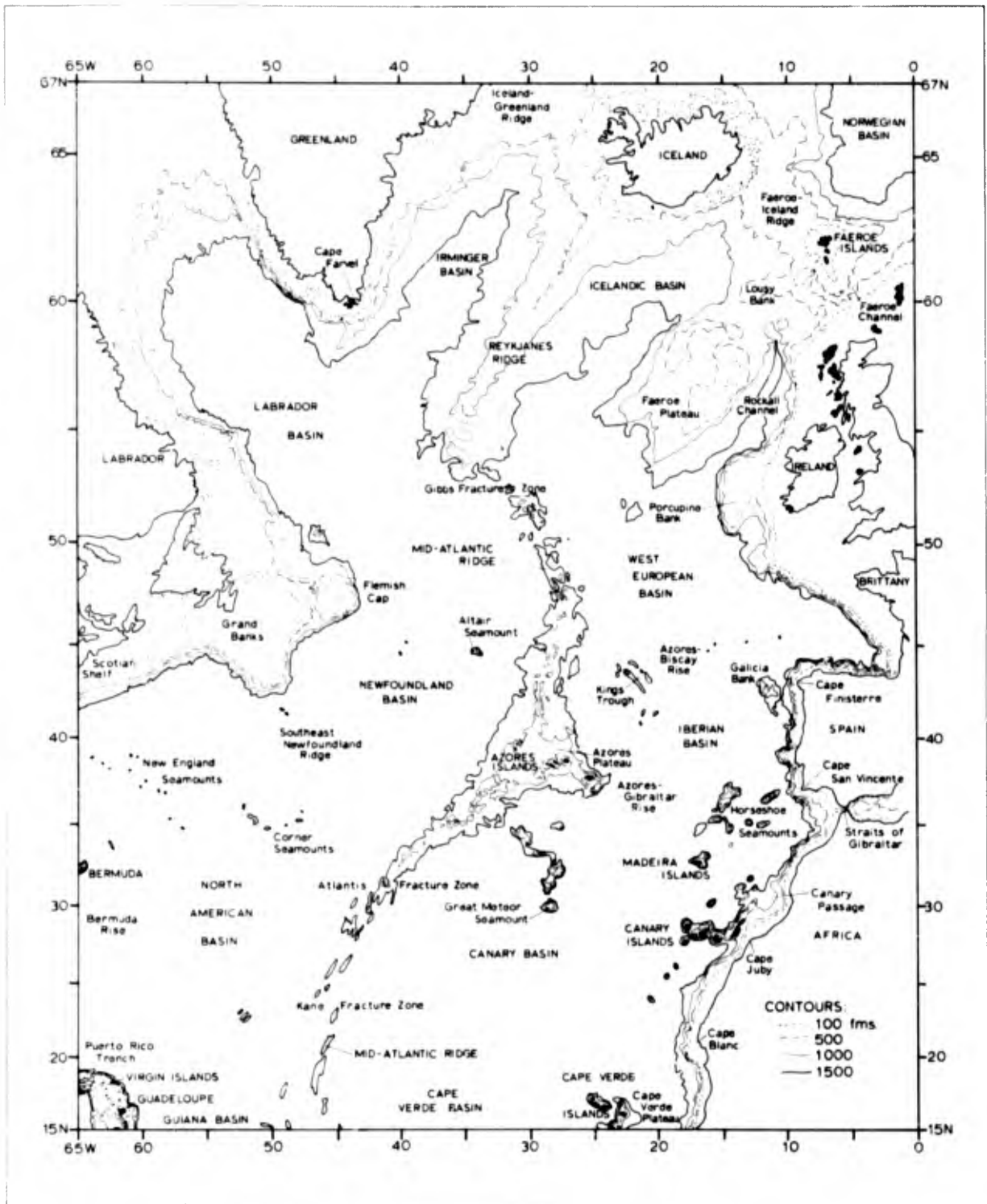
FIGURE 1. NAMES OF SELECTED PHYSICAL FEATURES.

velocity maxima effectively are ABSENT. The treatment of data used in the construction of the sound velocity cross-sections and sound velocity/T-S comparisons is discussed in Appendices A and B, respectively.

The four standard seasons of winter (January through March), spring (April through June), summer (July through September), and autumn (October through December) are used in this report. These seasons were chosen because the area extends from subtropical through subarctic latitudes. The four standard seasons seem typical between about 30° and 55° N. latitude. However, in the northern part of the area, winter extends through April, while in the southern part of the area October appears to be more typical of summer than autumn.

GENERAL OCEANOGRAPHY AS RELATED TO SOUND VELOCITY STRUCTURES

A general knowledge of the circulation and water mass structure of any oceanic area is a prerequisite to the understanding of sound velocity structures. Figure 2 shows generalized circulation at the surface and intermediate depths that primarily effects sound velocity structures in the area. The T-S indices of various water masses discussed in the following paragraphs are given on Figure B-1.
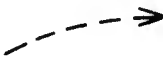
The surface oceanography of three-quarters of the area is dominated by the warm, saline Gulf Stream/North Atlantic Current system and its offshoots north of the Subtropical Convergence and by the North Equatorial/Antilles Current system south of the Subtropical Convergence. These current systems circulate North Atlantic Central Water (NACW) that is modified throughout the area by contact with various subsurface and intermediate water masses. Throughout much of the North Atlantic, sound velocity structures consist of a surface mixed layer, a negative velocity gradient to deep axial depth (generally deeper than 900 meters), and a positive sound velocity gradient from deep axial depth to the bottom. Figure B-27 shows a sound velocity structure typical of unmodified NACW.

The surface oceanography of the northwest quadrant of the area is dominated by the cold dilute Labrador, East Greenland, and West Greenland Currents. These currents circulate water masses having a salinity minimum at the surface. Sound velocity structures throughout this region generally consist of an extremely strong negative velocity gradient from the surface to deep axial depth (generally shoaler than 300 meters) and a positive velocity gradient from deep axial depth to the bottom. Figure B-18 shows a sound velocity structure typical for unaltered Labrador Current Water (LCW). In this region, winter cooling often results in the formation of positive velocity gradients from

3

FIGURE 2
GENERALIZED CIRCULATION AT THE SURFACE AND INTERMEDIATE DEPTHS
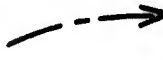
LEGEND:
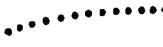
Warm, saline surface and near-surface currents as follow:
- A: Gulf Stream
- B: Slope Water Current
- C: North Atlantic Current
- D: Northern extension of North Atlantic Current
- E: Irminger Current
- F: Southern extension of North Atlantic Current
- G: Southeast offshoot of Gulf Stream
- H: Canary Current
- I: North Equatorial Current
- J: Antilles Current

Cold, dilute surface and near-surface currents as follow:
- K: Labrador Current
- L: East Greenland Current
- M: West Greenland Current

Warm, highly saline flow of Mediterranean Intermediate Water (MIW) at 900 to 1600 meters (annotations indicate percent unmixed MIW at salinity maximum)

Cold, dilute flow of Arctic Intermediate Water (AIW) at 800 to 1800 meters

Cold, very dilute flow of Antarctic Intermediate Water (AAIW) at 800 to 1000 meters (annotations indicate percent unmixed AAIW at salinity minimum)

Oceanic convergences as follow:
  Polar Front (PF)
  Subarctic Convergence (SaC)
  Subtropical Convergence for winter and summer (StC)

Atmospheric Arctic Front for winter and summer (AAF)

Region of marked prevalence of "18° Water"

Region markedly influenced by upwelling, particularly during winter

NOTE: This figure shows direction of flow only, and does not indicate current magnitudes.
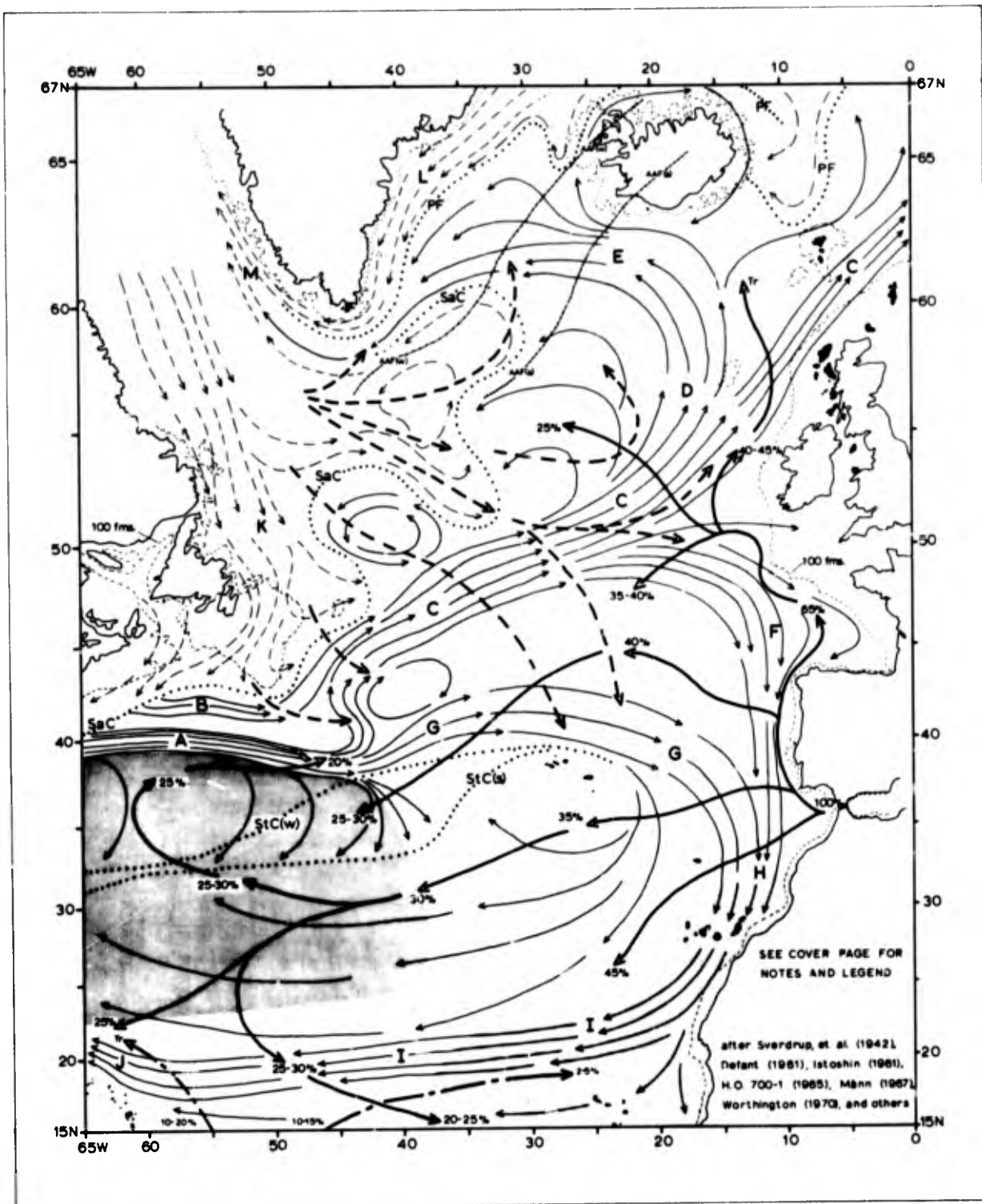
FIGURE 2. GENERALIZED CIRCULATION AT THE SURFACE AND INTERMEDIATE
DEPTHS.

5

surface to bottom that are dissipated during summer by surface warming (Figure B-11 in West Greenland Current).

The warm water regime of the Gulf Stream/North Atlantic Current system is separated from the cold water regime of the Labrador Current by the Subarctic Convergence and from the cold water regimes of the East Greenland Current, West Greenland Current, and the Norwegian Sea by the Polar Front. Both the Subarctic Convergence and the Polar Front cause rapid changes in sound velocity structures over relatively short distances. This is particularly noticeable in the region south of Grand Banks. Figures B-25, B-26, and B-30 describe a cross-section extending from north of the Labrador Current across the Gulf Stream and indicate the extremely strong variations in sound velocity structure encountered crossing the Subarctic Convergence. A similar variation across the Polar Front can be seen by comparing Figure B-3 with B-5 and Figure B-4 with B-7.

In the southeast corner of the area, cold relatively dilute upwelled waters cause somewhat lower surface and near-surface sound velocities than normally expected for a subtropical region, particularly during winter when upwelling is at its peak (Defant, 1961). Figure B-52 shows an example of this situation. Although upwelled water is carried to the west by the North Equatorial Current, it does not effect surface sound velocities west of about 35° W. longitude or north of about 30° N. latitude.

In the region west of the Mid-Atlantic Ridge and south of the Gulf Stream, sound velocity structures are altered by the presence of "18° Water" (Worthington, 1959 and Istoshin, 1961). This subsurface water mass is characterized by a nearly isothermal layer between about 200 and 400 meters and most likely is formed by winter cooling in the vicinity of the Subtropical Convergence. "18° Water" is found in varying concentrations throughout the Sargasso Sea. This water mass retards the formation of negative velocity gradients below the surface mixed layer (e.g., see winter profile on Figure B-45) and in high concentrations can cause the development of a sound velocity minimum followed by a velocity maximum at the bottom of the "18° Water" layer. Figure B-40 shows examples of upper sound channels and subsurface sound velocity maxima formed by "18° Water".

At intermediate depths, sound velocity structures throughout the area are altered by intrusions of Mediterranean Intermediate Water (MIW; upper North Atlantic Deep Water of Defant, 1961), Antarctic Intermediate Water (AAIW; sub-Antarctic Intermediate Water of Defant, 1961), and Arctic Intermediate Water (AIW; sub-Arctic Intermediate Water of Bubnov, 1968). In this area, MIW is characterized by a salinity maximum between about 900 and 1600 meters, AAIW by a salinity minimum between about 800 and 1000 meters, and AIW by a salinity minimum between about 800 and 1800 meters.

6

The effects of MIW intrusions on sound velocity structures have been documented by Piip, Apr 1968 in the Canary and Iberian Basins; by Katz, Jun 1969 over the central Mid-Atlantic Ridge; and by Fenner and Bucca, Dec 1969 throughout the Northeast Atlantic. In the presence of high to intermediate concentrations of MIW, a sound velocity minimum is formed at the interface with NACW, a subsurface sound velocity maximum is formed at the approximate depth of the high salinity core, and deep axial depths are markedly depressed. Figures B-37 and B-38 show examples of sound velocity structures in the presence of intermediate and high MIW concentrations, respectively. In the presence of lesser MIW concentrations, the upper sound channel and subsurface sound velocity maximum tend to merge into a broad deep sound channel with an axis 100- to 300-meters deeper than normally expected (e.g., see Figure B-42). Lesser concentrations of MIW may also lead to sound velocity perturbations either above or below deep axial depth (see Figures B-31 and B-47, respectively).

The intrusions of AIW in the north and AAIW in the south tend to impede the spread of MIW and tend to counteract the effects of MIW on the depth and width of the deep sound channel. The summer sound velocity profile shown on Figure B-19 is a good example of a narrow deep sound channel formed at the approximate depth of AIW. However, throughout most of the northwest quadrant of the area the winter cooling/summer warming cycle has more effect on the deep sound channel structure than AIW, and AIW is found at depths below deep axial depth (winter profile on Figure B-19). The effects of AAIW in causing a narrower and shoaler deep sound channel are far more pronounced than those of AIW, even in the presence of diluted concentrations of MIW (e.g., see Figure B-49). Along the southern boundary of the area, the deep sound channel structure is controlled by AAIW, as previously noted for the northern Guiana Basin by Piip, Jan 1966.

The circulation of North Atlantic Deep and Bottom Water does not normally change the basic shape of the positive velocity gradient found below deep axial depths. Although sound velocity values vary somewhat from basin to basin in the North Atlantic (as shown by Moore, Nov 1965), sound velocity profiles below about 2000 meters are predictable throughout most of the study area. However, throughout the Irminger, Labrador, and western Icelandic Basins; cold, dilute Norwegian Sea Overflow Water (NSOW) can cause a sound velocity minimum just above the bottom and/or a sound velocity maximum at the interface between NSOW and "resident" North Atlantic Bottom Water. This situation has been studied in detail by Guthrie, Jun 1964 in the central Irminger Basin. Figures B-5 and B-10 show examples of NSOW effects in the Irminger and Labrador Basins, respectively. The warmer, more saline form of NSOW found in the eastern Icelandic Basin leads to the shoaler deep axial

7

depths found over the Faeroe-Iceland Ridge (Figure B-4). The colder, more dilute NSOW enters the North Atlantic over the Iceland-Greenland Ridge; the warmer, more saline NSOW over the Faeroe-Iceland Ridge and through the Faeroe Channel. The circulation of both types of NSOW is given in detail by Worthington, 1970.

UPPER SOUND CHANNEL

In this area, an upper sound channel can be caused by one or more of the following factors:

- interaction of warm, saline MIW with relatively cold, dilute NACW

- the annual heating/cooling cycle

- T-S inversions in the near-surface layer (commonly associated with oceanic frontal zones)

- high concentrations of "18° Water".

The first two cases were examined in detail for the Northeast Atlantic by Fenner and Bucca, Dec 1969. Interaction between MIW and NACW causes an upper sound channel throughout large sections of the Canary and Iberian Basins (Figure B-38). Winter cooling followed by summer warming to a lesser depth causes a sound velocity minimum (Figure B-20) in the region north of Cape Finisterre and Galicia Bank. However, winter cooling must exceed the maximum depth of summer warming. If the reverse situation occurs, no upper sound channel is formed (Figure B-17). This second mechanism, combined with the effects of T-S inversions in the near-surface layer, apparently causes upper sound channels throughout the North Atlantic other than in the Canary and Iberian Basins and the Sargasso Sea. In the Sargasso Sea, nearly isothermal "18° Water" causes an upper channel by retarding the near-surface negative velocity gradient (Figure B-40). Regions of transitory upper sound channels result from the attenuation of causitive forces (i.e., dilution of MIW or "18° Water" and/or less severe winter cooling).

Figure 3 shows the areal extent and average axial depth of the upper sound channel for winter. East of the Mid-Atlantic Ridge, the northern limit of a transitory upper sound channel corresponds well with the surface position of Central North Atlantic Front during winter (Laevastu and LaFond, Oct 1970). North of this front, winter cooling extends to greater than 400 meters, precluding the formation of an upper sound channel. In the Sargasso Sea, the lack of a permanent upper sound channel may be related to the relative
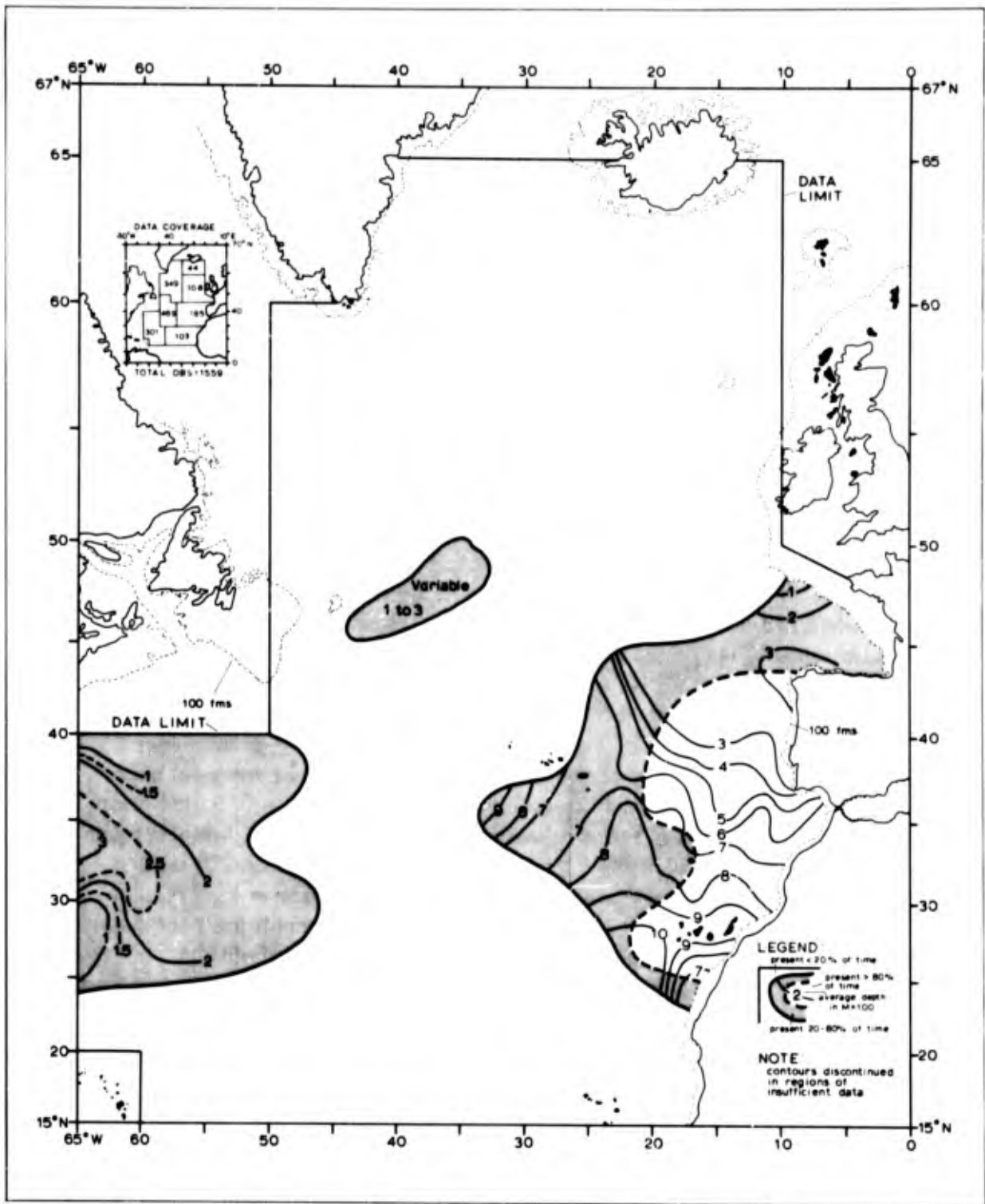
FIGURE 3. AREAL EXTENT AND AVERAGE AXIAL DEPTH OF UPPER SOUND
CHANNEL FOR WINTER (JAN-MAR).

absence of "18° Water" during winter, but also is caused by cooling of the surface and near-surface layers. Upper sound channels found east of Grand Banks probably result from mixing of the North Atlantic and Labrador Currents.

The various sound velocity cross-sections demonstrate the winter upper sound channel structure in the vertical dimension. Figure A-4 shows a rapidly shoaling upper sound channel north of the Azores-Gibraltar Rise that terminates abruptly at about 45° N. latitude coincident with the surfacing of the 1505-meter/second (m/sec) sound velocity isoline and the rapid shoaling of the 1500- and 1495-m/sec isolines. Surfacing or rapid shoaling of velocity isolines is characteristic of mixing, generally along a frontal zone. In the center of the area, Figure A-6 shows the lack of a winter upper channel over the Newfoundland Basin except for that associated with the surfacing of the 1500- and 1495-m/sec isolines at about 48° N. latitude (North Atlantic/Labrador Current confluence). Farther west, Figures A-8 and A-10 show complex and transitory upper sound channels in the Sargasso Sea during winter. The structure begins at about 25° N. latitude coincident with the surfacing of the 1530-m/sec and the deepening of the 1520-m/sec isolines. A wide-spacing between the 1520- and 1530-m/sec isolines is generally indicative of high to intermediate concentrations of "18° Water". In the east-west direction, Figure A-15 shows transitory upper channels off Brittany during winter. As expected, Figures A-17 and A-19 show the total absence of upper channels in the northern half of the area during winter.

Figure 4 shows the areal extent and average axial depth of the upper sound channel for spring. East of the Mid-Atlantic Ridge, the permanent upper sound channel extends as far north as Iceland due to increased surface insolation. However, north of the spring surface position of the Central North Atlantic Front (Laevastu and LaFond, Oct 1970), upper axial depths are less than 200 meters; whereas south of the front they deepen with decreasing latitude in the presence of increasing quantities of MIW. Transitory upper sound channels are continuous across the Reykjanes Ridge during spring and extend south throughout the Newfoundland and North American Basins into the Sargasso Sea. These structures result from sporadic warming of surface and near-surface layers characterized by relatively deep layer depths during winter. In the Sargasso Sea, increased surface warming in conjunction with more widespread "18° Water" causes an upper sound channel structure that is somewhat better defined than that found during winter. In a region surrounding Bermuda, this structure is permanent during spring. In the vertical dimension, Figure A-13 shows a deepening of the upper axis to the west over the Canary Basin, the total absence of this structure over the Mid-Atlantic Ridge, and well defined but transitory upper sound channels between about 100 and 200 meters over the North American Basin. The termination of an upper sound channel at about 30° W. longitude corresponds to the
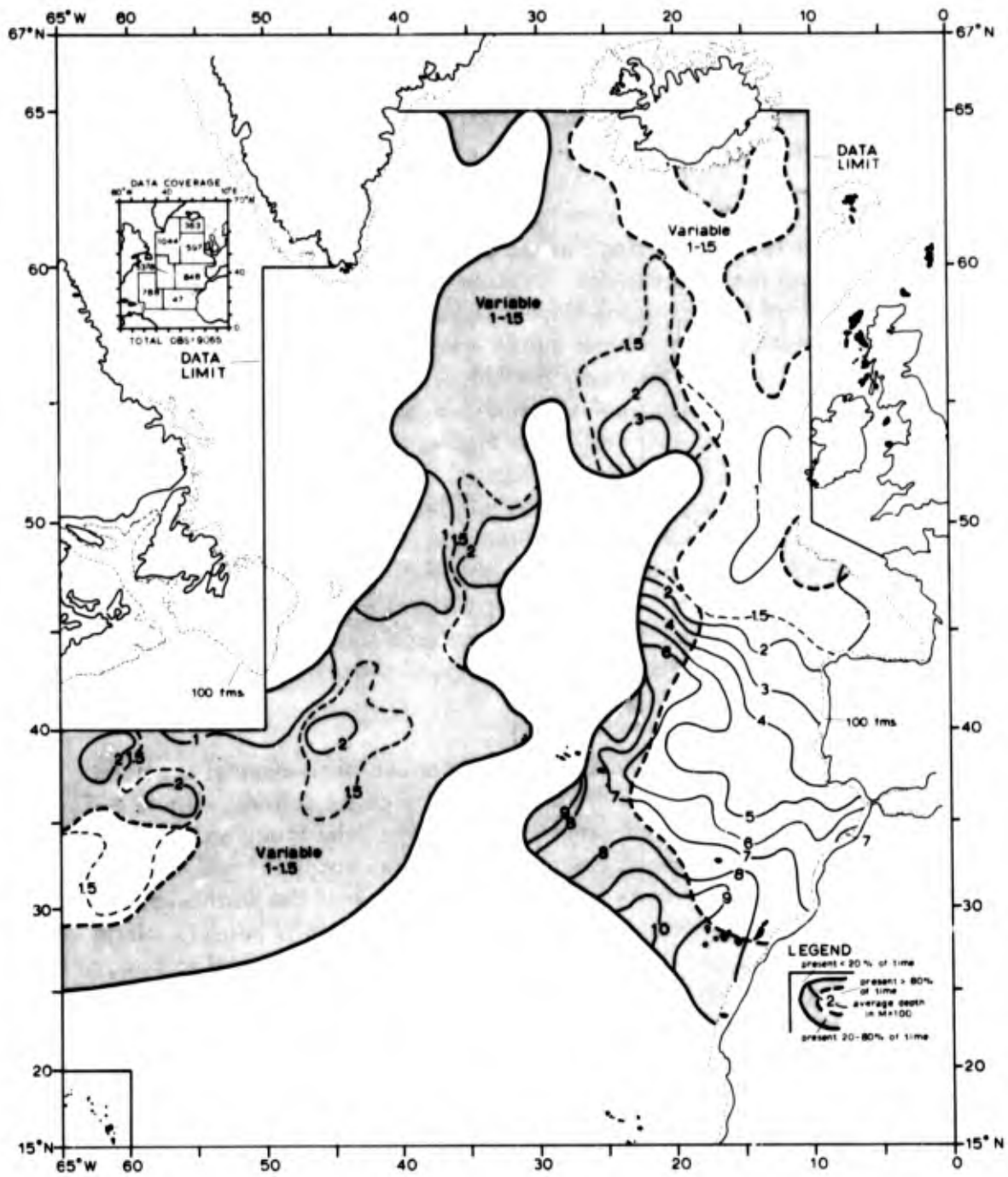
10

FIGURE 4. AREAL EXTENT AND AVERAGE AXIAL DEPTH OF UPPER SOUND CHANNEL FOR SPRING (APR-JUN).

disappearance of the greater than 1505-m/sec tongue (MIW). The reappearance of an upper sound channel west of the Mid-Atlantic Ridge roughly corresponds to the initial appearance of the 1520-m/sec sound velocity isoline ("18° Water"). The sound velocity perturbations at about 1000 meters just west of the Mid-Atlantic Ridge probably are caused by detached cells of MIW.

Figure 5 shows the areal extent and average axial depth of the upper sound channel for summer. During this season, there is a permanent upper channel throughout the Iberian, West European and Icelandic Basins and along the western flanks of the Reykjanes Ridge. Upper axial depths north of Cape Finisterre are about 50 meters deeper during summer than spring due to increased surface insolation. West of the Reykjanes Ridge, the permanent upper channel is caused by increased surface insolation and T-S inversions associated with the Subarctic Convergence (summer profiles on Figures B-12 and B-16). During summer, transitory upper sound channels occur farther west in the Labrador Basin but are absent in the region northwest of Altair Seamount where they are found during spring. This may be a result of preferential summer warming within the large gyre of the North Atlantic Current northeast of Flemish Cap (i.e., summer warming extends deeper than winter cooling, whereas spring warming does not). In the Sargasso Sea, upper axes are about 50 meters deeper during summer than during spring and the area of permanent upper sound channels extends northwest from Bermuda to about 39° N. Latitude.

The widespread and varied occurrence of upper sound channel structures during summer is best observed on the sound velocity cross-sections. Figure A-2 shows a permanent upper channel extending from Cape Juby to Iceland. Along this section, the upper axis shoals most rapidly between about 35° and 40° N. latitude and is coincident with an intrusion of a tongue from the north with sound velocities less than 1505 m/sec (NACW mixing with MIW below). North of about 45° N., the upper axis levels off at about 150 meters. Farther west, Figure A-3 shows distinctly transitory upper channels west of about 20° W. longitude and north of about 40° N. latitude in the presence of sporadic MIW cells. In the center of the area, Figure A-5 shows the absence of a continuous upper channel structure south of about 50° N. latitude except over the axis of the Mid-Atlantic Ridge (preferential east-west flow of MIW, see Figure 2). However, north of about 50° N. latitude a permanent upper sound channel is characterized by fluctuating velocities ranging from 1475 to 1485 m/sec (Subarctic Convergence). Figure A-7 shows transitory upper sound channels over the North American Basin associated with "18° Water" and the absence of these structures north of Grand Banks during summer. Along the eastern boundary of the area, Figure A-9 shows a better defined upper channel structure in the presence of greater surface warming and a wider interval between the 1530- and 1520-m/sec sound velocity isolines.
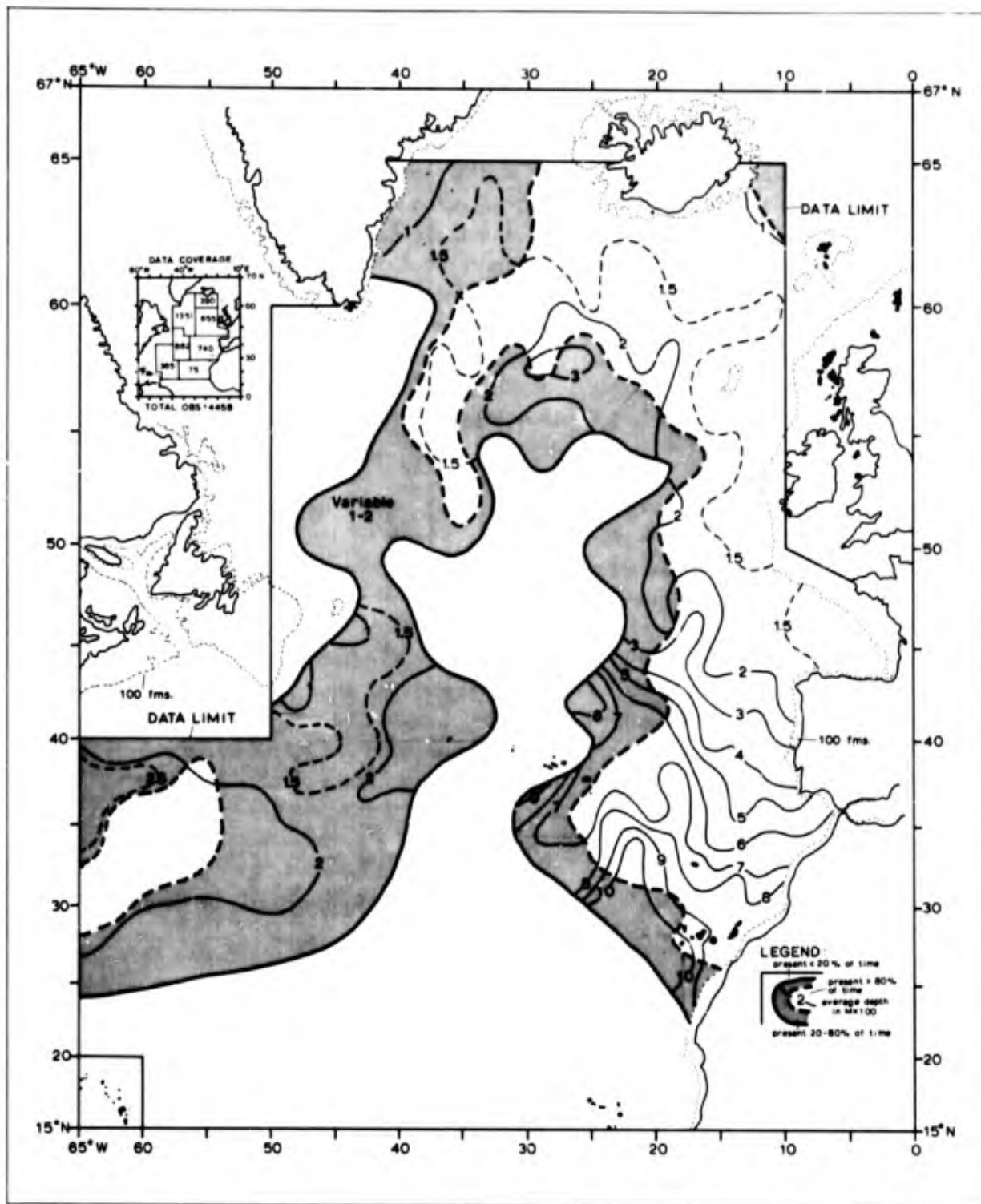
12

FIGURE 5. AREAL EXTENT AND AVERAGE AXIAL DEPTH OF UPPER SOUND
CHANNEL FOR SUMMER (JUL-SEP).

13

In the east-west direction, Figure A-14 shows a permanent upper channel structure during summer extending from Brittany across the West European Basin and terminating over the western flanks of the Mid-Atlantic Ridge coincident with a rapid shoaling of the 1500-m/sec sound velocity isoline. No such structure is found west of the Mid-Atlantic Ridge except at about 40° W. longitude associated with mixing east of Flemish Cap. Farther north, Figure A-16 shows two distinct regions with upper channels, one extending from Ireland to the Faeroe Plateau and the other over the western flanks of the Reykjanes Ridge. The first of these terminates coincidently with the rapid shoaling of the 1495-m/sec isoline (dilution of MIW). The second is associated with marked fluctuations of the 1480-m/sec isoline and the initial appearance of velocities less than 1475 m/sec (Subarctic Convergence). South of Iceland Figure A-18 shows a stable upper axis at about 150 meters that extends from the Faeroe Islands west across the Reykjanes Ridge. This structure rapidly terminates after the initial appearance of velocities less than 1480 m/sec.

Figure 6 shows the areal extent and average axial depth of the upper sound channel for autumn. Description of this feature is hindered by inadequate historical data south of the Azores Islands and over the central Labrador Basin and southern Reykjanes Ridge. The areal extent during autumn is simular to that for spring (Figure 4). However, upper axial depths north of Cape San Vicente and throughout the region west of the Mid-Atlantic Ridge are about 50 meters deeper than those for summer and about 100 meters deeper than those for spring. This is probably due to a seasonal heat lag and the absence of a surface Central North Atlantic Front during autumn (Laevastu and LaFond, Oct 1970). No sound velocity cross-sections are available for autumn north of 25° N. latitude.

SUBSURFACE SOUND VELOCITY MAXIMUM

Subsurface sound velocity maxima in the North Atlantic can be caused by one or more of the following factors:

- the high salinity MIW core (salinity maximum)

- the annual heating/cooling cycle

- T-S inversions in the near-surface layer

- interaction between the bottom of the "18° Water" layer and NACW.

The first two cases were discussed for the Northeast Atlantic by Fenner and Bucca, Dec 1969. The first case applies between the Canary Islands and Cape Finistere; the second north of about 50° N. latitude. In the first case, maxima
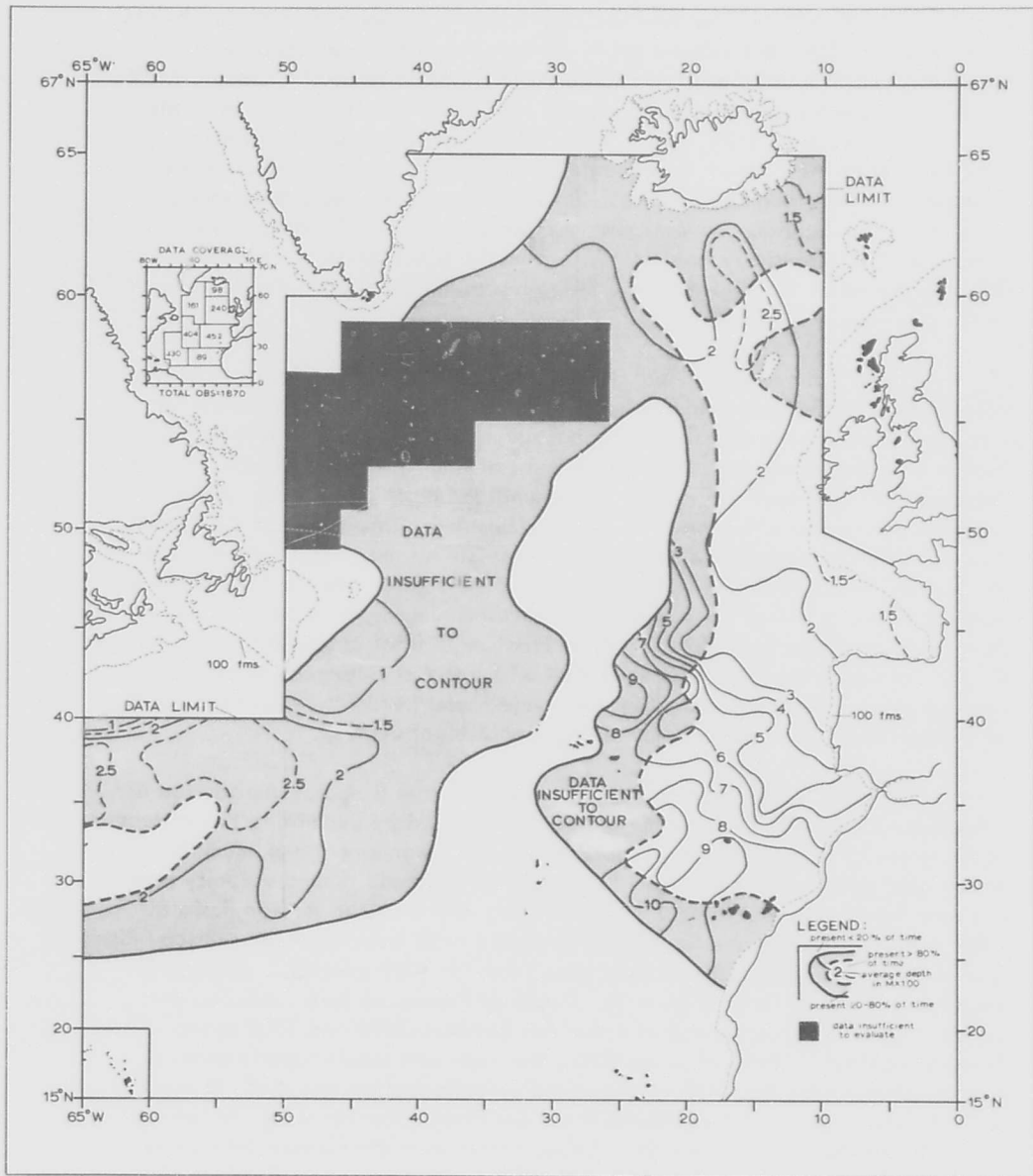
14

FIGURE 6. AREAL EXTENT AND AVERAGE AXIAL DEPTH OF UPPER SOUND
CHANNEL FOR AUTUMN (OCT-DEC).

15

correspond well with the depth of the MIW salinity maximum (see Figure B-38); in the second with the maximum depth of winter cooling (see Figure B-9). Between Cape Finisterre and the Faeroe Plateau and in Rockall Channel, MIW tends to deepen subsurface sound velocity maxima originally caused by winter cooling (Figures B-7, B-20, and B-24). Winter cooling and T-S inversions associated with the Subarctic Convergence probably cause maxima over the Labrador and Newfoundland Basins. In the Sargasso Sea, subsurface sound velocity maxima correspond well with the bottom of the "18° Water" layer (Figure B-40). Transitory maxima result from the attenuation of causitive forces and west of the Mid-Atlantic Ridge represent sonic layer depths (except in the presence of "18° Water").

Figure 7 shows the annual areal extent and average axial depth of the subsurface sound velocity maximum. An annual presentation was chosen for this parameter since seasonal two-degree square averages vary less than 100 meters from annual averages throughout most of the Northeast Atlantic, in the Sargasso Sea, and over the central Newfoundland Basin. However, large seasonal variations in the depth of the maximum were found west of the Canary Islands, over the Faeroe-Iceland and Iceland-Greenland Ridges, and between the Azores-Biscay Rise and Porcupine Bank. These three regions correspond to oceanic fronts at either the surface, intermediate depths, or both (i.e., front demarking southern limit of MIW, Polar Front, and front caused by North Atlantic Current at the surface and mixing of AIW with MIW at intermediate depths, respectively). Seasonal variations also were found in regions where the depth of the maximum was less than 300 meters (sonic layer depths).

The complicated vertical and areal extent and temporal distribution of subsurface sound velocity maxima are best understood by examining the various sound velocity cross-sections. Figure A-2 shows a permanent maximum that shoals gradually to the north from Cape Juby to Iceland. Sound velocity maxima are associated with a greater than 1510-m/sec cell over the Iberian Basin (at 1200 meters) and with greater than 1505-m/sec cells over the Azores-Biscay Rise and along the southern edge of Porcupine Bank (at 1000 meters). These cells coincide with MIW flows (Figure 2). North of Porcupine Bank, maxima are found at about 800 meters and at velocities between 1495 and 1500 m/sec (winter cooling). North of Lousy Bank, the maximum shoals rapidly upon initial contact with the 1490-m/sec sound velocity isoline and tends to merge with the upper sound channel along the Polar Front. Farther west, Figure A-4 shows the existance of two maxima during winter over the Canary Basin, one at about 100 meters (sonic layer depth) and one at intermediate depths with sound velocities of 1500 to 1505 m/sec. The deeper maximum shoals rapidly to the north and merges with the upper maximum and upper sound channel at about 45° N. latitude (surface Central North Atlantic Front, Laevastu and
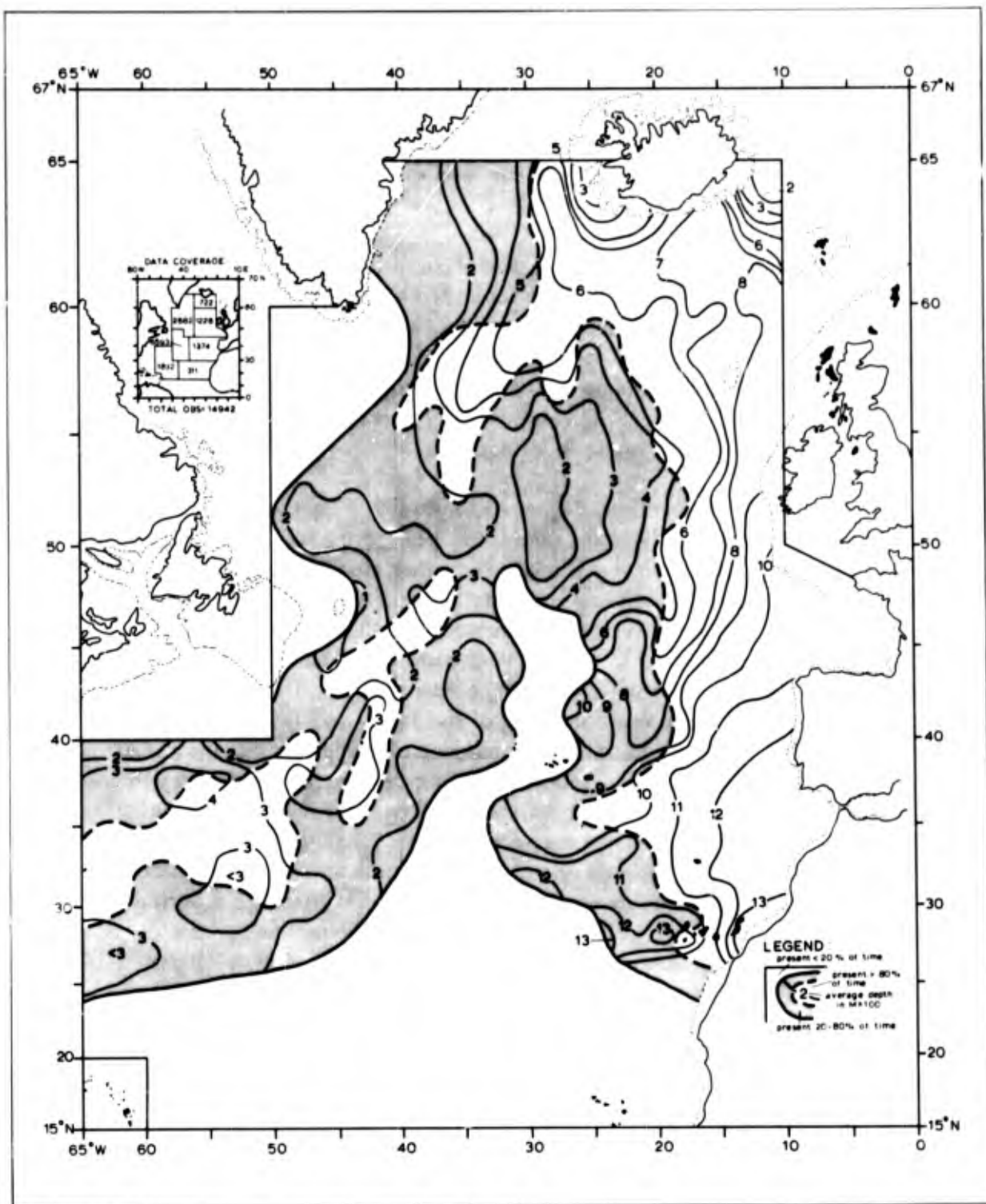
16

FIGURE 7. ANNUAL AREAL EXTENT AND AVERAGE DEPTH OF SUBSURFACE
SOUND VELOCITY MAXIMUM.

LaFond, Oct 1970). North of 45° N. latitude, the subsurface sound velocity maxima represent the maximum depth of winter cooling. A more transitory maximum occurs along this same meridian during summer (Figure A-3). Figures A-3 and A-4 show the merging of the deep maximum, upper sound channel, and the deep sound channel at about 26° N. latitude. South of 26° N. latitude, a sound velocity maximum and minimum are found below deep axial depth (also see Figure A-12).

In the center of the area, Figure A-6 shows a continuous maximum from 30° N. latitude to the Polar Front (sonic layer depth) during winter. During summer (Figure A-5), maxima disappear over the Newfoundland Basin, but still are present over the Reykjanes Ridge. Along the western boundary of the area, Figures A-9 and A-10 show maxima during both seasons at velocities greater than 1520 m/sec ("18° Water"). During winter, a second maximum is found above the "18° Water" layer (sonic layer depth).

In the east-west direction, Figure A-13 shows a permanent sound velocity maximum that shoals gradually to the west from Spain to the axis of the Mid-Atlantic Ridge. This maximum merges with the upper sound channel where velocities greater than 1505 m/sec disappear. West of the Mid-Atlantic Ridge a shoaler maximum is found at velocities greater than 1520 m/sec. Farther north during winter, Figure A-17 shows a very complex sound velocities maximum structure associated with the disappearance of velocities greater than 1500 m/sec (MIW), the rapid shoaling of the 1490- and 1495-m/sec sound velocity isolines, and the initial appearance of velocities less than 1480 m/sec. Over the Faeroe Plateau, sound velocity maxima associated with winter cooling and the MIW core coexist on the same profile. Between the Faeroe Plateau and the Subarctic Convergence, a continuous sound velocity maximum occurs at about 200 meters during winter. This maximum terminates coincidently with the initial appearance of sound velocities less than 1470 m/sec. During summer (Figure A-16) maxima only occur over Rockall Channel and in the vicinity of the Subarctic Convergence. South of Iceland, Figures A-18 and A-19 show a continuous maximum during summer and winter that extends from the Faeroe Islands to the Subarctic Convergence. Over the Icelandic Basin, maxima occur at velocities of nearly 1495 m/sec (interaction of NACW with a much diluted MIW core). However, just east of the Reykjanes Ridge, sound velocity maxima during both seasons represent the maximum depth of winter cooling. Over the Irminger Basin, winter cooling extends below deep axial depth (greater than 1000 m, Holzkamm, et al., 1964), causing a positive velocity gradient from top to bottom. Therefore, permanent subsurface sound velocity maxima are not found in this region. In the northern and central Labrador Basin and over Grand Banks and Flemish Cap, subsurface sound velocity maxima are effectively absent, due to deep winter cooling and the presence of a salinity minimum at the surface (LCW).

18

DEEP SOUND CHANNEL

Figure 8 shows the annual average depth of the deep sound channel axis. An annual presentation was chosen for this parameter since in any given two-degree square seasonal variations were as great as annual variations. In addition, deep axial depths at any given latitude do not appear to be related to the annual heating/cooling cycle (i.e., deeper values during summer, shoaler during winter). However, seasonal variations in deep axial depth were found in the western Irminger Basin, northern and central Labrador Basin, and east of Grand Banks and Flemish Cap. In these regions, extreme surface cooling causes the formation of positive velocity gradients during winter that extend from the surface to the bottom. During the warmer seasons, surface insolation causes a deep axis at depths shoaler than 400 meters. North of about 55° N. latitude, the eastern limit of semipermanent positive velocity gradients corresponds well with the winter position of the Atmospheric Arctic Front (Figure 2). South of Cape Farvel, semipermanent positive velocity gradients occur throughout the year (Figure B-8).

Two major tongues are apparent on Figure 8. The first is bounded by the 1200-meter axial depth isoline and extends west southwest from Spain across the North Atlantic to Bermuda. The second is bounded by the 900-meter axial depth isoline and extends from the Labrador Basin to the Faeroe Plateau along about 55° N. latitude. Anomalously deep values of this parameter found in the first tongue are caused by high salinity MIW. Anomalously shoal values in the second tongue are caused by low salinity AIW. Both tongues correspond well with salinity contours at the 4.0°C potential temperature surface shown by Worthington and Wright, 1970. In addition, Figure 8 shows four regions of rapid change in deep axial depth: west of Iceland (Polar Front), over the Faeroe-Iceland Ridge (Polar Front and dilution of MIW), east of Grand Banks and Flemish Cap (Subarctic Convergence), and west of the Canary Islands (dilution of MIW).

The various sound velocity cross-sections illustrate these and other overall features of the deep axial depth distribution. Figure A-2 shows a gradual shoaling of deep axial depths from Cape Juby to Porcupine Bank, rather constant deep axial depths between Porcupine and Lousy Banks, and a rapid shoaling between Lausy Bank and Iceland. Along this section, axial velocities range from less than 1505 m/sec in the south (MIW) to less than 1485 m/sec in the north (the warmer, more saline form of NSOW). Farther west, Figures A-3 and A-4 show axial depths that deepen between the Cape Verde Plateau and the Azores-Gibraltar Rise and then shoal to the north. During both seasons, axial velocities are less than 1495 m/sec over the Cape Verde Plateau (AAIW), greater than 1500 m/sec over the Azores-Gibraltar
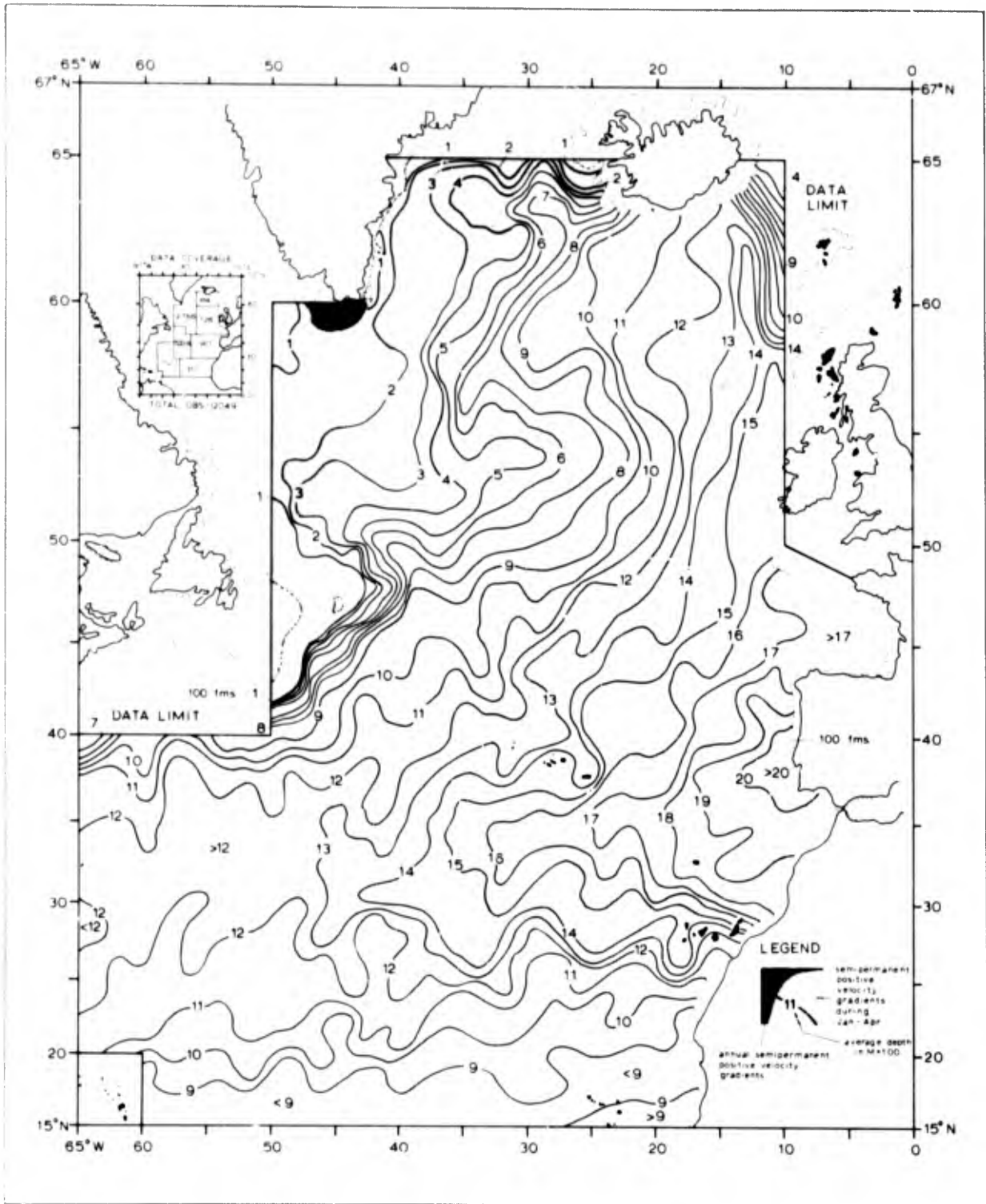
19

FIGURE 8. ANNUAL AVERAGE DEPTH OF DEEP SOUND CHANNEL AXIS.

Rise (MIW), and less than 1490 m/sec north of King's Trough (AIW and/or the warmer, more saline form of NSOW). Figures A-3 and A-4 also show a merging of the deep sound channel, subsurface sound velocity maximum, and upper sound channel at about 26° N. latitude. Along the 50° W meridian, Figures A-7 and A-8 show that axial depths deepen slightly between 15° N. latitude and the Corner Seamounts and then shoal rapidly between the Corner Seamounts and Grand Banks (Subarctic Convergence). North of Grand Banks, axial depths vary from 100 to 200 meters during summer and from 0 to 50 meters during winter (semipermanent positive velocity gradients). Axial velocities less than 1490 m/sec found south of 20° N. latitude are caused by AAIW, whereas low axial velocities found north of about 35° N. latitude are caused by either AIW (1485 to 1490 m/sec) or LCW (1440 to 1485 m/sec).

In the east-west direction, Figure A-11 shows less than 900-meter axial depths and axial velocities less than 1490 m/sec over the Cape Verde and Guiana Basins (AAIW). Between the Cape Verde and Canary Islands, Figure A-12 shows axial depths that deepen between the African coast and about 30° W. longitude and then remain at about 1200 meters between 30° and 65° W. longitude. Over the Canary Basin, a sound velocity maximum/minimum structure occurs below the deep axis (caused by MIW). This structure merges with the deep axis at about 30° W. longitude. Farther north, Figure A-13 shows 1800- to 2000-meter axial depths east of the Mid-Atlantic Ridge (high concentrations of MIW) and 1200- to 1600-meter axial depths west of the Ridge (diluted MIW). Axial velocities range from less than 1505 m/sec off Spain to about 1490 m/sec at 65° W. longitude. Across the center of the area, Figures A-14 and A-15 show axial depths during summer and winter than shoal from 2000 meters off Spain to about 1200 meters over the Mid-Atlantic Ridge, vary between 1000 and 1200 meters over the Newfoundland Basin, shoal rapidly after the initial appearance of the 1485-m/sec sound velocity isoline (Subarctic Convergence), and then vary between 200 meters (summer) and the surface (winter) west of the Subarctic Convergence. Axial velocities decrease steadily to the west, being greater than 1495 m/sec over the West European Basin (MIW), less than 1490 m/sec over the Newfoundland Basin (AIW), and less than 1475 m/sec west of the Subarctic Convergence (LCW). Over the Icelandic Basin, Figures A-18 and A-19 show axial depths of 1000 to 1200 meters and axial velocities of 1490 to 1495 m/sec during both seasons. Both depths and velocities decrease rapidly east of about 13° W. longitude (warmer, more saline form of NSOW). West of the Reykjanes Ridge, axial depths shoal gradually to the west during summer. During winter, semipermanent positive velocity gradients occur west of about 35° W. longitude. During both seasons, axial velocities vary from about 1485 m/sec over the Reykjanes Ridge to less than 1450 m/sec off the Greenland Coast.

21

SOUND VELOCITY PERTURBATIONS

In addition to the upper sound channel, subsurface sound velocity maximum, and deep sound channel, other sound velocity maximum/minimum structures are frequently found above and below the deep sound channel axis and just above the bottom. For purposes of the following discussion, such features will be referred to as sound velocity perturbations. These structures generally are transitory and normally are not effective channels for sound transmission.

Sound velocity perturbations near the deep sound channel axis generally are due to mixing of MIW, AAIW, and/or LCW with NACW. Figure A-13 and Figures B-35 and B-37 (all along the 35° N. parallel) show good examples of sound velocity perturbations above deep axial depth caused by the interaction of MIW and NACW. Figure A-12 and Figure B-47 (both along the 25° N. parallel) show good examples of sound velocity perturbations below deep axial depth due to the same process. Sound velocity perturbations resulting from intrusions of MIW into the main thermocline are quite common along the axis of the Mid-Atlantic Ridge, where shoal bathymetry impedes the flow of this high salinity water mass (Katz, Jun 1969). The winter profile on Figure B-50 shows an example of a perturbation above deep axial depth caused by an intrusion of AAIW into NACW. The perturbation below deep axial depth on this same profile is due to an intrusion MIW. The winter profiles on Figures B-21 and B-25 show examples of perturbations below deep axial depth caused by intrusions of NACW into a layer of LCW. Such perturbations occur along the Subarctic Convergence during all seasons (see Figures A-8, A-9 and A-14).

Sound velocity perturbations found at or just above the bottom in the Irminger, Labrador, and western Icelandic Basins are due to cold, dilute NSOW flowing across the Iceland-Greenland Ridge. A sound velocity minimum is formed coincident with the cold, low salinity core when this core lies just above the bottom, but is absent if the core is in contact with the bottom. A more frequently found maximum is formed at the interface between the overflow water core and "resident" North Atlantic Bottom Water. Figure B-5 shows an example of both cases for the north central Irminger Basin. Near-bottom sound velocity maxima are shown on the following cross-sections:

- Figures A-5, A-6, A-18 and A-19 (Irminger Basin)

- Figure A-7 (Labrador Basin)

- Figures A-3 and A-4 (Icelandic Basin).

22

The maximum shown on Figure A-7 lies within the Mid-Ocean Canyon. Near-bottom sound velocity minima were found only during winter and only in close proximity to the Iceland-Greenland Ridge (Figures A-6 and A-19).

As shown above, NSOW entering the North Atlantic over the Iceland-Greenland Ridge causes sound velocity perturbations just above the bottom. However, NSOW entering the North Atlantic over the Faeroe-Iceland Ridge and through the Faeroe Channel causes a rapid shoaling of deep axial depth (see Figures A-2, A-18 and A-19). Bottom water flows over the Icealnd-Greenland Ridge are much colder and much less saline than flows over the Faeroe-Iceland Ridge and through the Faeroe Channel (Lee and Ellett, 1965) and hence are found deeper in the water column. In addition, deep axial depths west of the Reykjanes Ridge are considerably shoaler than those in the eastern Icelandic Basin in the presence of diluted MIW.

SUMMARY AND CONCLUSIONS

This report supplements a previous partial summary of sound velocity characteristics for the North Atlantic Ocean (Fenner, et al., Jun 1971) in terms of:

- the extent and average axial depth of the upper sound channel for the four standard seasons of winter, spring, summer and autumn

- the annual extent and average depth of the subsurface sound velocity maximum

- the annual average depth of the deep sound channel axis.

Each of the above parameters is defined using areal contour charts, vertical sound velocity cross-sections to a maximum depth of 5000 meters, and sound velocity/temperature-salinity (T-S) profile comparisons. In addition, a brief discussion is given of sound velocity perturbations found above and below deep axial depth and just above the bottom.

Upper sound channels are found during all seasons over the Iberian Basin caused by an interaction of warm, saline Mediterranean Intermediate Water (MIW) with cold, dilute North Atlantic Central Water (NACW). In the Sargasso Sea, a similar structure at lesser depths is caused by high concentrations of "18° Water". During spring, summer and autumn, upper sound channels also are found north of about 45° N. latitude on both sides of the Mid-Atlantic Ridge. These structures are caused by warming of surface and near-surface

layers characterized by positive velocity gradients during winter and by T-S inversions found in conjunction with various oceanic frontal zones.

Subsurface sound velocity maxima just below the upper sound channel are caused by the high salinity MIW core, interaction between the bottom of the "18° Water" layer and NACW, winter cooling, and T-S inversions found along frontal zones. The depth of this feature is relatively constant throughout the year in the Northeast Atlantic, in the Sargasso Sea, and over the central Newfoundland Basin. However, seasonal variations were encountered along various oceanic fronts and in regions where the subsurface sound velocity maximum was shoaler than 300 meters (sonic layer depth).

Deep axial depths are deeper than 1200 meters in a region extending west southwest from Spain across the North Atlantic to Bermuda due to the influence of MIW. Anomalously shoal values of this parameter (less than 900 meters) are found in a tongue along 55° N. latitude due to low salinity Arctic Intermediate Water (AIW) and along the southern boundary of the area due to low salinity Antarctic Intermediate Water (AAIW). Deep sound channels are anomalously wide in the presence of MIW (particularly in diluted concentrations), but are constructed by AIW and AAIW.

Sound velocity perturbations above and below deep axial depth throughout the area are due to mixing of MIW, AAIW, and/or Labrador Current Water (LCW) with NACW. Sound velocity perturbations are found just above the bottom in the Irminger, Labrador and western Icelandic Basins in conjunction with cold, dilute Norwegian Sea Overflow Water (NSOW).

The pronounced effects of various surface, subsurface and intermediate water masses on sound velocity profiles indicates that a general knowledge of circulation and water masses is prerequisite to understanding the predicting of sound velocity structures. This is particularly important in areas of mixing between water masses, such as along the Subarctic Convergence, Polar Front, and along the front between the Azores-Biscay Rise and Porcupine Bank. Truly synoptic oceanographic observations are needed to fully understand the complex temporal and spatial variability of sound velocity in areas of marked oceanic activity.

REFERENCES

Bubnov, V. A., 1968, The intermediate Subarctic waters in the northern part of the Atlantic Ocean: Okeanol. Issled., v. 19, p. 136-153 (translated from Russian as Naval Oceano. Off. Transl. no. 545, 1971).

Defant, A., 1961, Physical oceanography, v. 1: New York, Pergamon Press, 729 p.

Fenner, D. F. and Bucca, P. J., Dec 1969, The upper and deep sound channel in the Northeast Atlantic: Naval Oceano. Off. Informal Rept no. 69-94.

Fenner, D. F., Bucca, P. J., and Davis, C. L., Jun 1971, Sound velocity and bottom characteristics for LRAPP Atlantic areas I, II, and III: Naval Oceano. Off. Informal Rept, no. 71-2. CONFIDENTIAL

Fuglister, F. C., 1960, Atlantic ocean atlas of temperature and salinity profiles and data from the International Geophysical Year of 1957-1958: Woods Hole Oceano. Inst. Atlas Series, v. 1, 209 p.

Guthrie, R. C., Jun 1964, Sound velocity distribution in the Irminger Sea: Proc. First U. S. Navy Symp. Mil. Oceano., v. 1, p. 97-111.

Holzkamm, F., Krause, G., and Siedler, G., 1964, On the processes of renewal of North Atlantic deep water in the Irminger Sea: Deep-Sea Res., v. 11, p. 881-890.

Husby, D. M., Jun 1967, Oceanographic observations; North Atlantic Ocean Station Delta, 44° N., 41° W.; July 1966-August 1967: U. S. Coast Guard Oceano. Rept. no. 23 (CG 373-23).

Istoshin, Y. V., 1961, Formative area of "eighteen degree" water in the Sargasso Sea: Okeanologiya, v. 1, no. 4, p. 600-607 (translated from Russian in Deep-Sea Res., v. 9, p. 384-390, 1962).

Jones, L. M., and VonWinkle, W. A., May 1965, Sound velocity profiles in an area south of Bermuda: U. S. Navy Underw. Sound Lab. Rept. no. 632.

Katz, E. J., Jun 1969, Variableness of the sound velocity profile about the Mid-Atlantic Ridge axis: Woods Hole Oceano. Inst. Ref. no. 69-50 (unpublished manuscript).

REFERENCES (CONTINUED)

Laevastu, T., and LaFond, E. C., Oct 1967, Oceanic fronts and their seasonal positions on the surface: Naval Undersea Res. and Dev. Center Tech. Pub. 204.

Lee, A. and Ellett, D., 1965, On the contribution of overflow water from the Norwegian Sea to the hydrographic structure of the North Atlantic Ocean: Deep-Sea Res., v. 12, p. 129-142.

Mann, C. R., 1967, The termination of the Gulf Stream and the beginning of the North Atlantic Current: Deep-Sea Res., v. 14, p. 337-359.

Moore, C. T., Nov 1965, Tables of sound speed at the bottom below 1,000 fathoms in the North Atlantic Ocean: Naval Oceano. Off. Informal Rept. no. 0-52-65 (unpublished manuscript).

Morgan, C. W., 1967, Oceanography of the Grand Banks region of Newfoundland in 1967: U. S. Coast Guard Oceano. Rept no. 19 (CG 373-19).

Naval Oceanographic Office, 1962, Tables of sound speed in sea water, Special Pub. 58 (supplement to H. O. Pub. 614).

_____ , 1965, Oceanographic atlas of the North Atlantic Ocean, section I, tides and currents: H. O. Pub. no. 700.

Piip, A. T., Jan 1966, Precision sound velocity profiles in the ocean, v. I, the sound channel in the Bermuda-Barbados region (November-December 1963): Lamont Geol. Observ. Tech. Rept. no. 3 (CU-3-66), prepared for Off. Naval Res. under contract Nonr 266(65).

_____ , Apr 1968, Precision sound velocity profiles in the ocean, v. IV, Canary Islands-Gibraltar-Bay of Biscay, sound speed, temperature, etc. (June-July 1965): Lamont Geol. Observ. Tech. Rept. no. 6 (CU-6-68), prepared for Off. Naval Res. under contract Nonr 266(65).

Schroeder, E., Stommel, H., Manzel, D., and Sutcliffe, W., Jr., 1959, Climatic stability of eighteen degree water at Bermuda: Jour. Geophys. Res., v. 64, no. 3, p. 363-366.

Sverdrup, H. U., Johnson, M. W., and Fleming, R. H., 1942, The oceans, their physics, chemistry, and general biology: Englewood Cliffs, Prentice Hall, 1087 p.

REFERENCES (CONTINUED)

Wilson, W. D., 1960, Equation for the speed of sound in sea water: Jour. Acoustical Soc. Am., v. 32, no. 10, p. 1357.

Worthington, L. V., 1959, The 18° water in the Sargasso Sea: Deep-Sea Res., v. 5, p. 297-305.

_____, 1970, The Norwegian Sea as a mediterranean basin: Deep-Sea Res., v. 17, p. 77-84.

Worthington, L. V. and Wright, W. R., 1970, North Atlantic Ocean atlas of potential temperature and salinity in the deep water including temperature, salinity and oxygen profiles from the Erika Dan cruise of 1962: Woods Hole Oceano. Inst. Atlas Series, v. 2, unpaginated.

APPENDIX A

SELECTED SOUND VELOCITY CROSS-SECTIONS

PRECEDING PAGE BLANK

29

APPENDIX A

SELECTED SOUND VELOCITY CROSS-SECTIONS

Figure A-1 gives the locations of the 18 sound velocity cross-sections shown as Figures A-2 through A-19. Figures A-3/A-4, A-5/A-6, A-7/A-8, A-9/A-10, A-14/A-15, A-16/A-17, and A-18/A-19 are seasonal pairs along the same parallel or meridian (summer and winter, respectively). Existing data were inadequate to construct a winter profile corresponding to Figure A-2. Figures A-11, A-12, and A-13 can be considered to be a seasonal (i.e., representative of both summer and winter) except for the first 100 to 200 meters of the water column. Figures A-6 and A-8 (both winter) are aseasonal south of 30° N. latitude, and are the same as Figures A-7 and A-9 (both summer). Figures A-11, A-12, and A-13 correspond to temperature and salinity sections shown by Fuglister, 1960 along 16°, 24°, and 36° N. latitude, respectively. Figure A-17 corresponds to temperature, salinity, and oxygen sections shown along 53° N. latitude by Worthington and Wright, 1970.

The basic contour interval used on the sound velocity cross-sections is 10 m/sec (shown by a thick, solid line). Subsidiary 5-m/sec contours (thin, solid line) have been added for better definition as necessary. When present, the following sound velocity features (dashed lines) are shown on each cross-section:

- deep sound channel axis (primary sound velocity minimum)

- secondary subsurface sound velocity minima (including upper sound channel axis, sound velocity perturbations, and near-bottom sound velocity minima)

- subsurface sound velocity maxima (including sonic layer depths, near-bottom maxima, and maxima caused by MIW and "18° Water"

- limiting (critical depth.

Limiting depth is defined as that depth where the sound velocity is equal to the maximum sound velocity found at the surface or at sonic layer depth (bottom of surface mixed layer).

The locations of individual sound velocity profiles are shown by ticks inside the bottom margin on each cross-section. These profiles were plotted

PRECEDING PAGE BLANK

31

at the NODC standard depths and analyzed at 5- and/or 10-m/sec intervals to either the bottom or a maximum depth of 5000 meters. The bathymetric profiles shown on the cross-sections were drawn from a large number of sources, including:

- Bathymetric profiles shown by Fuglister, 1960

- NAVOCEANO North Atlantic Regional Charts compiled in 1969

- Charts of A. S. Laughton (National Institute of Oceanography, Wormley, England) compiled in 1966

- Charts contoured by NAVOCEANO prior to 1960 as part of the National Intelligence Survey (NIS) program.

These profiles are highly generalized and only show large-scale bathymetric features that influence sound velocity structures.
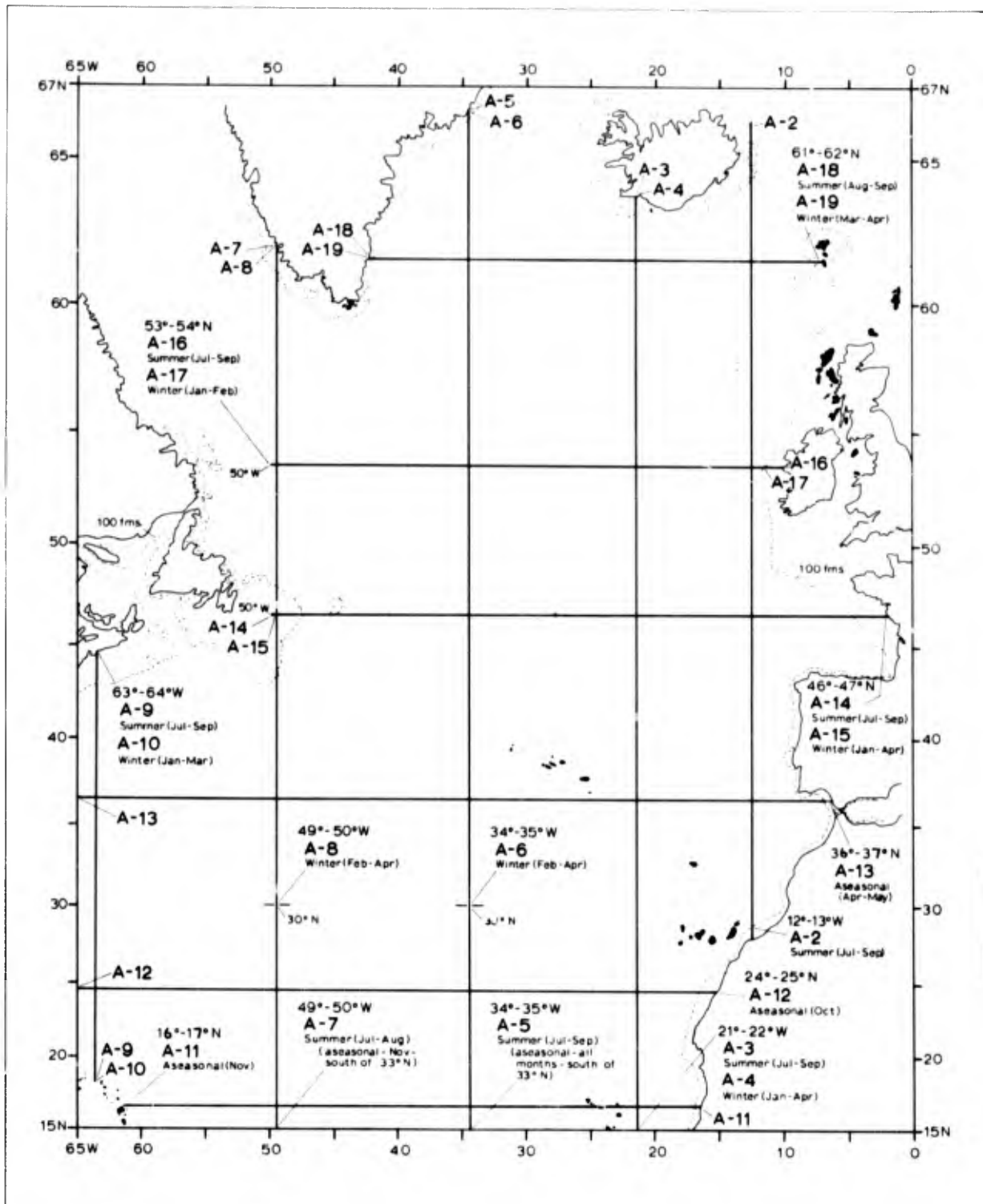
FIGURE A-1. LOCATION OF SELECTED SOUND VELOCITY CROSS-SECTIONS
(FIGURES A-2 THROUGH A-19).

33
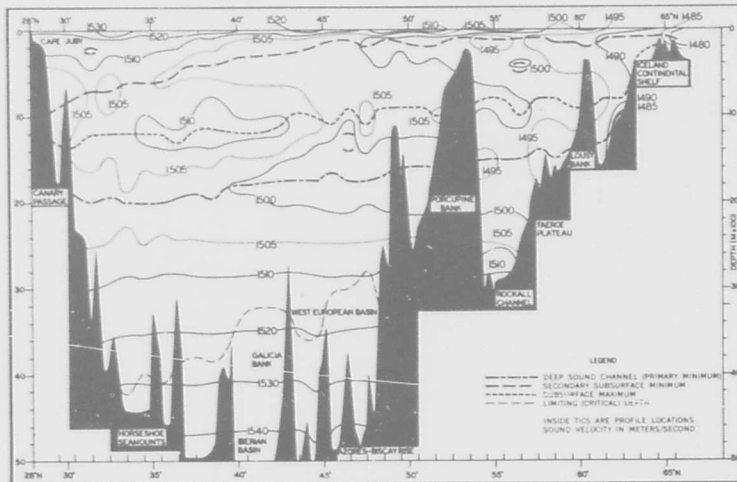
FIGURE A-2. SOUND VELOCITY CROSS-SECTION BETWEEN 12° AND 13° W. LONGITUDE FOR SUMMER (JUL-SEP).
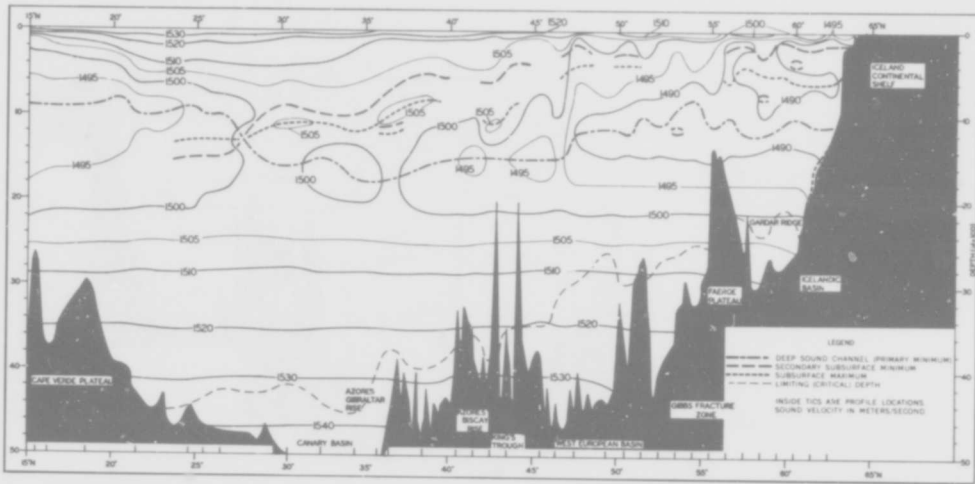
FIGURE A-3. SOUND VELOCITY CROSS-SECTION BETWEEN 21° AND 22°
W. LONGITUDE FOR SUMMER (JUL-SEP).
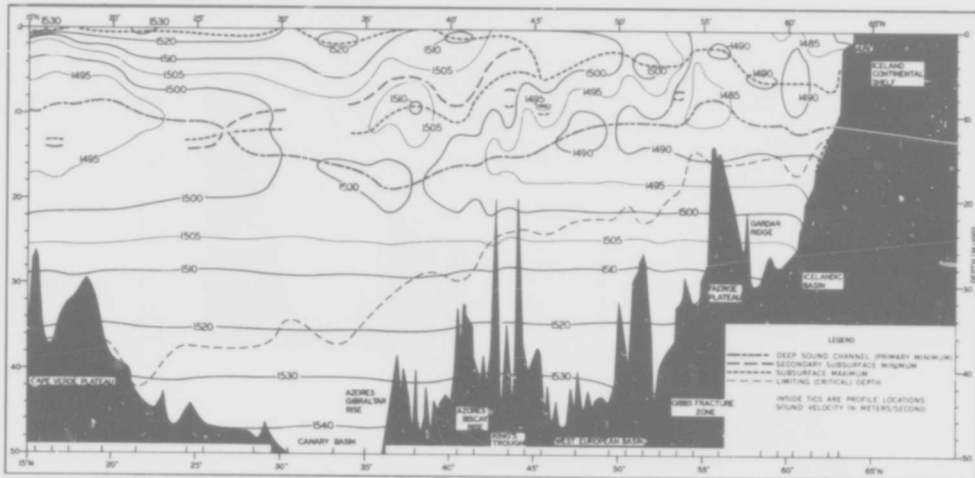
FIGURE A-4. SOUND VELOCITY CROSS-SECTION BETWEEN 21° AND 22°
W. LONGITUDE FOR WINTER (JAN-APR).
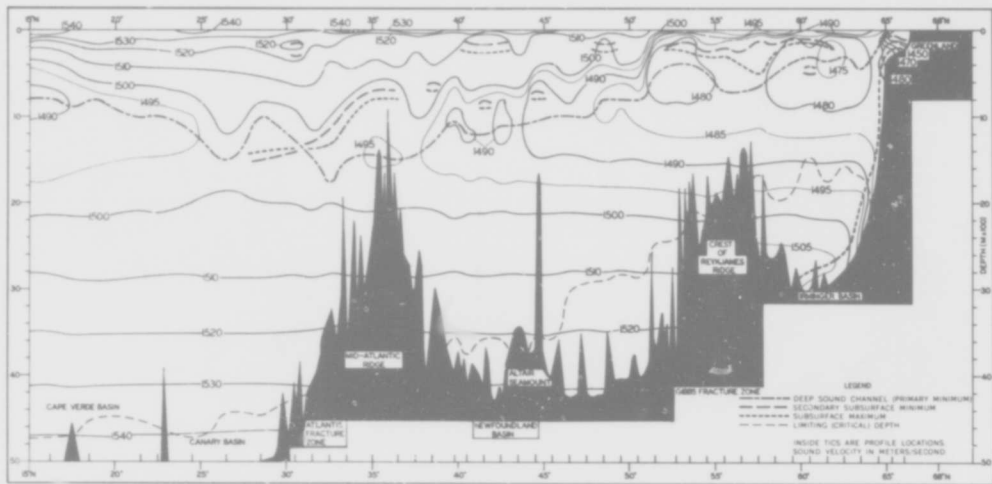
FIGURE A-5. SOUND VELOCITY CROSS-SECTION BETWEEN 34° AND 35°
W. LONGITUDE FOR SUMMER (JUL-SEP, ALL MONTHS
SOUTH OF 33° N. LATITUDE).
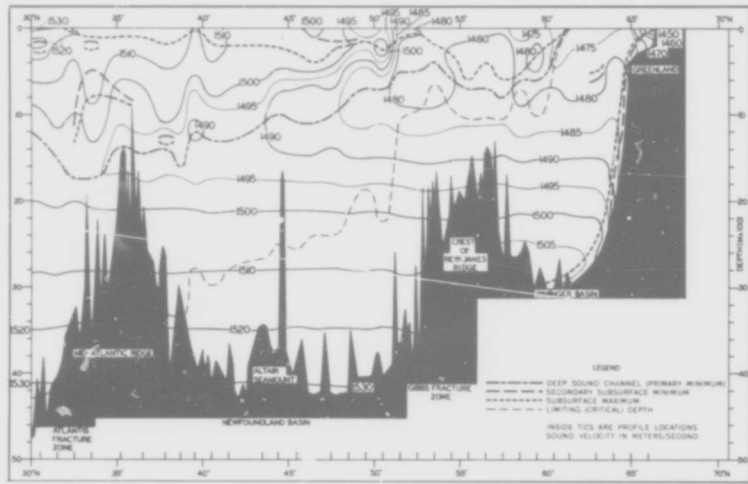
FIGURE A-6. SOUND VELOCITY CROSS-SECTION BETWEEN 34° AND 35°
W. LONGITUDE FOR WINTER (FEB-APR).

36
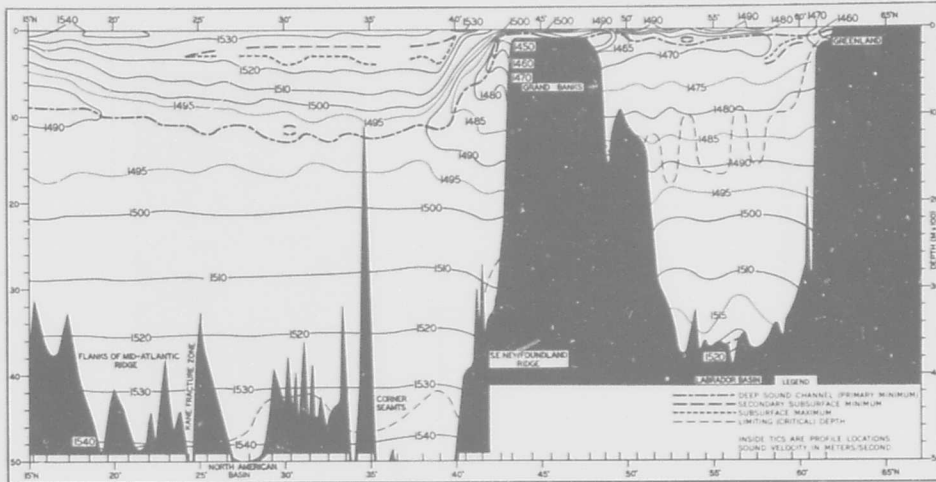
FIGURE A-7. SOUND VELOCITY CROSS-SECTION BETWEEN 49° AND 50°
W. LONGITUDE FOR SUMMER (JUL-AUG, NOV SOUTH OF
33° N. LATITUDE).
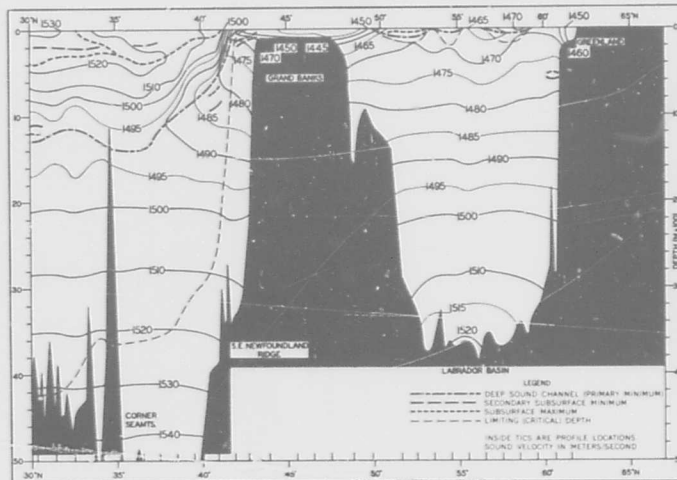
FIGURE A-8. SOUND VELOCITY CROSS-SECTION BETWEEN 49° AND 50°
W. LONGITUDE FOR WINTER (FEB-APR).

37
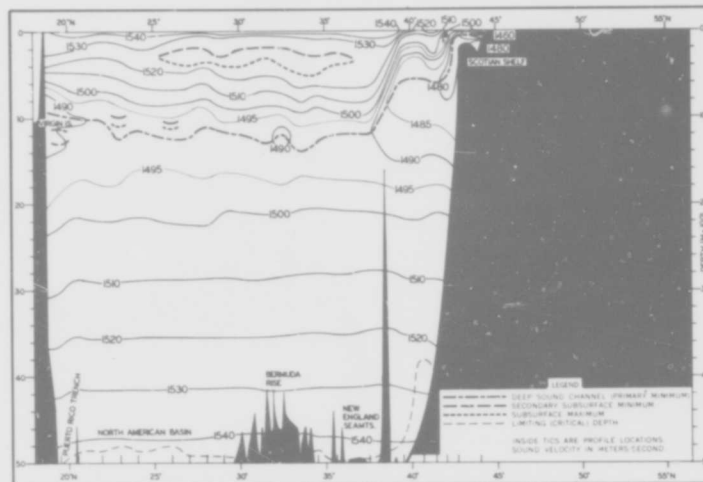
FIGURE A-9. SOUND VELOCITY CROSS-SECTION BETWEEN 63° AND 64°
W. LONGITUDE FOR SUMMER (JUL-AUG).
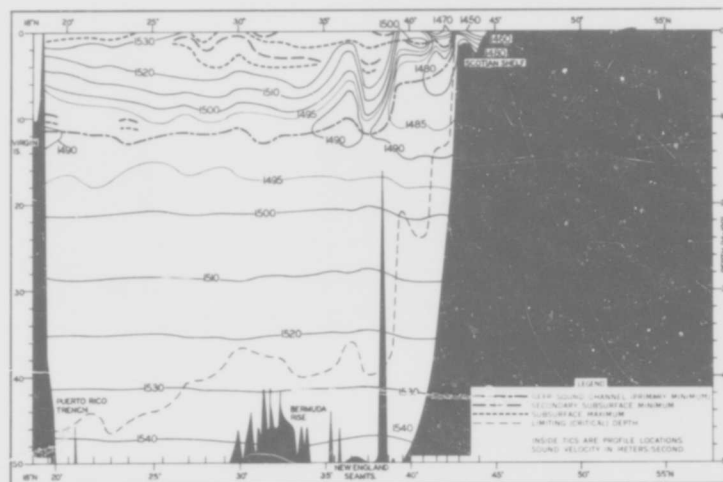
FIGURE A-10. SOUND VELOCITY CROSS-SECTION BETWEEN 63° AND 64°
W. LONGITUDE FOR WINTER (JAN-MAR).
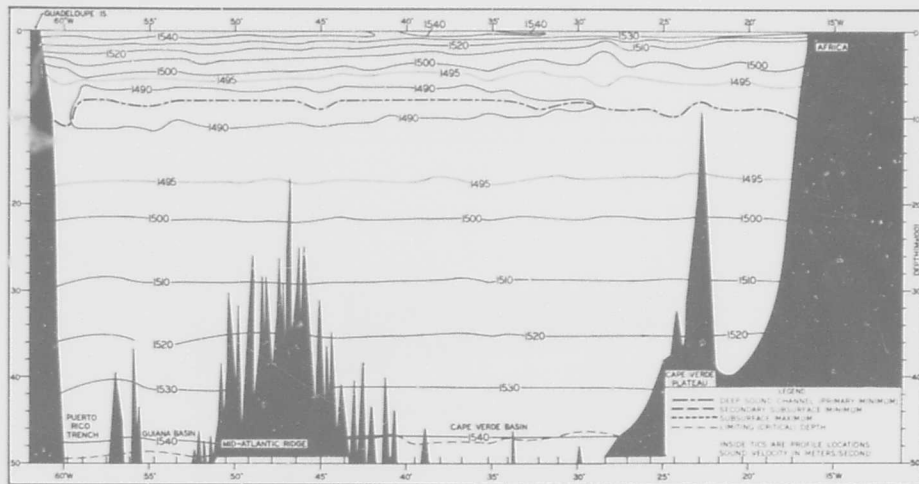
FIGURE A-11. SOUND VELOCITY CROSS-SECTION BETWEEN 16° AND 17°
N. LATITUDE (ASEASONAL, NOV).
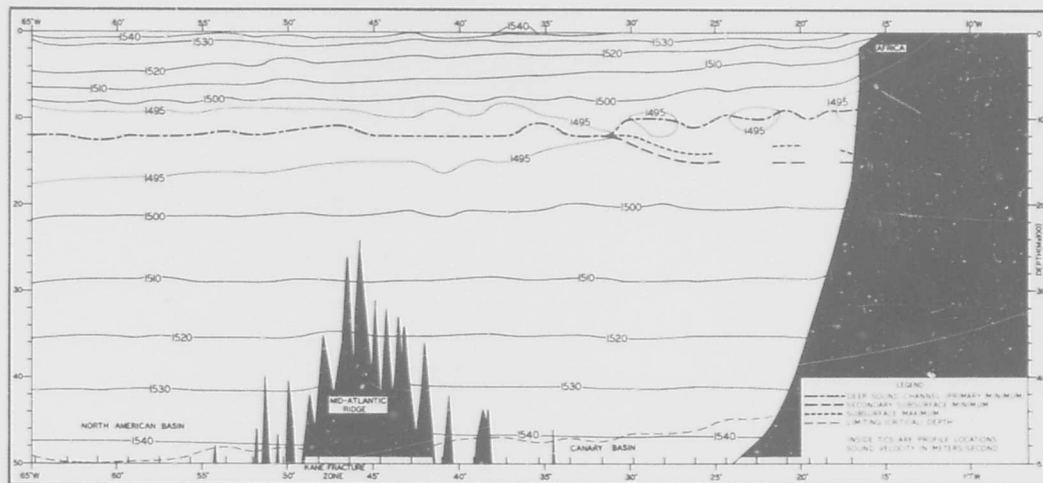
FIGURE A-12. SOUND VELOCITY CROSS-SECTION BETWEEN 24° AND 25°
N. LATITUDE (ASEASONAL, OCT).

39
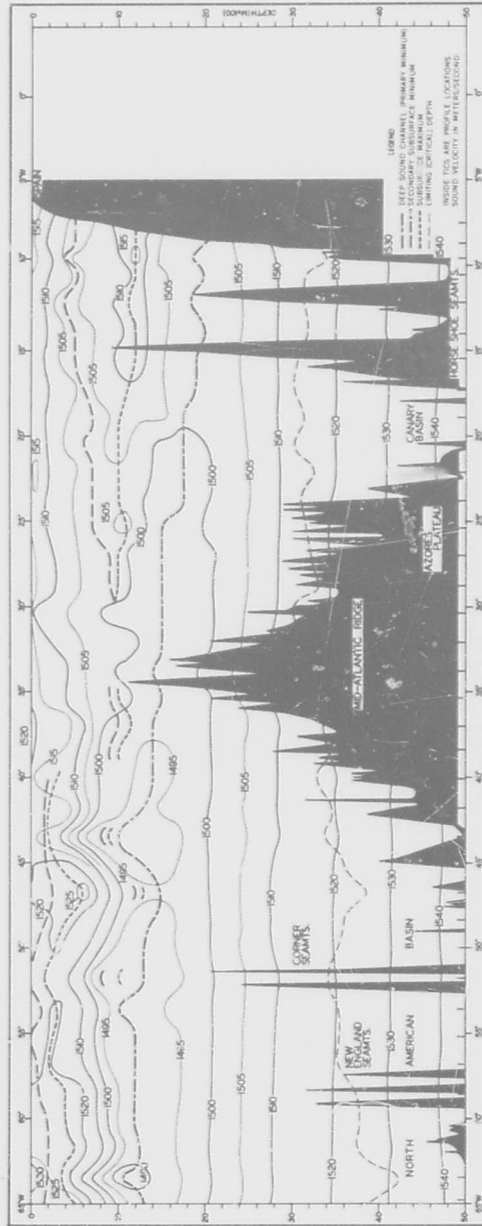
FIGURE A-13. SOUND VELOCITY CROSS-SECTION BETWEEN 36° AND 37° N. LATITUDE (ASEASONAL, APR-MAY)

40
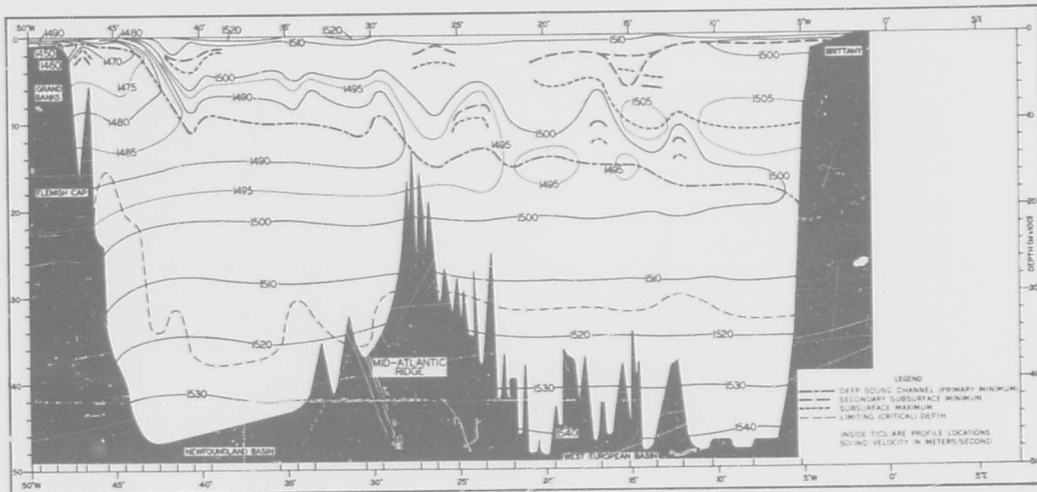
FIGURE A-14. SOUND VELOCITY CROSS-SECTION BETWEEN 46° AND 47°
N. LATITUDE FOR SUMMER (JUL-SEP).
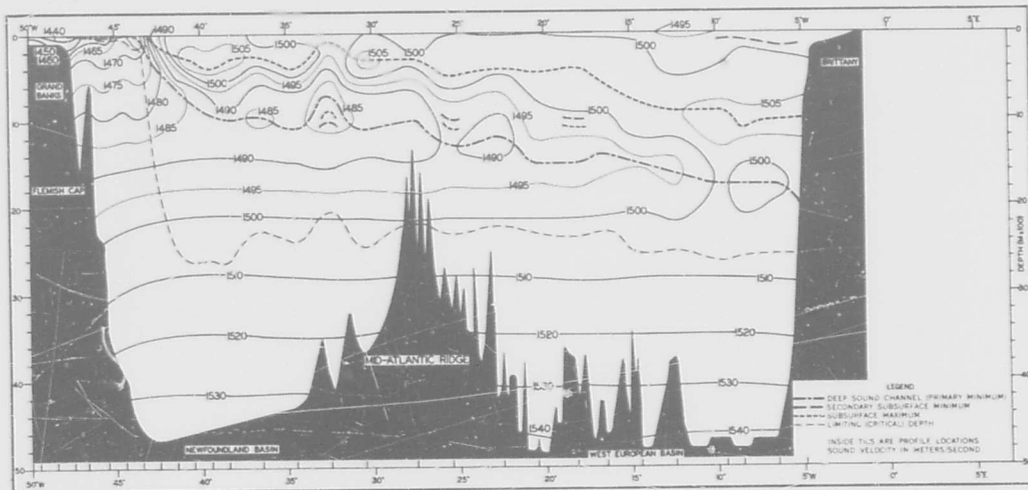
FIGURE A-15. SOUND VELOCITY CROSS-SECTION BETWEEN 46° AND 47°
N. LATITUDE FOR WINTER (JAN-APR).

41
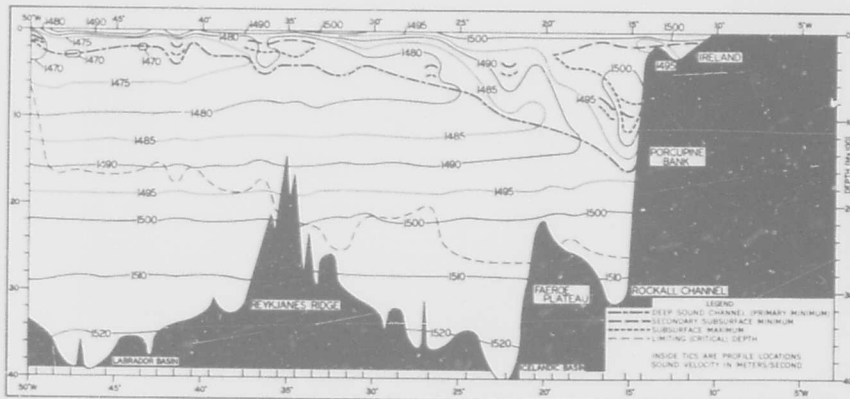
FIGURE A-16. SOUND VELOCITY CROSS-SECTION BETWEEN 53° AND 54°
N. LATITUDE FOR SUMMER (JUL-SEP).
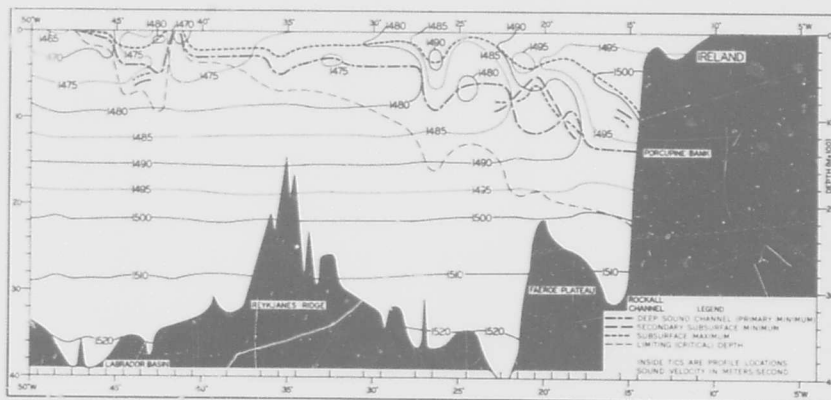
FIGURE A-17. SOUND VELOCITY CROSS-SECTION BETWEEN 53° AND 54°
N. LATITUDE FOR WINTER (JAN-FEB).

42
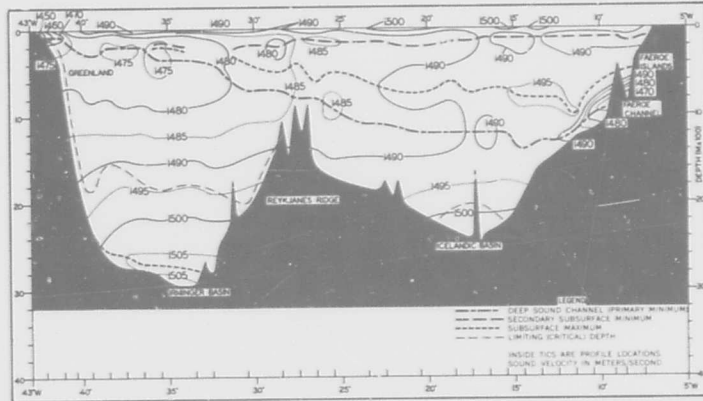
FIGURE A–18. SOUND VELOCITY CROSS-SECTION BETWEEN 61° AND 62° N. LATITUDE FOR SUMMER (AUG–SEP).
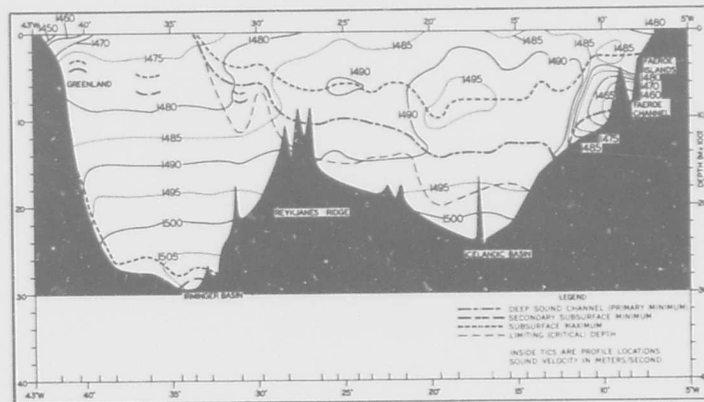
FIGURE A–19. SOUND VELOCITY CROSS-SECTION BETWEEN 61° AND 62° N. LATITUDE FOR WINTER (MAR–APR).

APPENDIX B

SELECTED SOUND VELOCITY AND T-S PROFILES

45

APPENDIX B

SELECTED SOUND VELOCITY AND T-S PROFILES

T-S RELATIONS IN THE NORTH ATLANTIC OCEAN

Figure B-1 shows a general T-S diagram for the major water masses of the North Atlantic Ocean that influence sound velocity structures. The T-S indices for NACW, Atlantic Subarctic Water (ASAW), and North Atlantic Deep and Bottom Water were taken directly from Sverdrup, et al., 1942. The curves showing the percent unmixed MIW at the salinity maximum and the percent unmixed AAIW at the salinity minimum are drawn from Defant, 1961. LCW is defined after Morgan, 1967 and is based on a 20-year average accumulated by the International Ice Patrol. The T-S range of AIW has been modified by the authors after that shown by Sverdrup, et al., 1942 and Bubnov, 1968 using considerable historical data from the northwest quadrant of the area. The T-S index for "18° Water" is taken from Schroeder, et al., 1959 and represents a long-term average taken just off Bermuda. Indices for the two NSOW subtypes are identical to those for Iceland-Greenland Overflow Water (colder, less saline subtype) and Iceland-Scotland Overflow Water (warmer, more saline subtype) given by Lee and Ellett, 1965.

GENERAL COMMENTS

Figure B-2 gives the locations of the 50 sound velocity/T-S comparisons shown as Figures B-3 through B-52. Each figure consists of a sound velocity and T-S profile representative of summer (S) and winter (W) conditions at the given location. The maximum depth of each sound velocity profile represents the approximate bottom depth. The depth limits of actual sound velocity data are indicated on the various figures by two parallel horizontal lines (=). Sound velocity profiles that have been extended below the depth of actual data are indicated by a dotted line. The T-S profiles have not been extended below the depth of actual data. The percentages of unmixed MIW and/or AAIW shown on the various figures were derived using the curves of Defant, 1961 (shown on Figure B-1).

To facilitate water mass identification and comparison between sound velocity and T-S profiles, the following legend has been used:

A: depth of MIW salinity maximum for winter

B: depth of MIW salinity maximum for summer

PRECEDING PAGE BLANK

47

C: bottom of unaltered NACW layer for winter (salinity minimum)

D: bottom of unaltered NACW layer for summer (salinity minimum)

E: depth of AIW or AAIW salinity minimum for winter

F: depth of AIW or AAIW salinity minimum for summer

G: depth of "18° Water" core for winter

H: depth of "18° Water" core for summer.

The "C" and "D" notations above are used only in the presence of MIW and/or AAIW. In the presence of AAIW, the "E" and "F" notations are always accompanied by annotations giving the percentage of unmixed AAIW. No percentages are available for unmixed AIW.

SOURCES AND TREATMENT OF DATA

All sound velocity profiles shown on Figures B-3 through B-52 were derived according to the equation of Wilson (1960) except for the winter profile on Figure B-35 and the summer profile on Figure B-44. These two profiles represent sound velocimeter data. The majority of the sound velocity profiles were retrieved from NODC in one-degree square seasonal and monthly summaries that also contained listings of temperature (in °C) at the various NODC standard depths. Whenever possible, Nansen cast observations of temperature and salinity were used in constructing T-S diagrams. These values were taken from Fuglister, 1960; Worthington and Wright, 1970; and the various sources given by Fenner, et al., Jun 1971. However, for the winter T-S profiles on Figures B-4, B-7, B-14, B-20, B-22, B-24, B-28, and B-38 and the summer profiles on Figures B-13, B-37, B-38, B-39, B-41, B-42, and B-43 salinities were computed from depth-temperature-sound velocity values using Wilson's tables (Naval Oceanographic Office, 1962). Although salinities computed in this manner are not as accurate as direct measurements, they are sufficiently accurate for constructing the T-S diagrams shown in this report. Sound velocity and T-S profiles for any given season and location represent the same single observations in all cases. No averaging processes were used in the construction of the profiles. Therefore, the given profiles are not typical of any large region, but only show general trends encountered throughout the area.

FIGURE B-1. T-S RELATIONS IN THE NORTH ATLANTIC OCEAN.
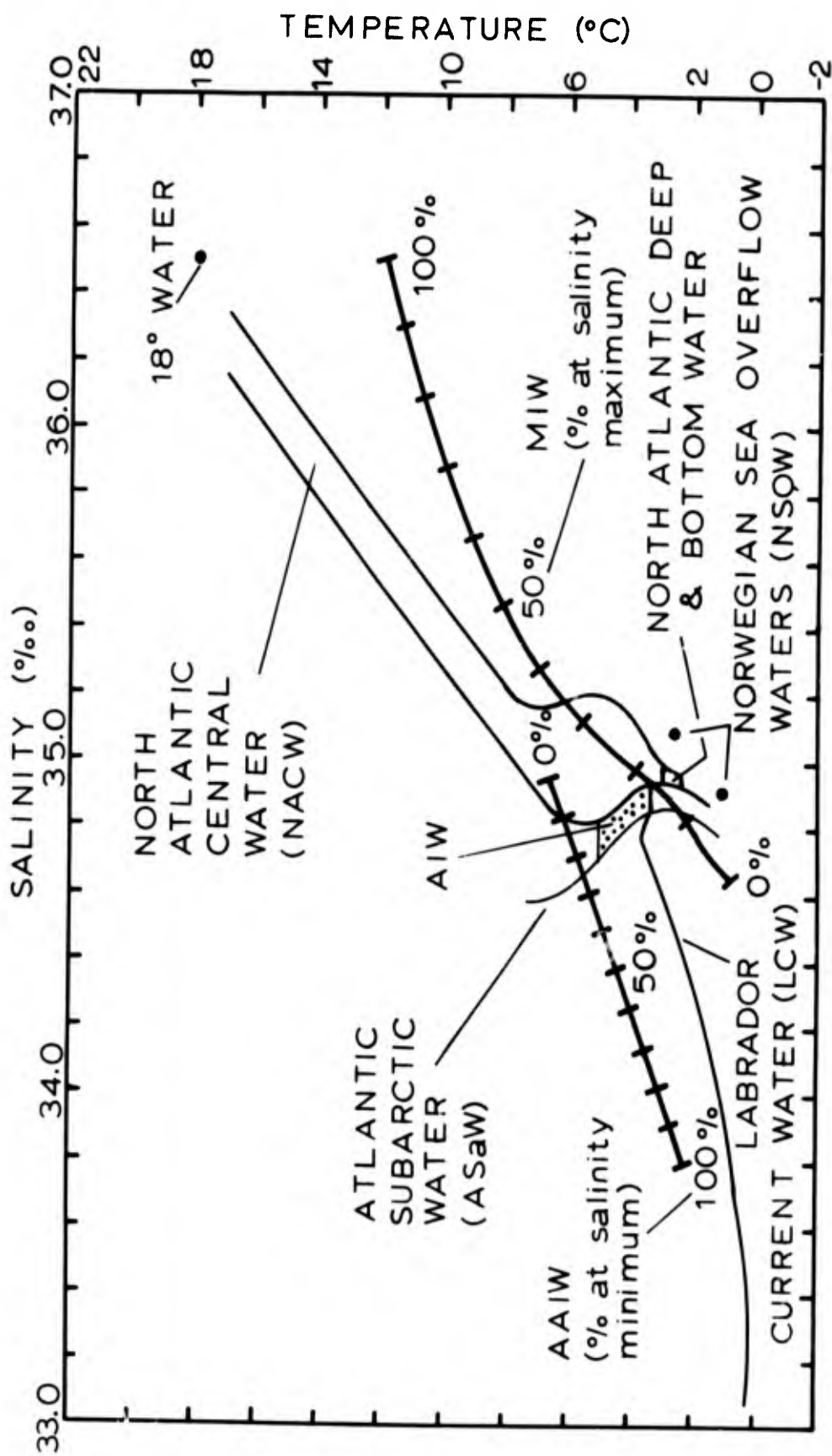
AAIW = Antarctic Intermediate Water
AIW   = Arctic Intermediate Water
MIW = Mediterranean Intermediate Water

after Sverdrup, et al. (1942)
Defant (1961), Morgan (1967)
and others.

49
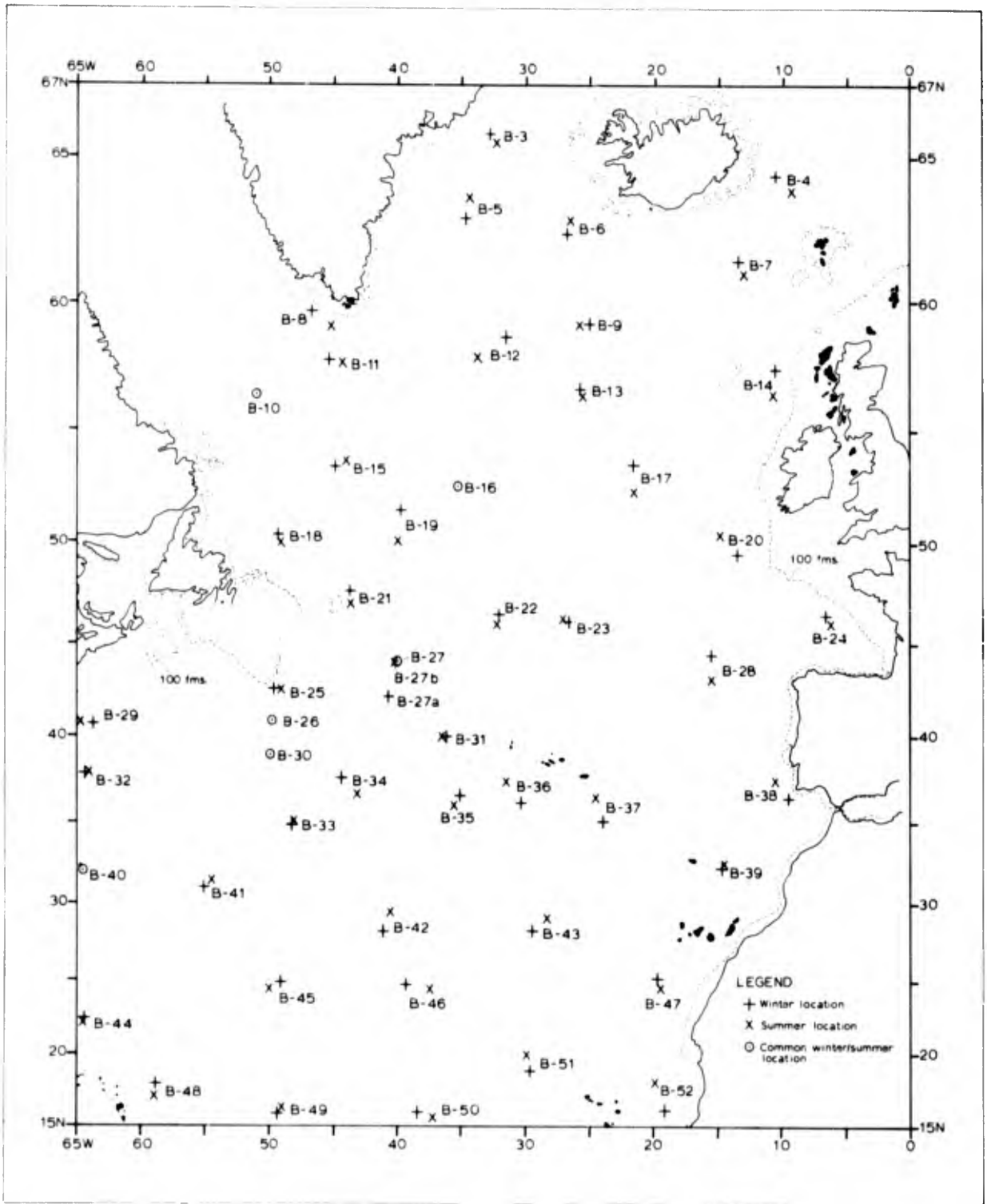
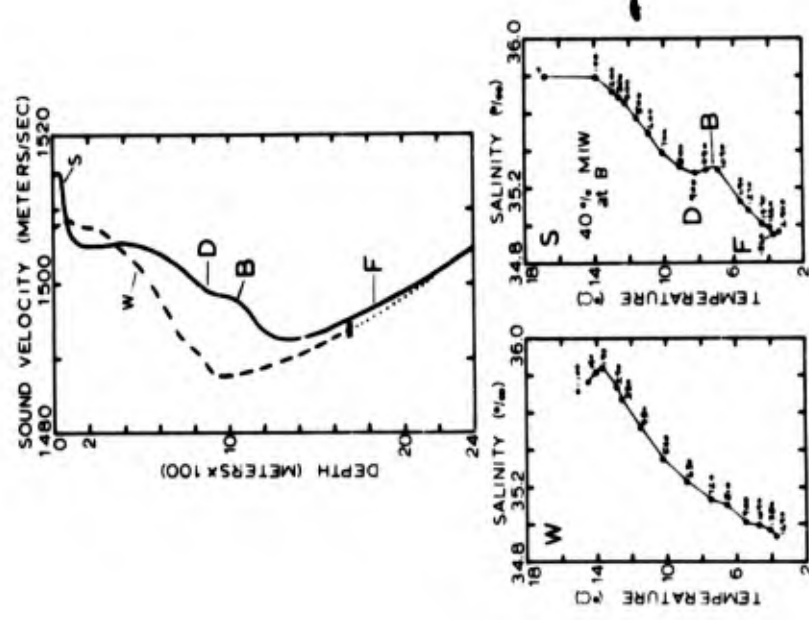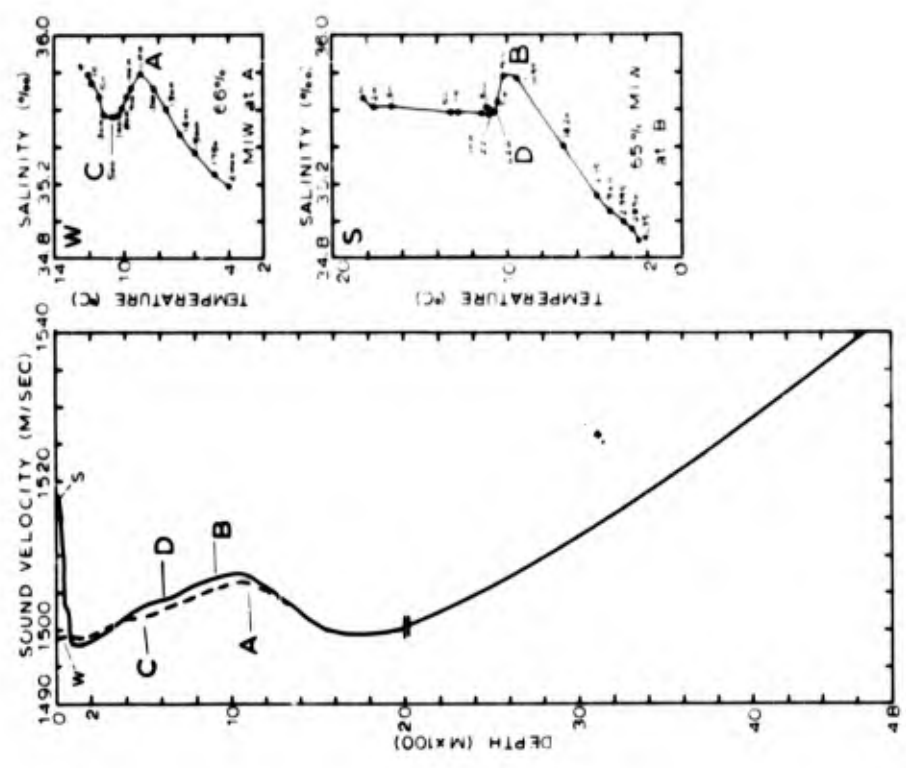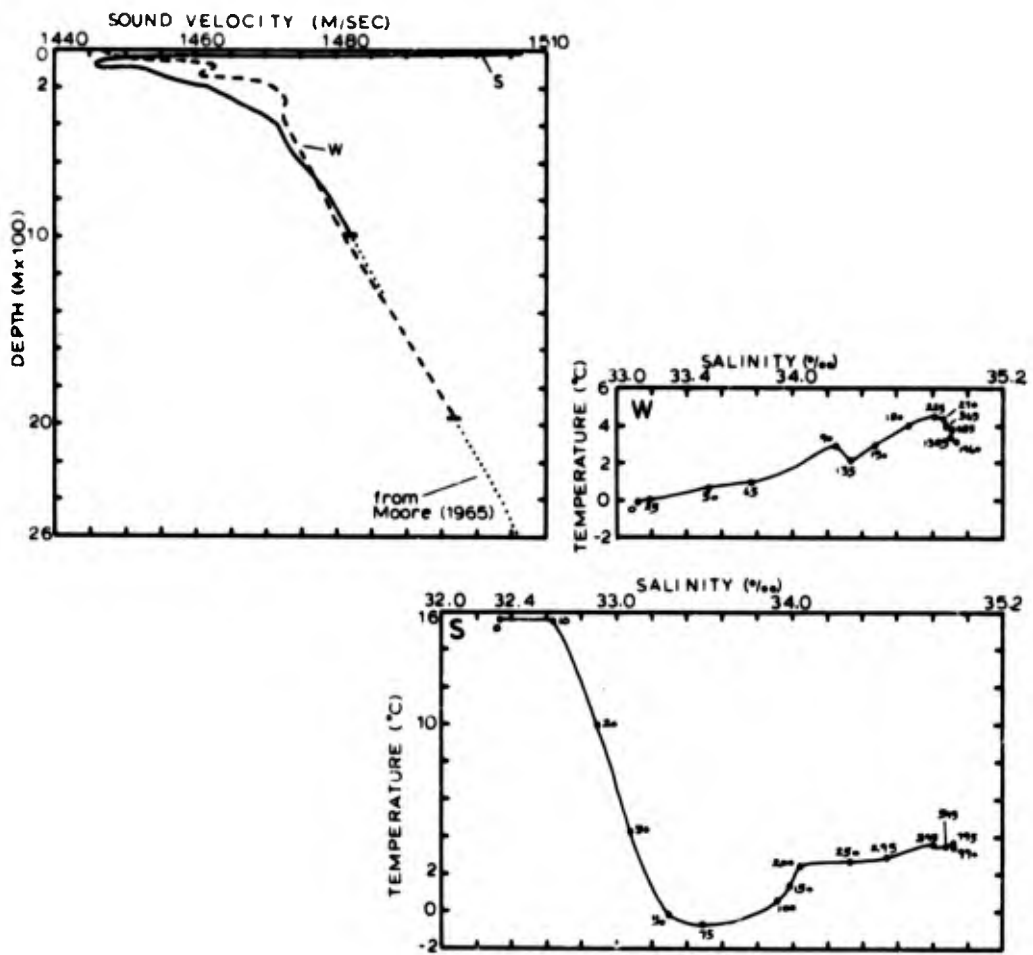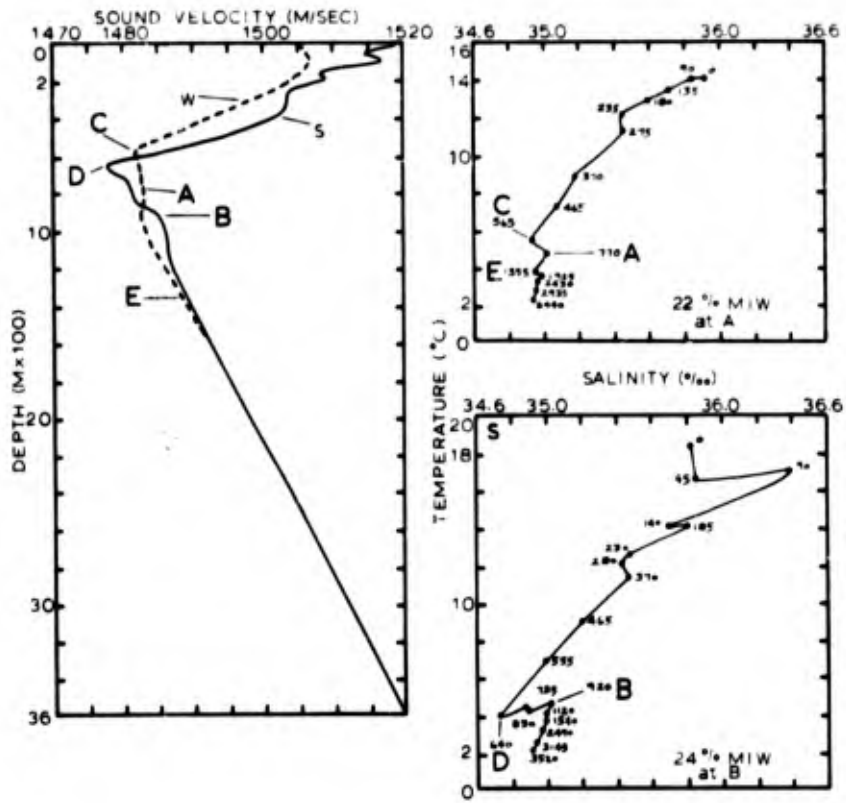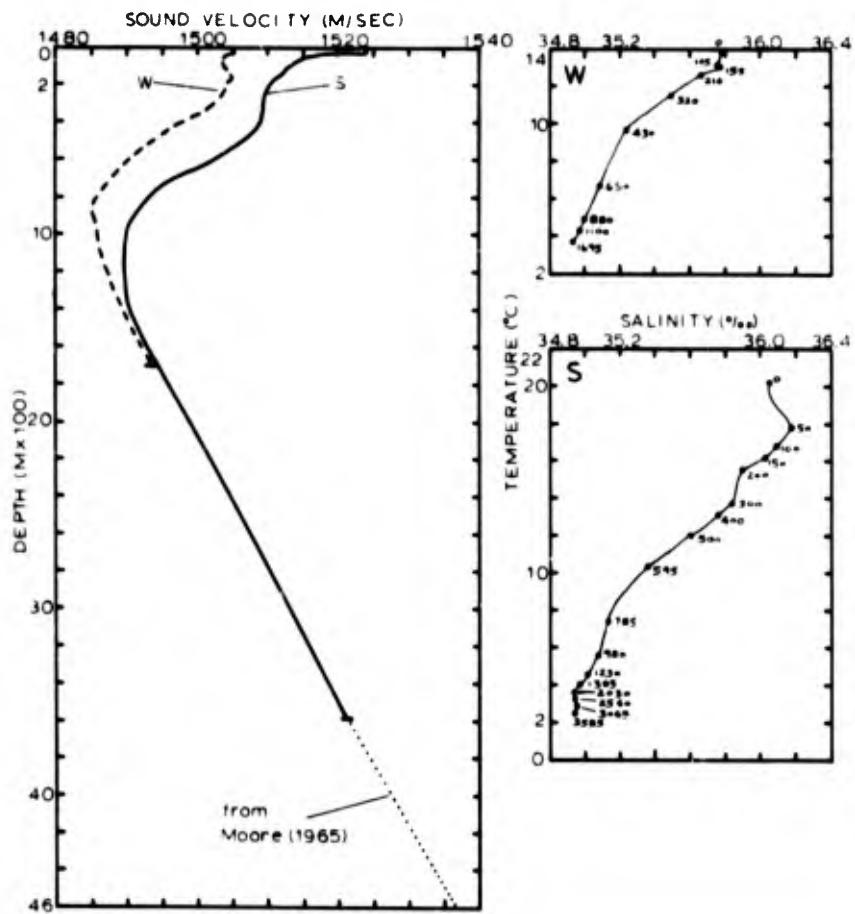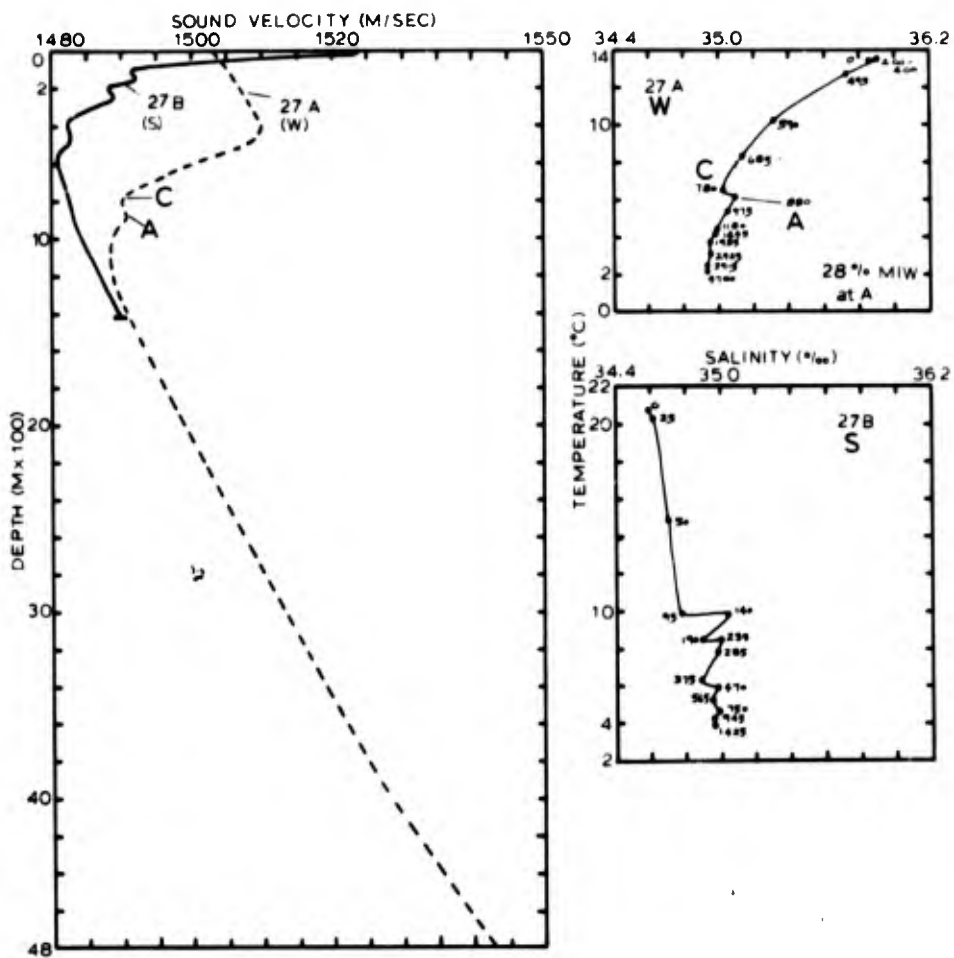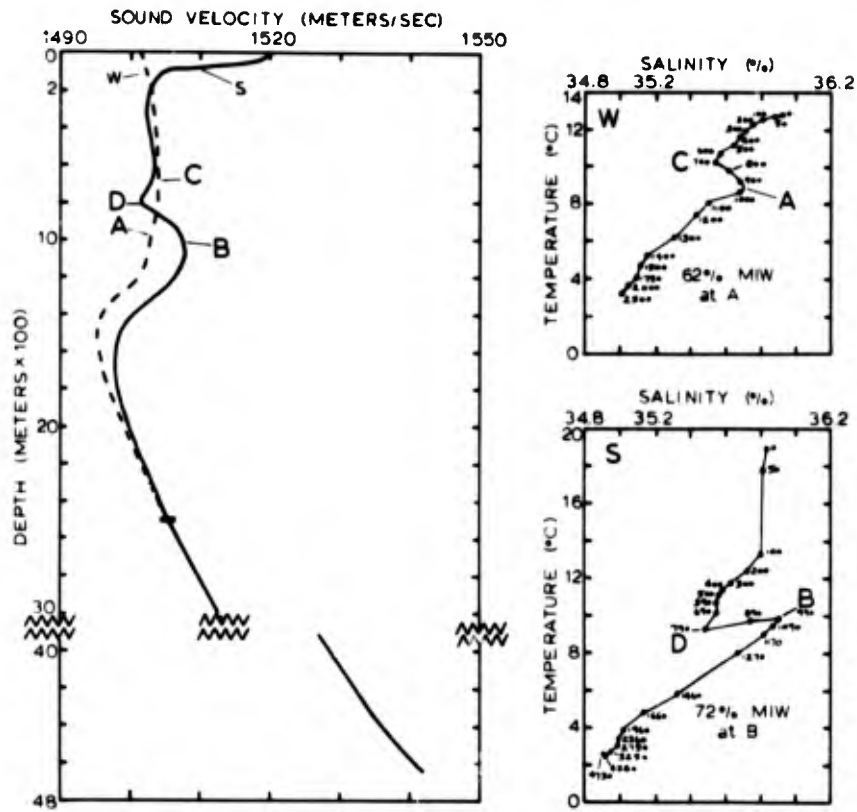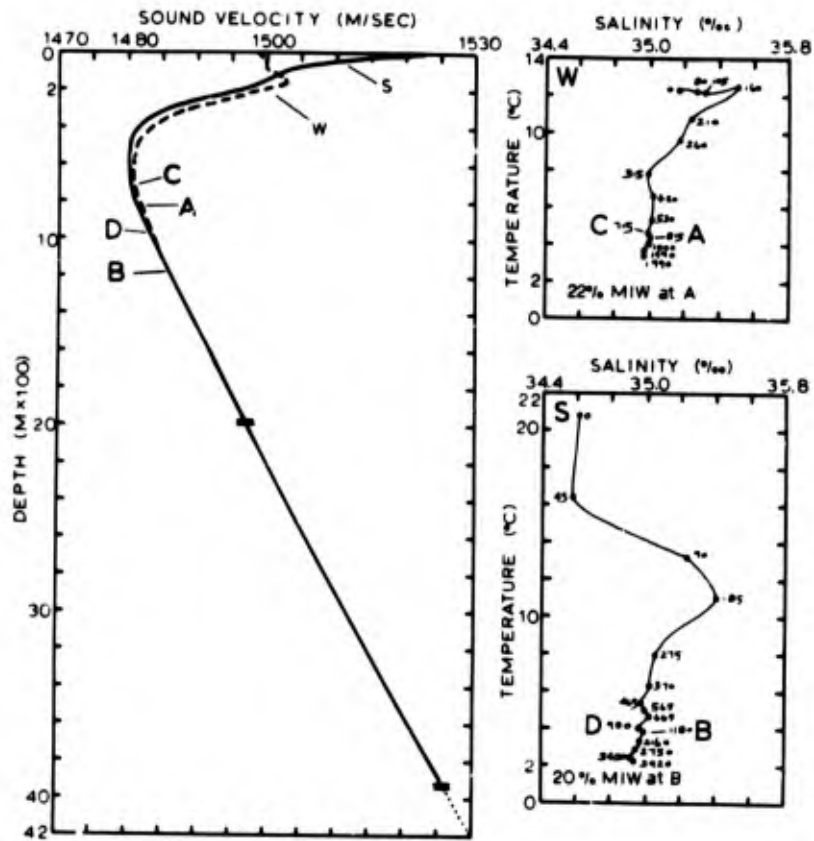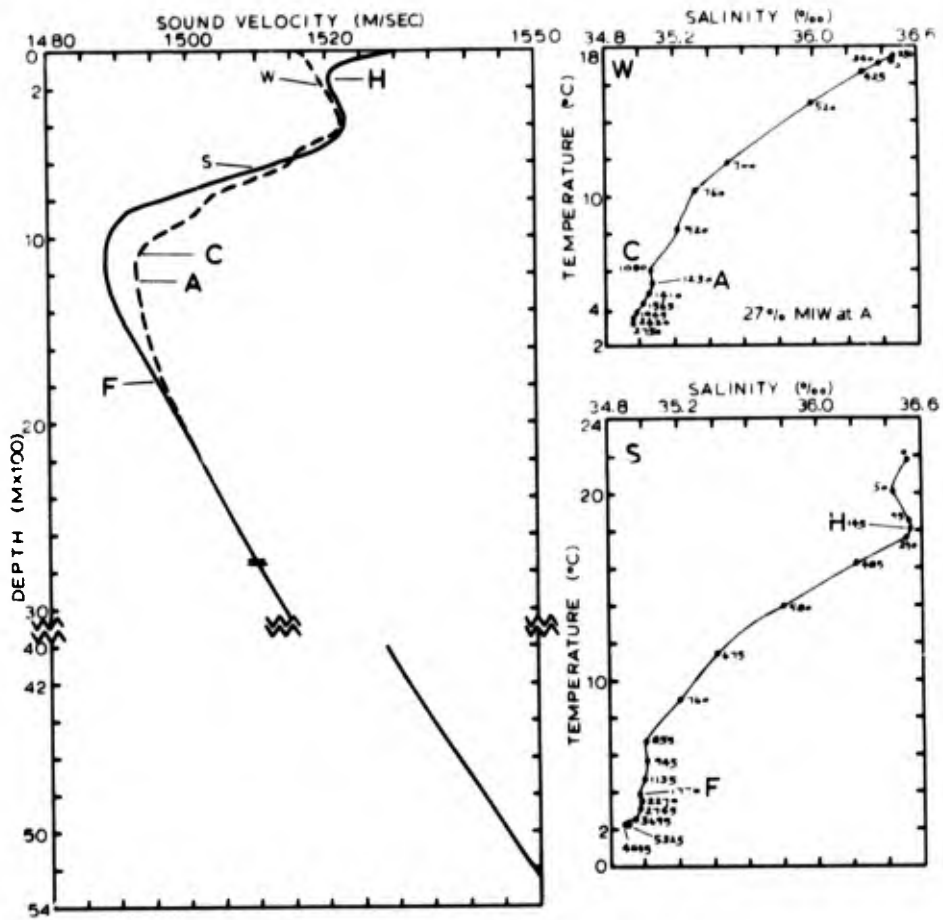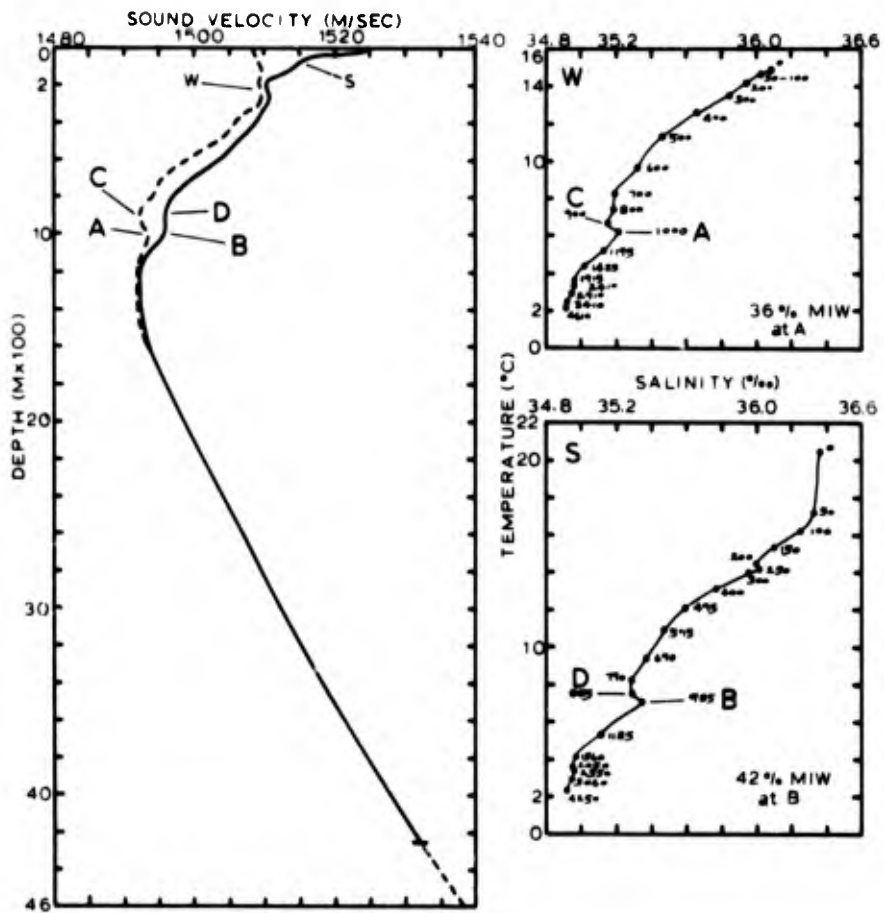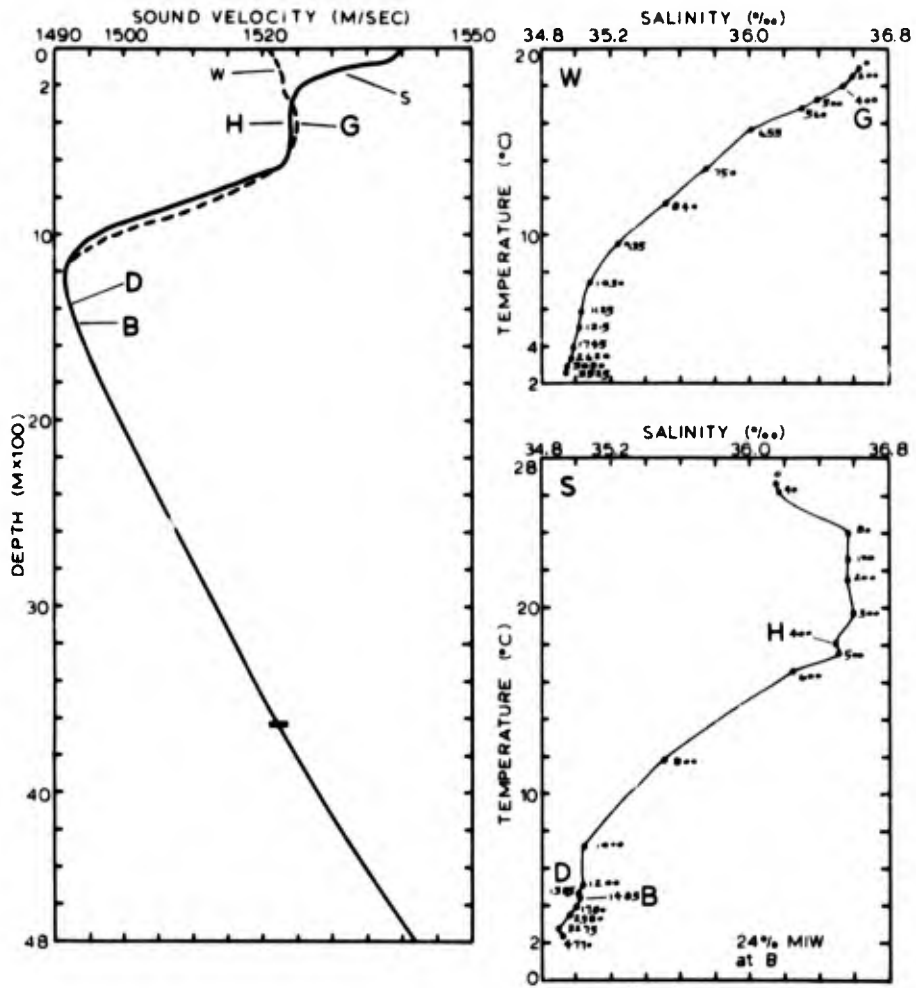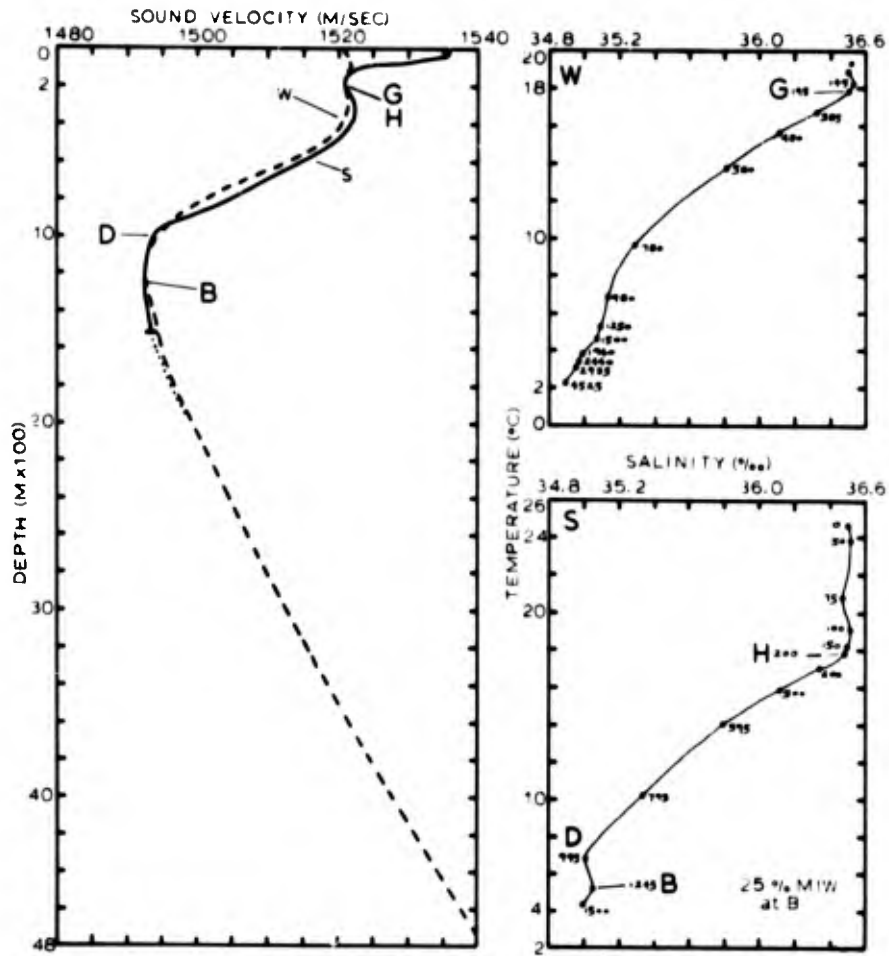FIGURE B-2. LOCATION OF SELECTED SOUND VELOCITY/T-S COMPARISONS (FIGURES B-3 THROUGH B-52).

50
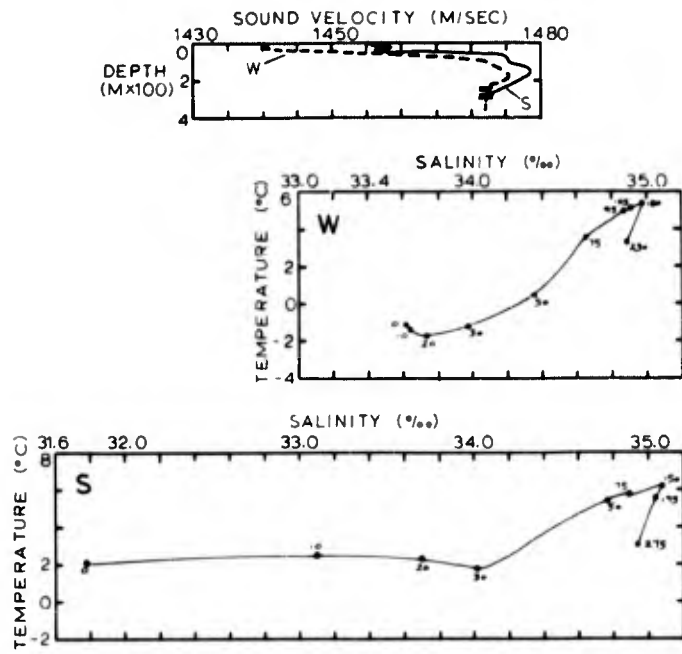
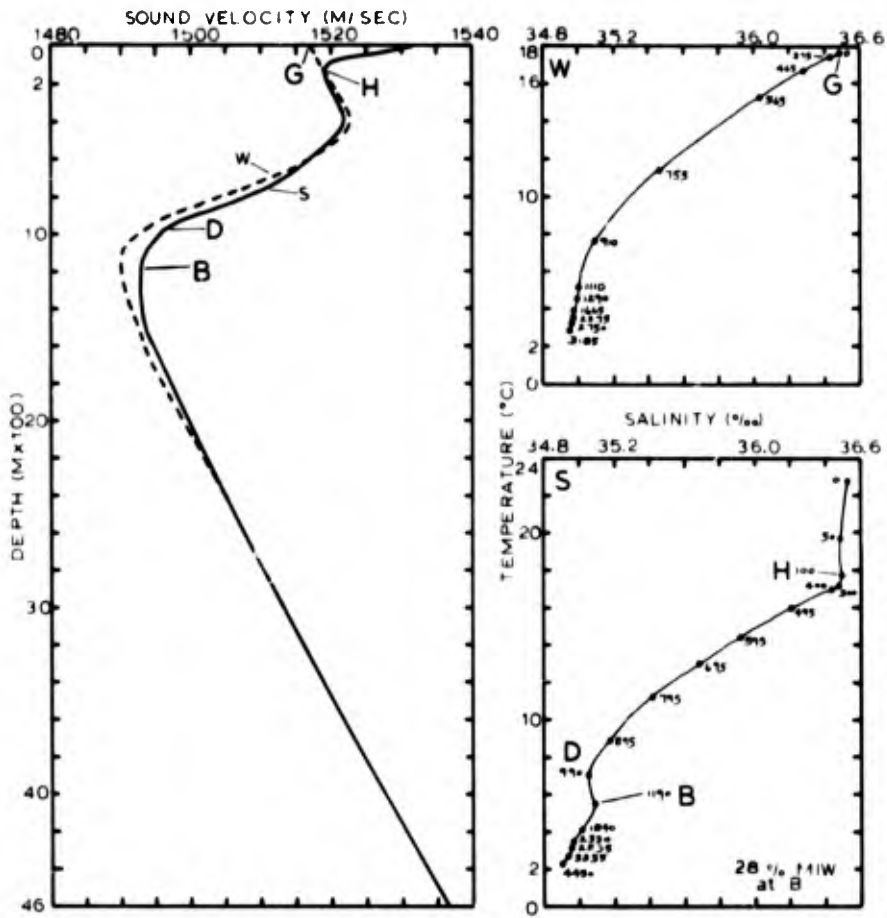FIGURE B-3. SELECTED SOUND VELOCITY/T-S COMPARISONS.
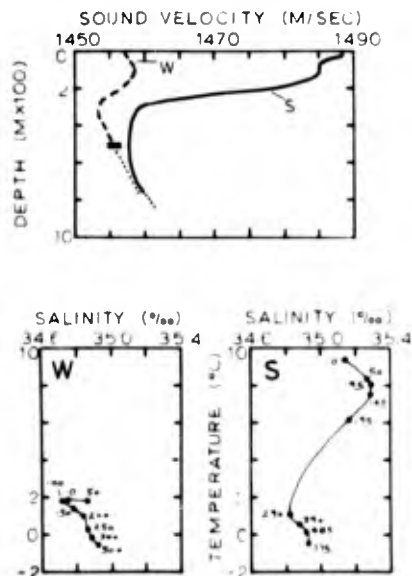
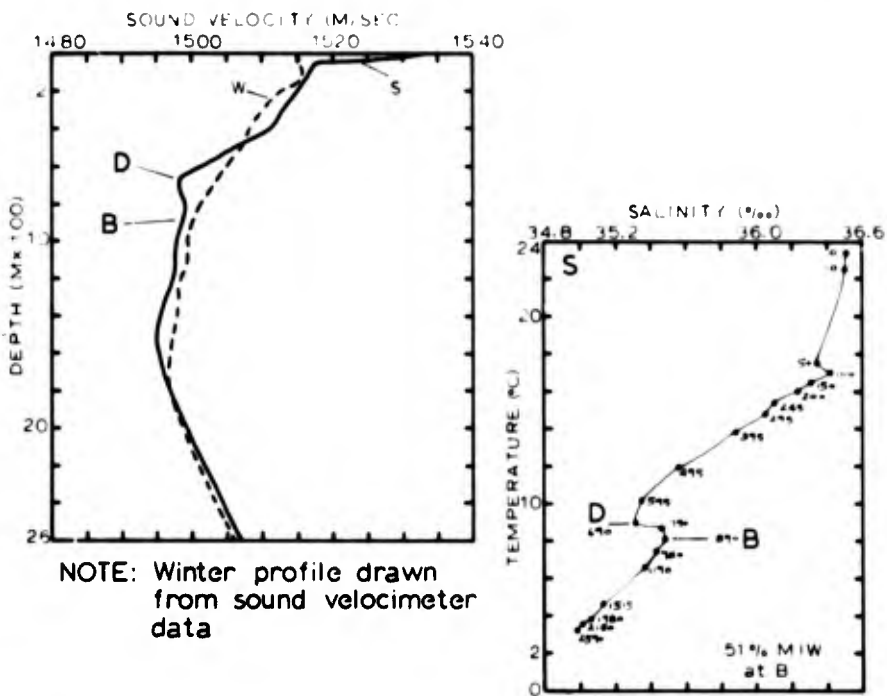FIGURE B-4. SELECTED SOUND VELOCITY/T-S COMPARISONS.

51
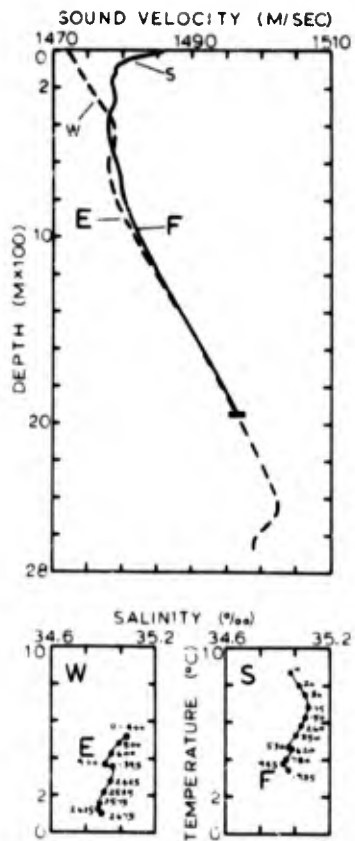
FIGURE B-5. SELECTED SOUND VELOCITY/T-S COMPARISONS.
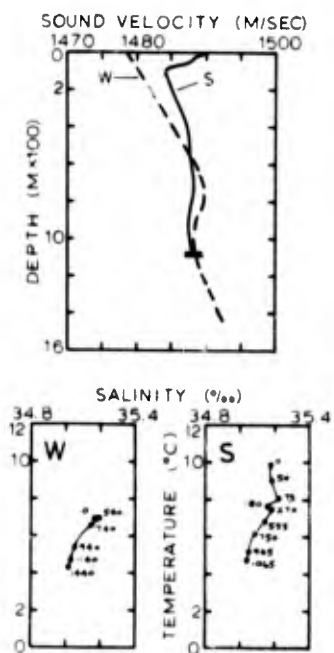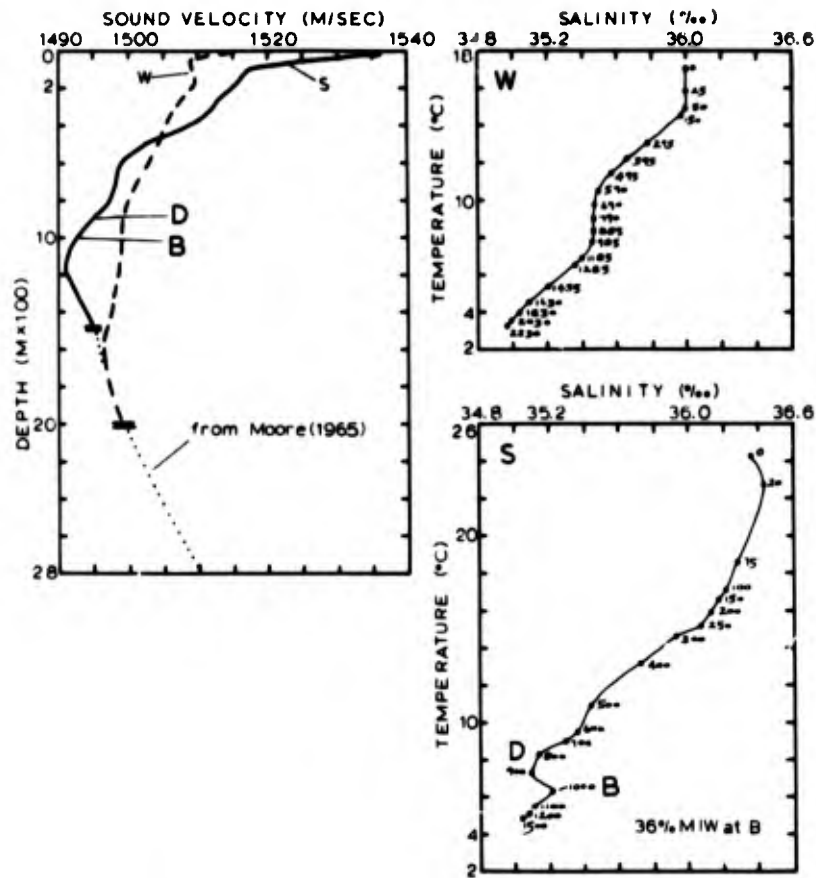

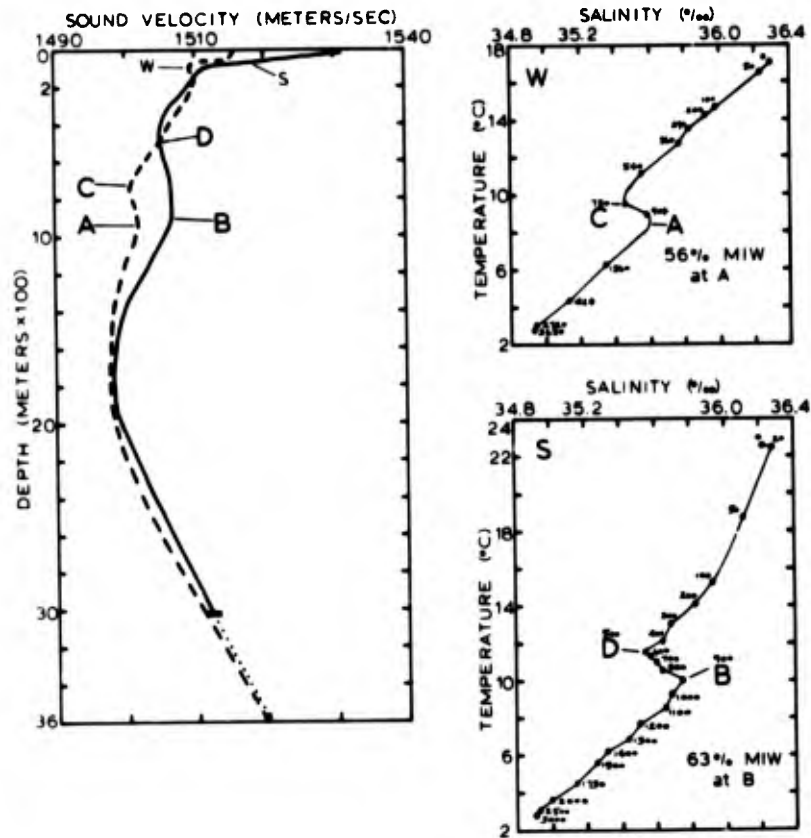FIGURE B-6. SELECTED SOUND VELOCITY/T-S COMPARISONS.

52
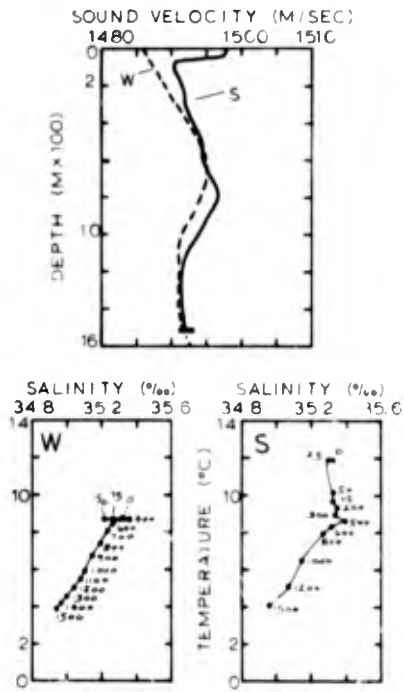
FIGURE B-7. SELECTED SOUND VELOCITY/T-S COMPARISONS.
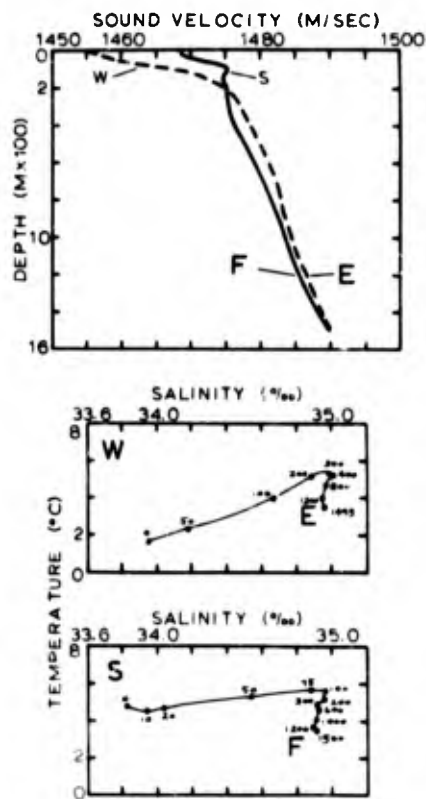
FIGURE B-8. SELECTED SOUND VELOCITY/T-S COMPARISONS.

53

FIGURE B-10. SELECTED SOUND VELOCITY/T-S COMPARISONS.

FIGURE B-9. SELECTED SOUND VELOCITY/T-S COMPARISONS.

54
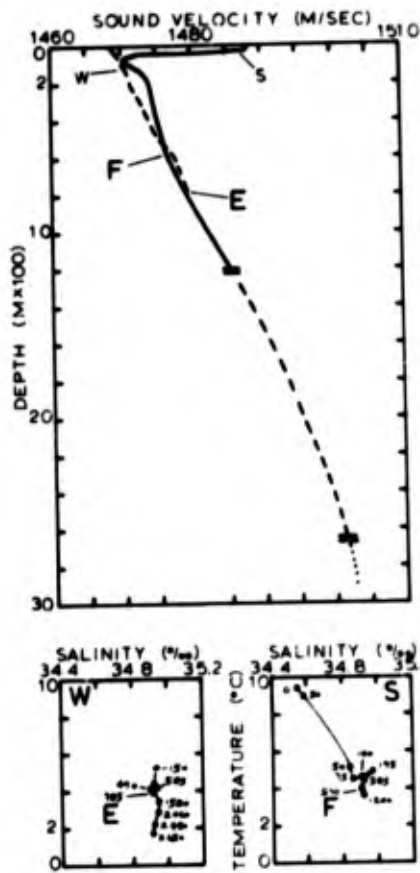
FIGURE B-11. SELECTED SOUND VELOCITY/T-S COMPARISONS.
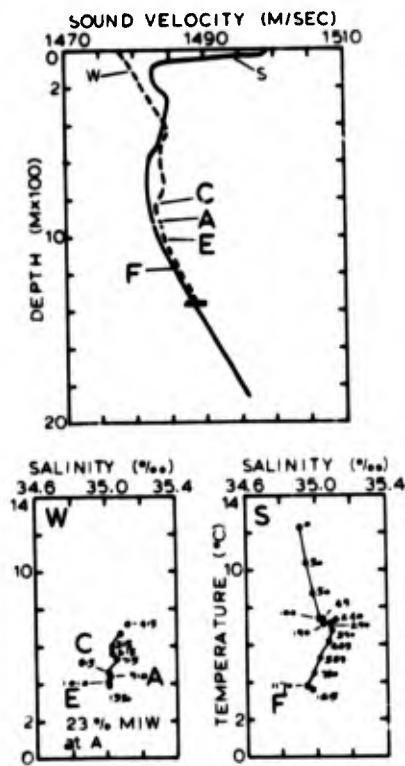
FIGURE B-12. SELECTED SOUND VELOCITY/T-S COMPARISONS.
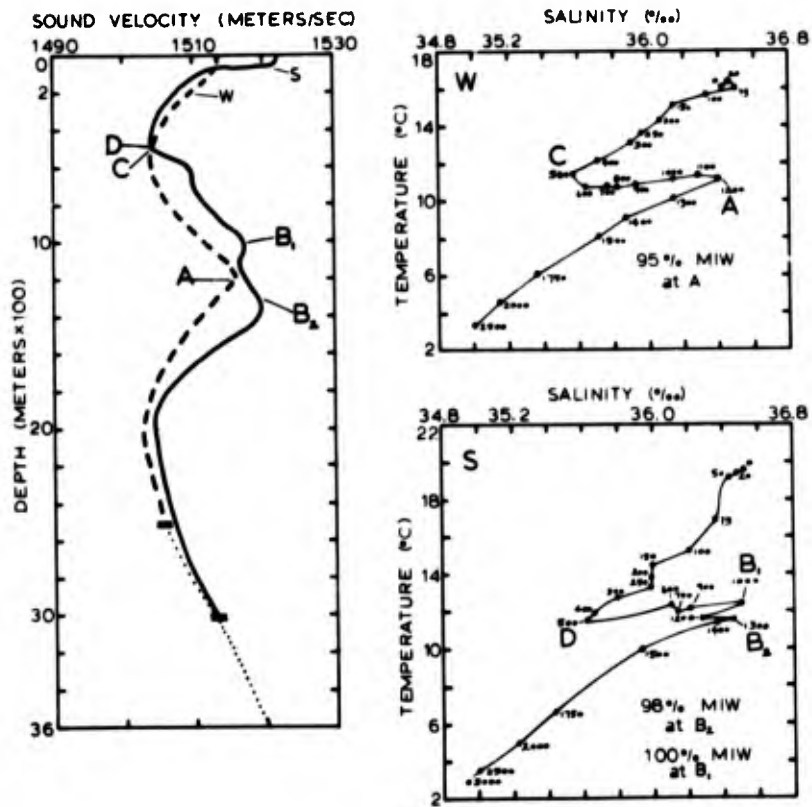
55

FIGURE B-14. SELECTED SOUND VELOCITY/T-S COMPARISONS.

FIGURE B-13. SELECTED SOUND VELOCITY/T-S COMPARISONS.

FIGURE B-16. SELECTED SOUND VELOCITY/T-S COMPARISONS.

FIGURE B-15. SELECTED SOUND VELOCITY/T-S COMPARISONS.
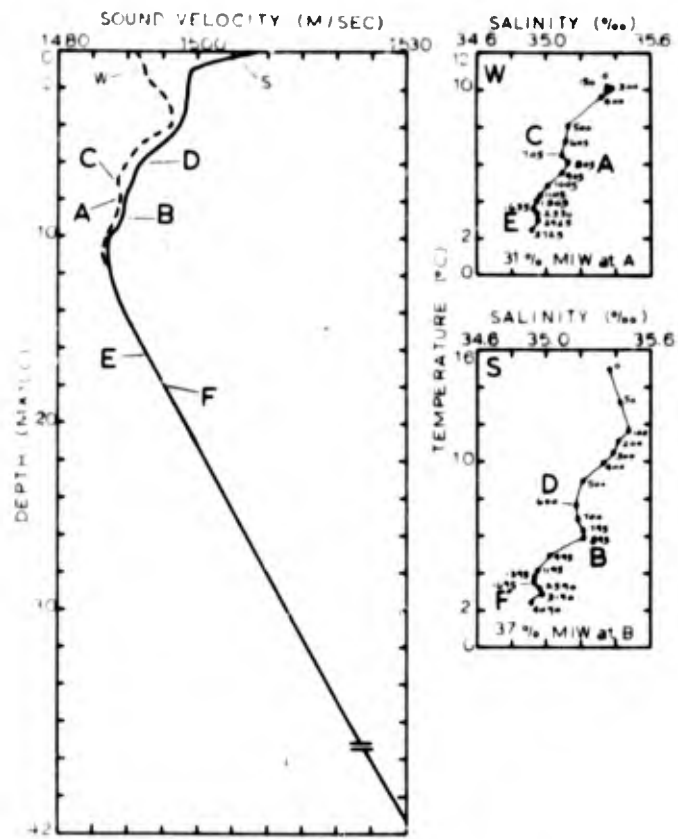
FIGURE B-17. SELECTED SOUND VELOCITY/T-S COMPARISONS.
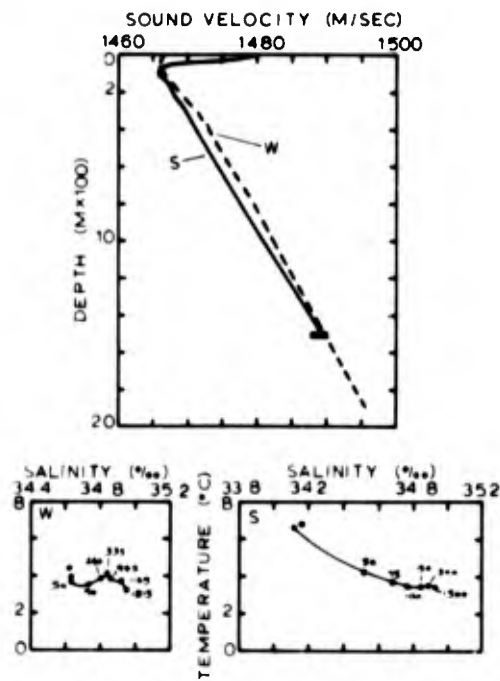
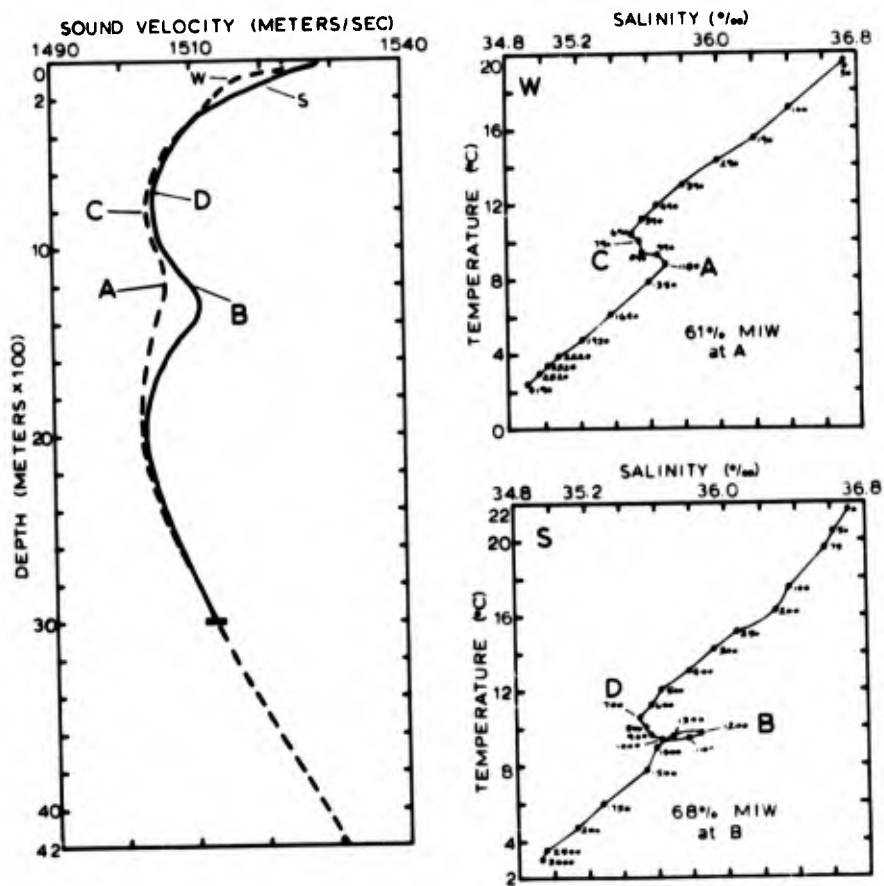FIGURE B-18. SELECTED SOUND VELOCITY/T-S COMPARISONS.
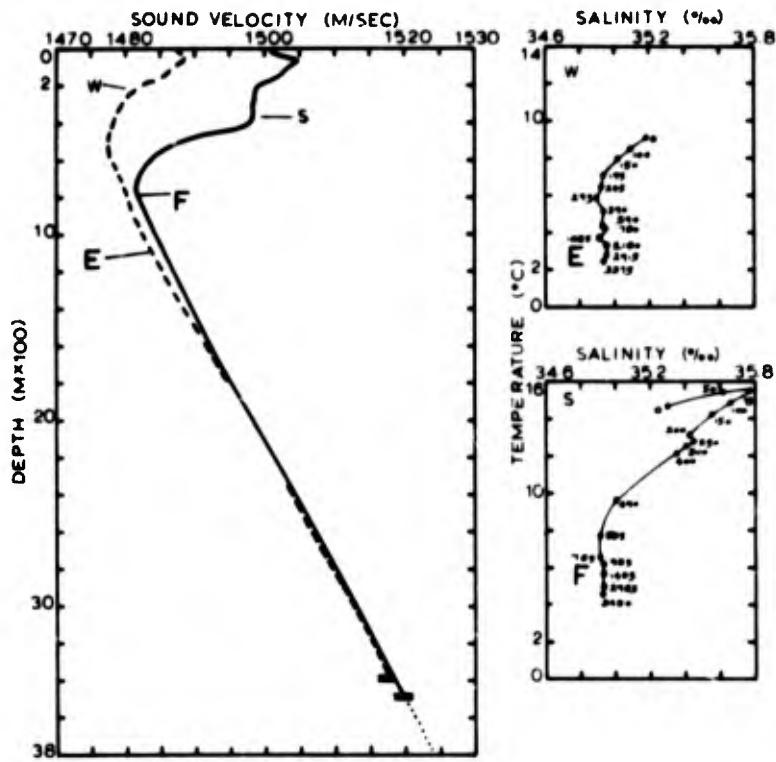
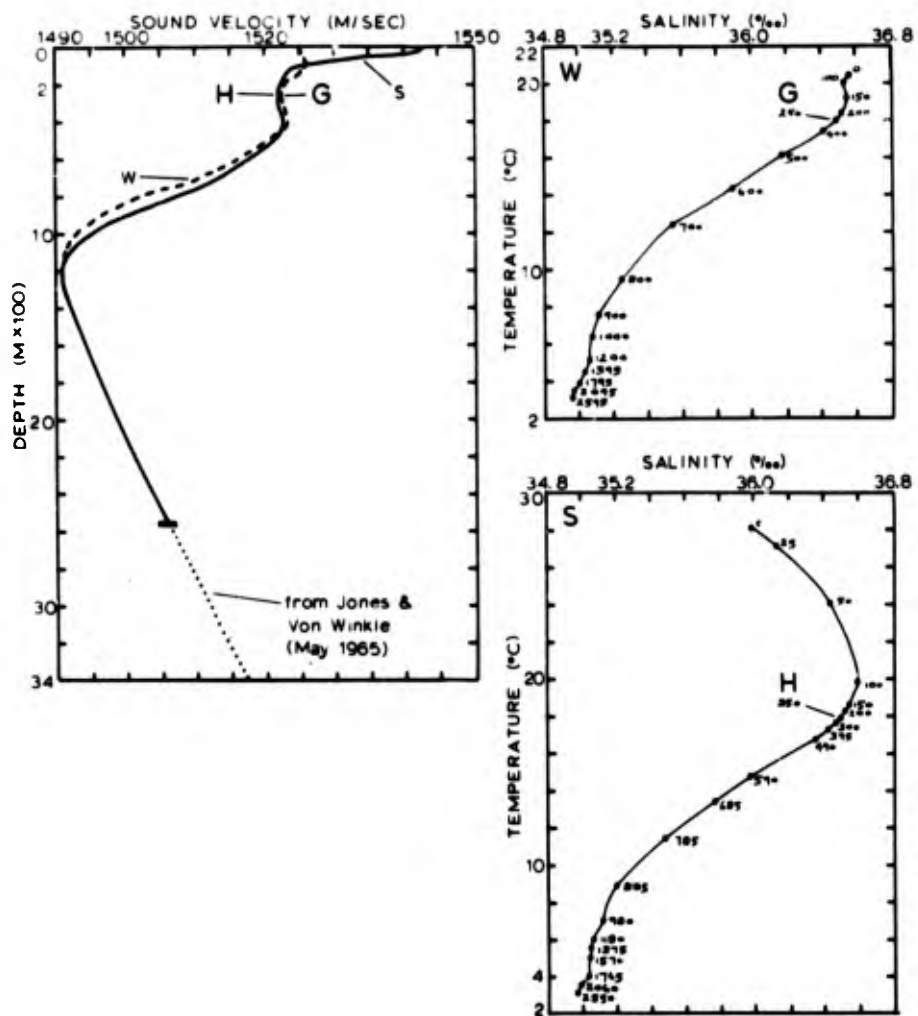FIGURE B-19. SELECTED SOUND VELOCITY/T-S COMPARISONS.
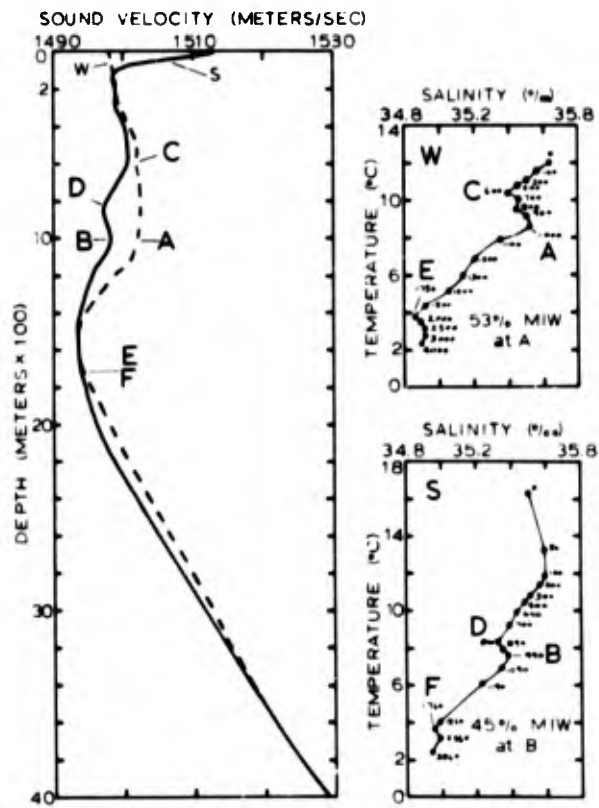
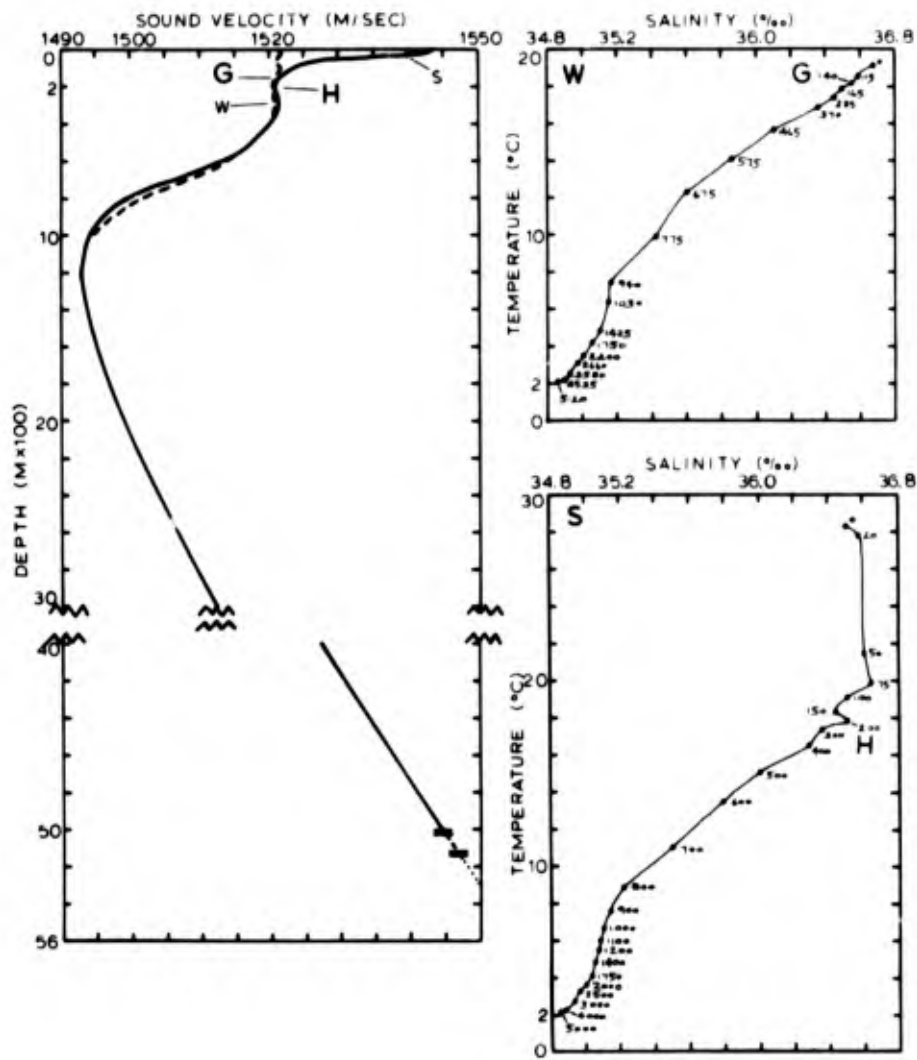FIGURE B-20. SELECTED SOUND VELOCITY/T-S COMPARISONS.
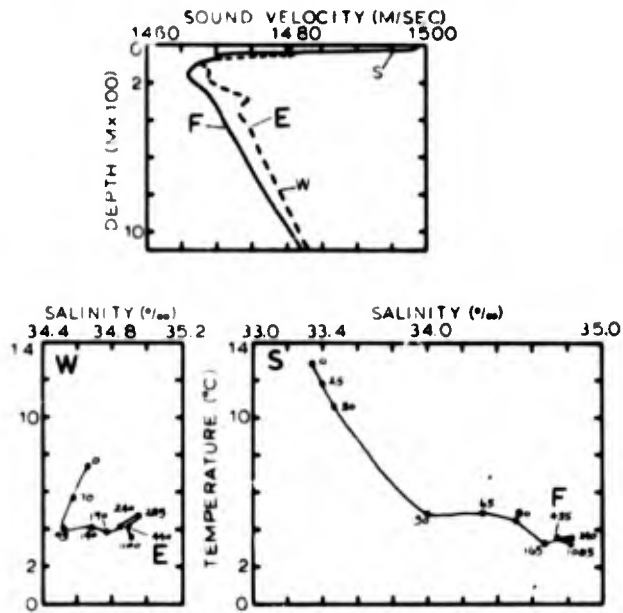
FIGURE B-21. SELECTED SOUND VELOCITY/T-S COMPARISONS.
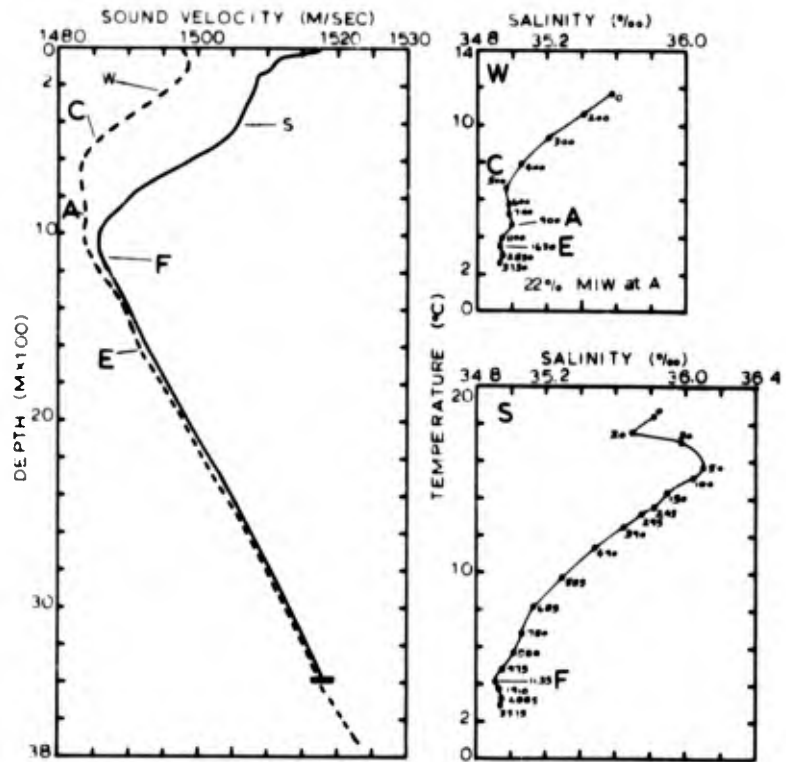
FIGURE B-22. SELECTED SOUND VELOCITY/T-S COMPARISONS.

FIGURE B-24. SELECTED SOUND VELOCITY/T-S COMPARISONS.

FIGURE B-23. SELECTED SOUND VELOCITY/T-S COMPARISONS.
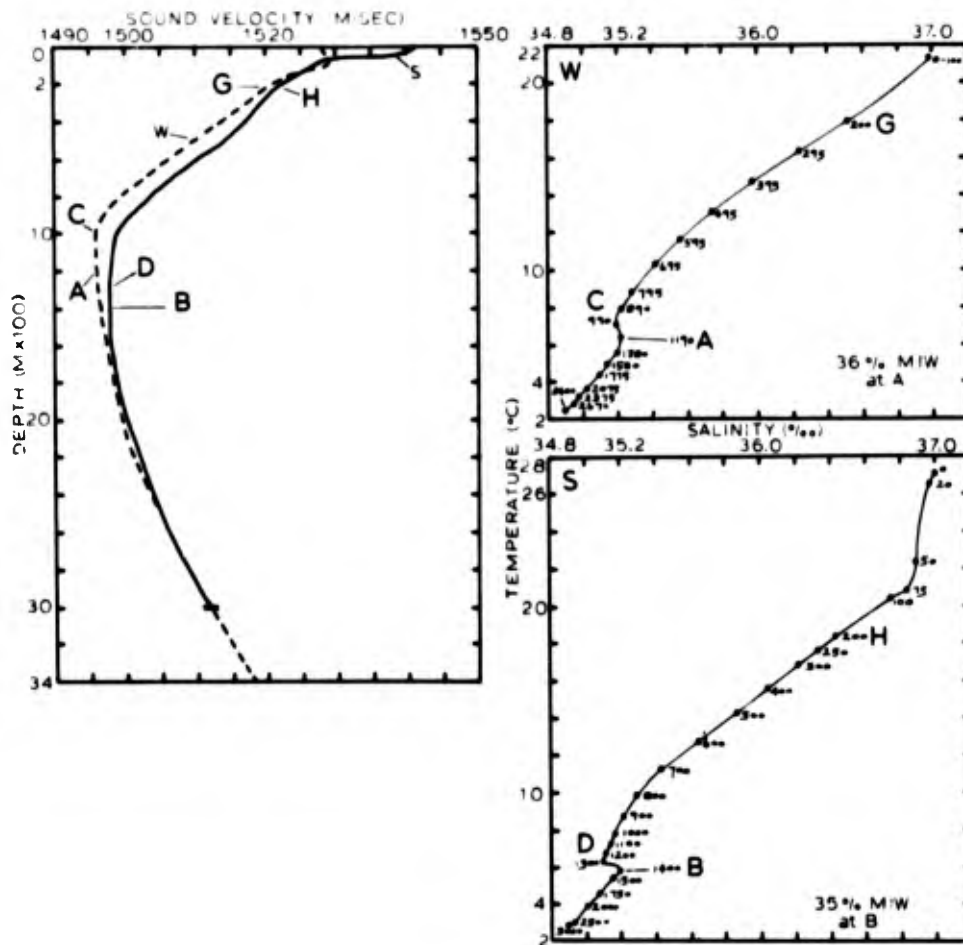
FIGURE B-25. SELECTED SOUND VELOCITY/T-S COMPARISONS.

FIGURE B-26. SELECTED SOUND VELOCITY/T-S COMPARISONS.

FIGURE B-27. SELECTED SOUND VELOCITY/T-S COMPARISONS.
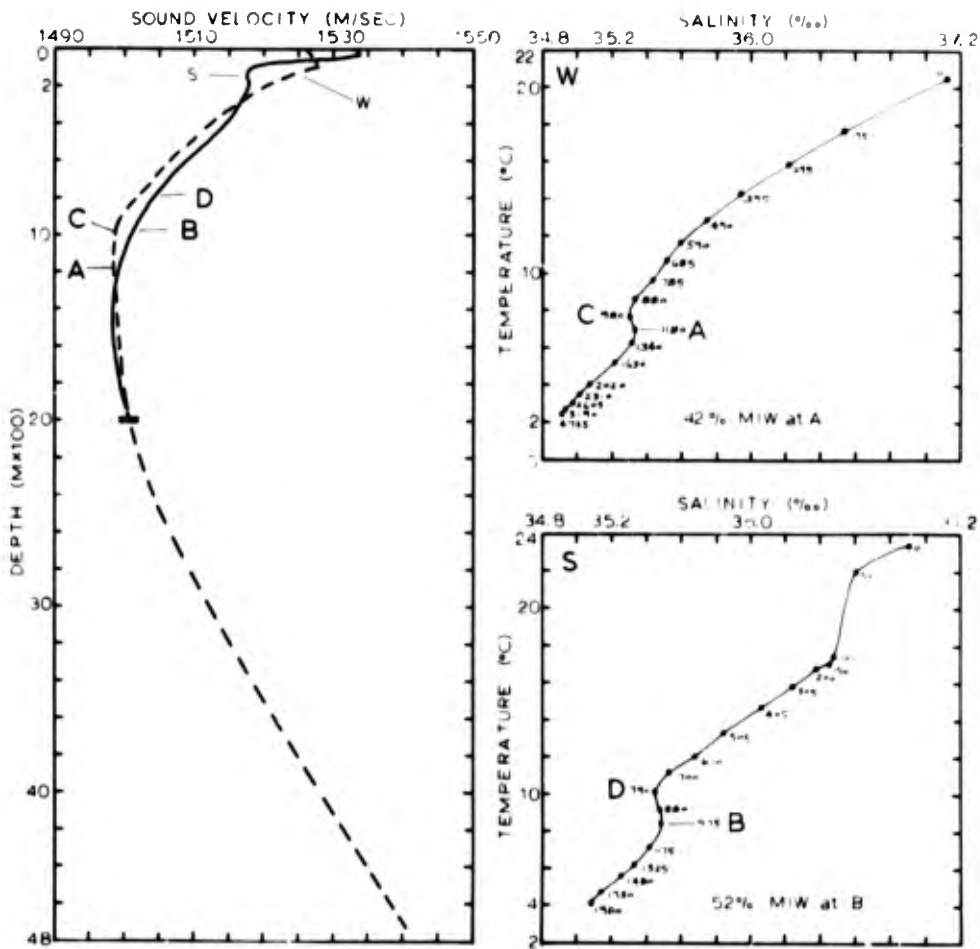
64

FIGURE B-27 A & B. SELECTED SOUND VELOCITY/T-S COMPARISONS.

FIGURE B-28. SELECTED SOUND VELOCITY/T-S COMPARISONS.

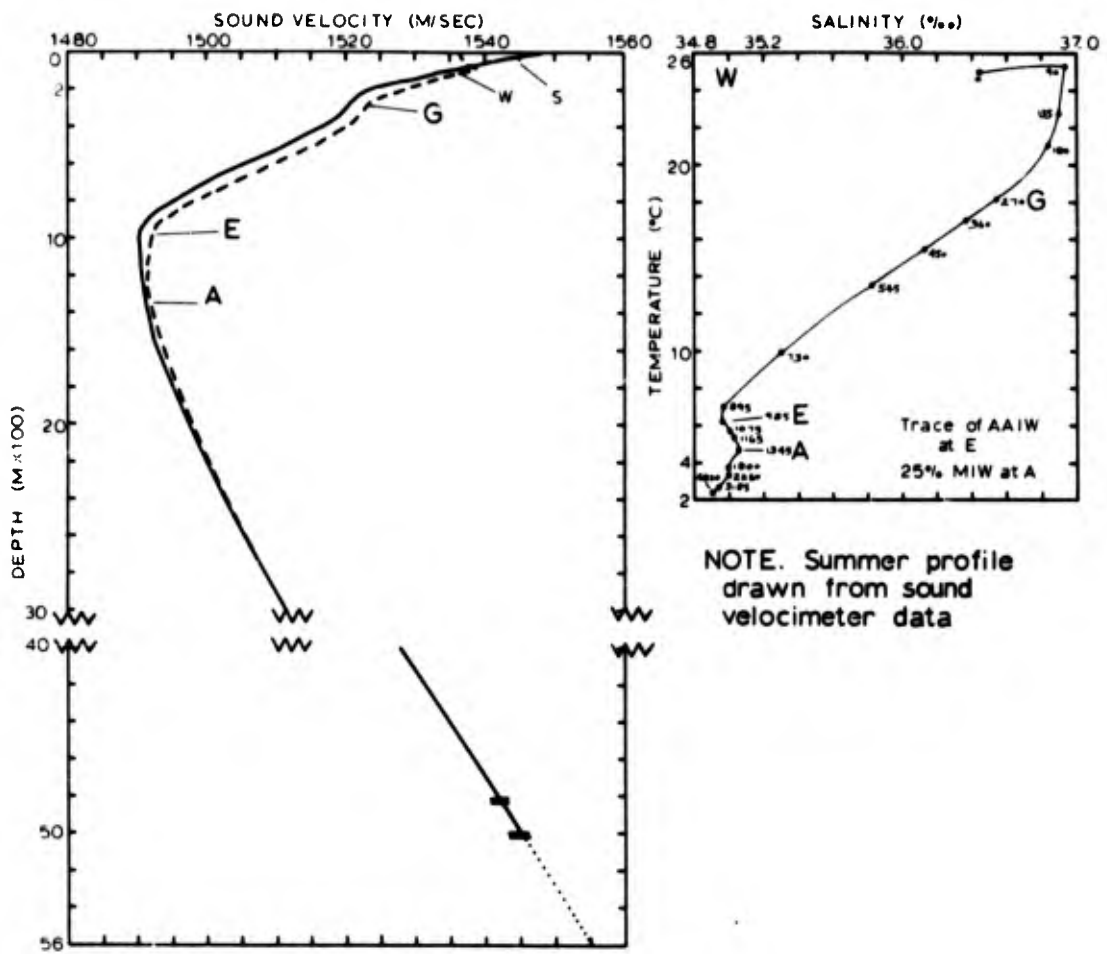FIGURE B-29. SELECTED SOUND VELOCITY/T-S COMPARISONS.

66

FIGURE B-30. SELECTED SOUND VELOCITY/T-S COMPARISONS.

FIGURE B-31. SELECTED SOUND VELOCITY/T-S COMPARISONS.

FIGURE B-32. SELECTED SOUND VELOCITY/T-S COMPARISONS.

FIGURE B-33.   SELECTED SOUND VELOCITY/T-S COMPARISONS.

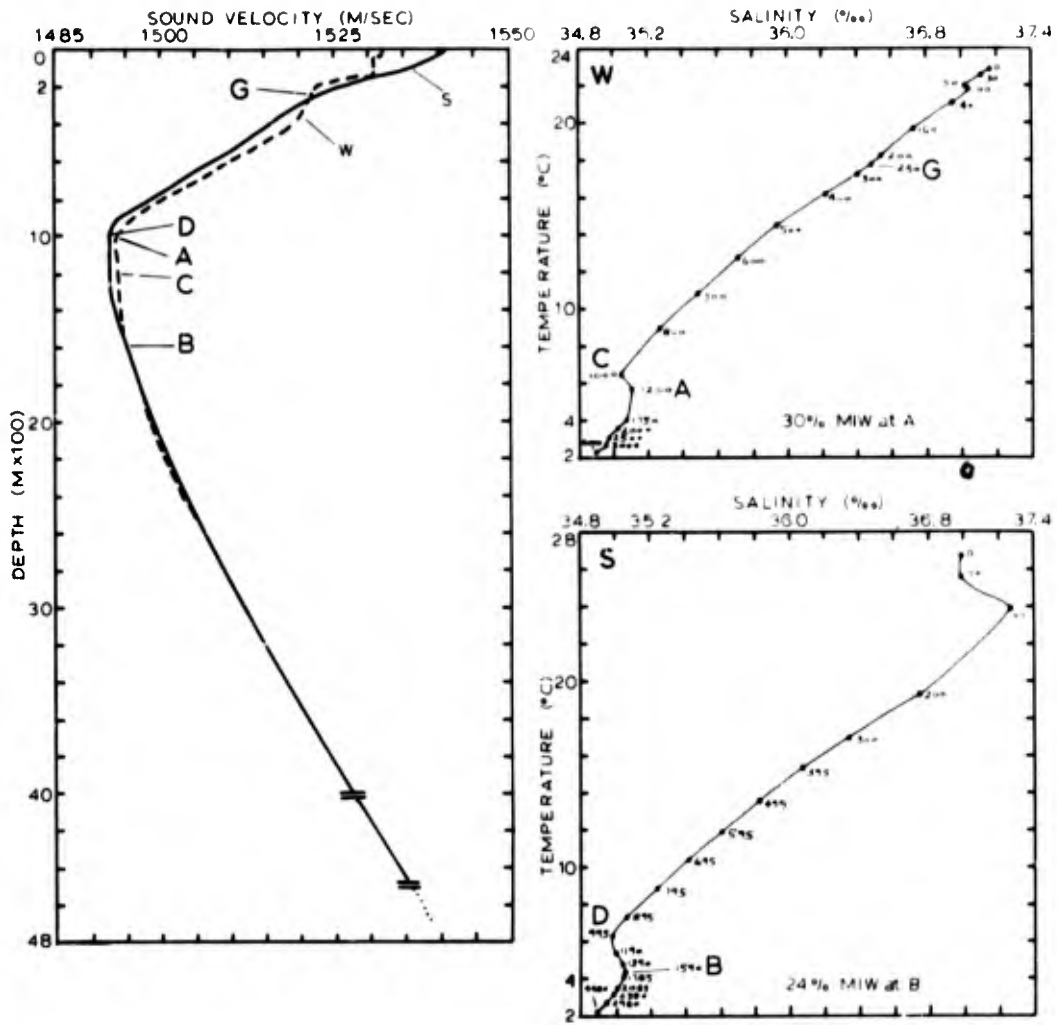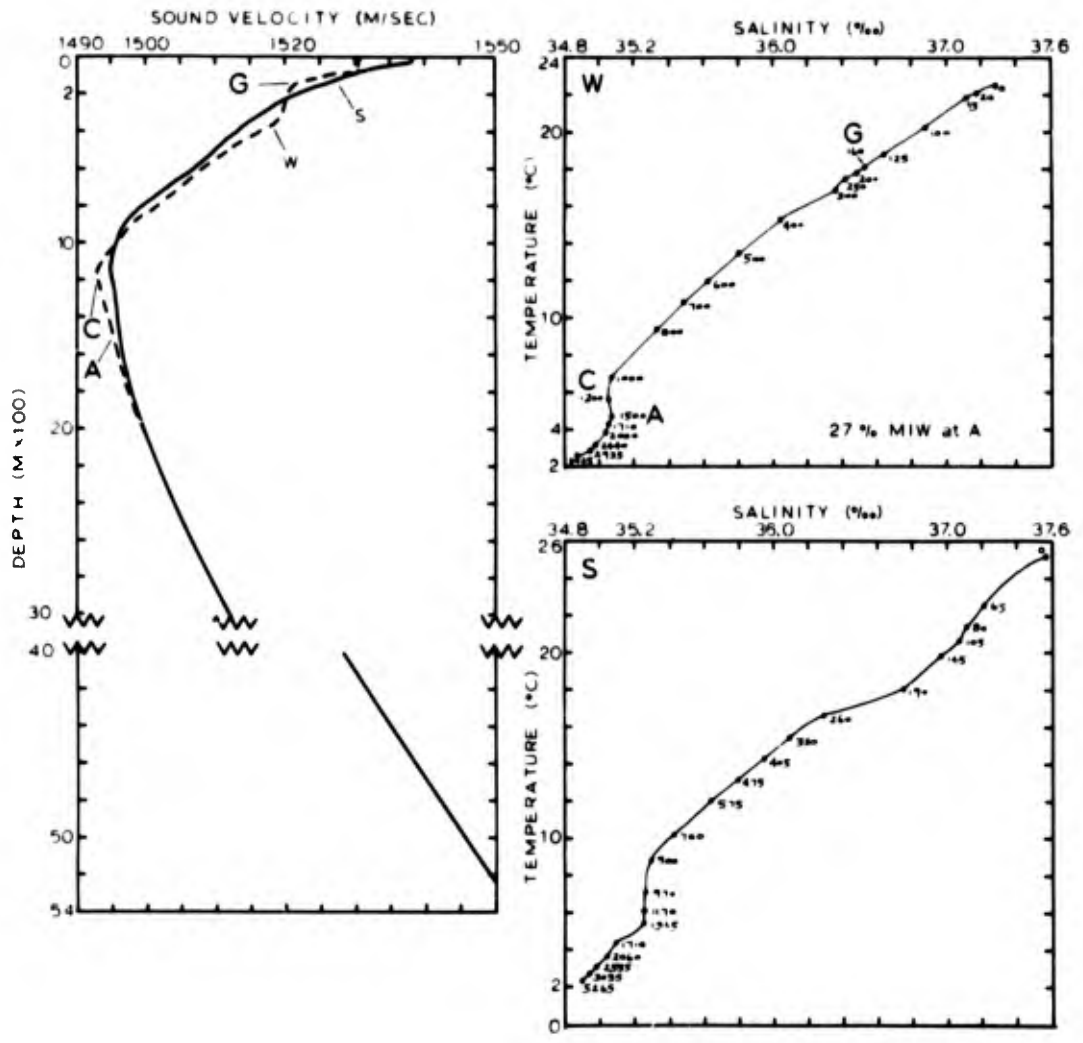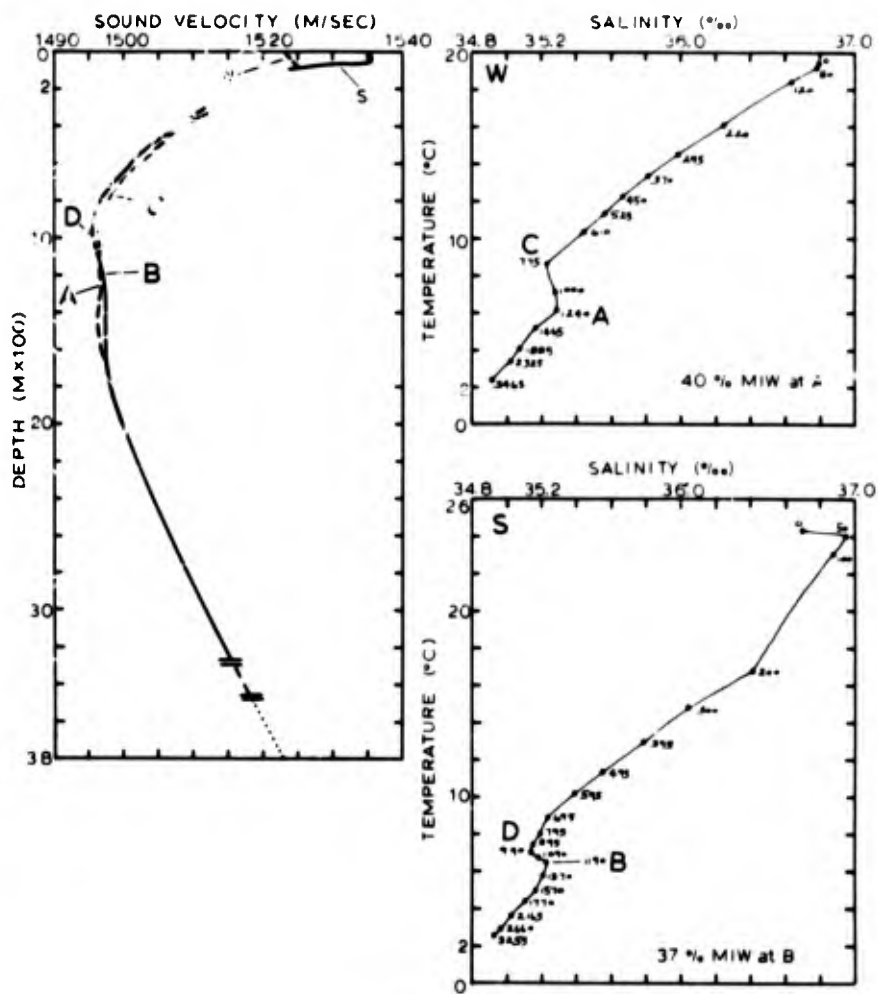FIGURE B-34.   SELECTED SOUND VELOCITY/T-S COMPARISONS.

NOTE: Winter profile drawn
        from sound velocimeter
        data

FIGURE B-35.   SELECTED SOUND VELOCITY/T-S COMPARISONS.

71

FIGURE B-36. SELECTED SOUND VELOCITY/T-S COMPARISONS.

FIGURE B-37. SELECTED SOUND VELOCITY/T-S COMPARISONS.

72

FIGURE B-38. SELECTED SOUND VELOCITY/T-S COMPARISONS.

FIGURE B-39. SELECTED SOUND VELOCITY/T-S COMPARISONS.

FIGURE B-40. SELECTED SOUND VELOCITY/T-S COMPARISONS.

74

FIGURE B-41. SELECTED SOUND VELOCITY/T-S COMPARISONS.

FIGURE B-42. SELECTED SOUND VELOCITY/T-S COMPARISONS.

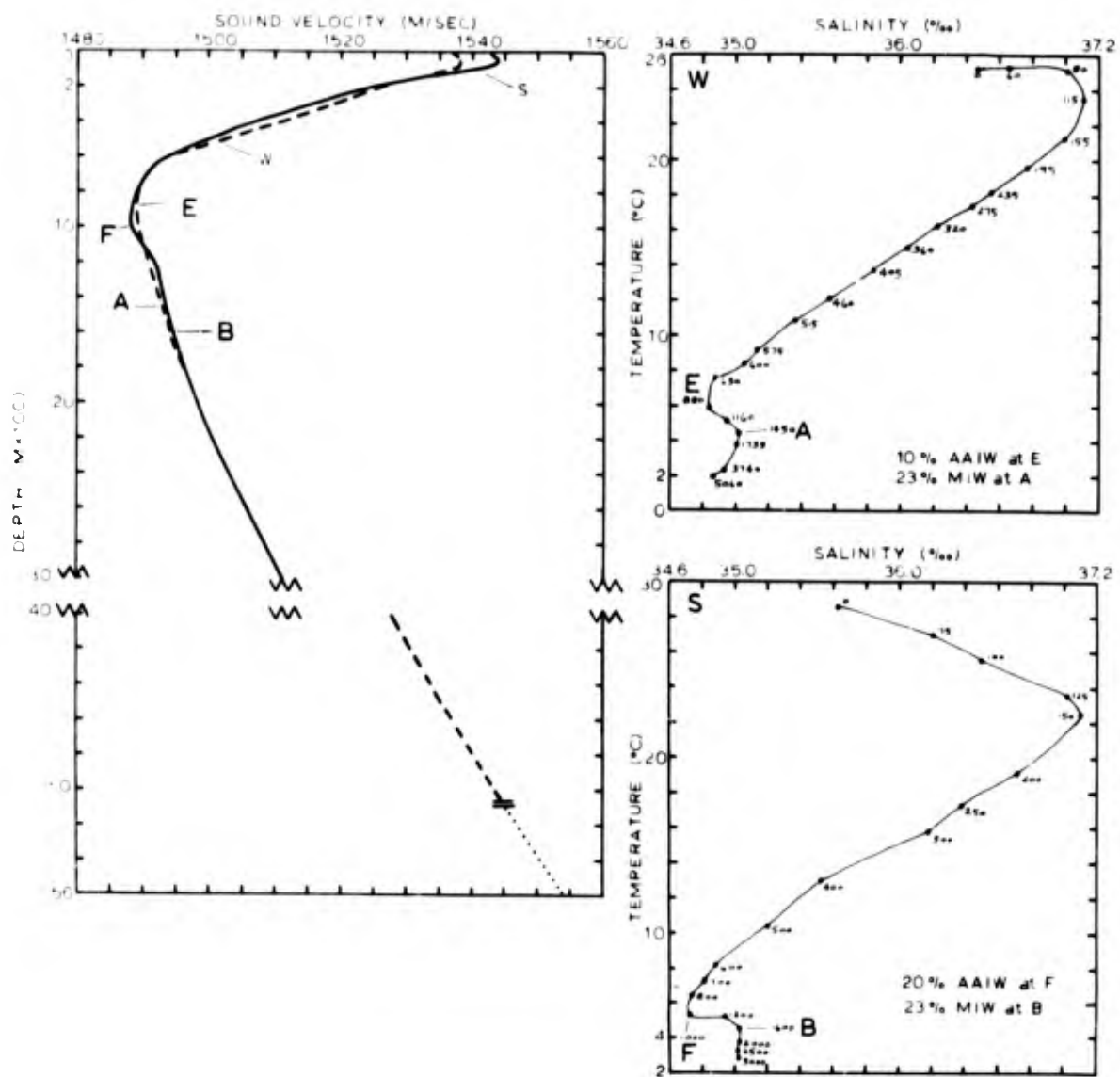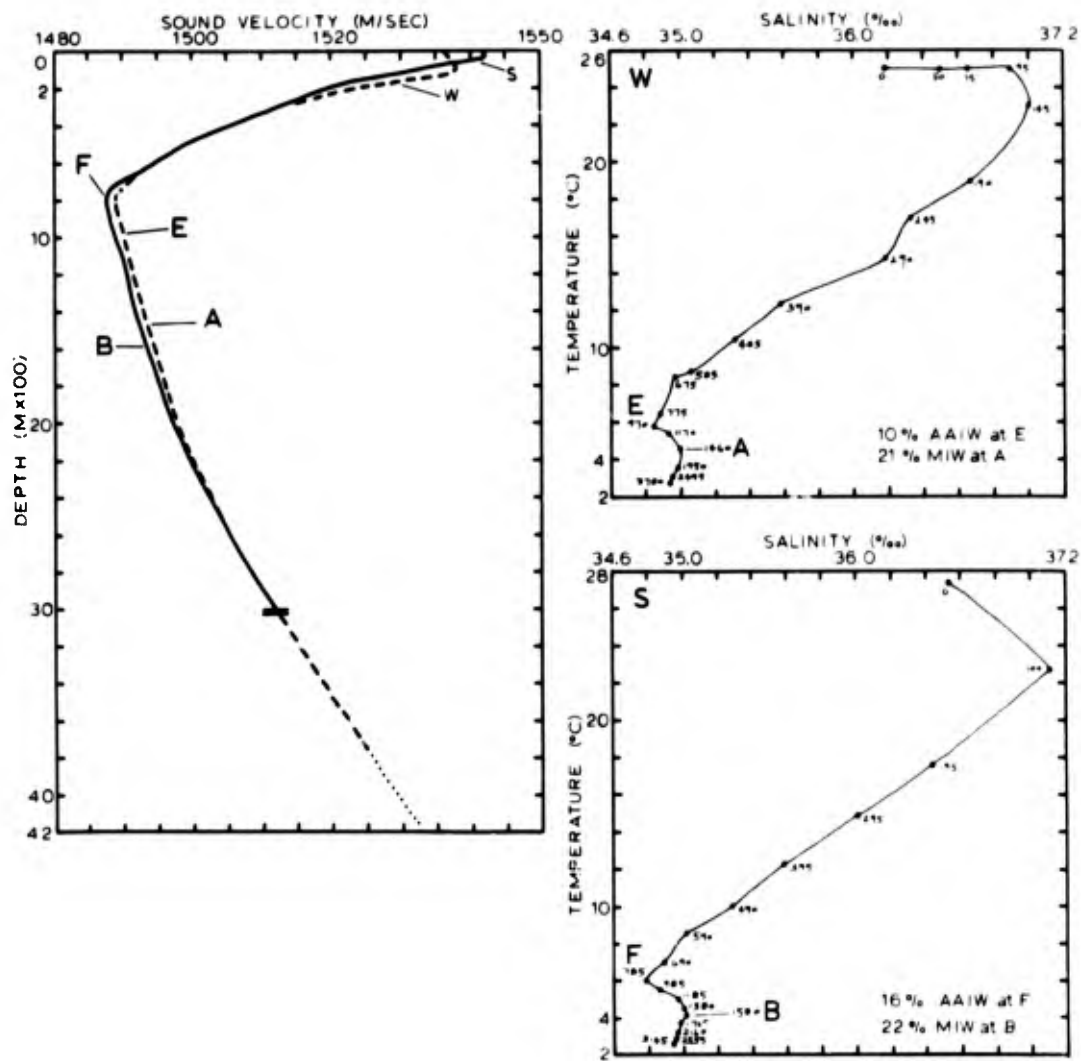FIGURE B-43. SELECTED SOUND VELOCITY/T-S COMPARISONS.

FIGURE B-44. SELECTED SOUND VELOCITY/T-S COMPARISONS.

FIGURE B-45. SELECTED SOUND VELOCITY/T-S COMPARISONS.

FIGURE B-46. SELECTED SOUND VELOCITY/T-S COMPARISONS.

FIGURE B-47. SELECTED SOUND VELOCITY/T-S COMPARISONS.

FIGURE B-48. SELECTED SOUND VELOCITY/T-S COMPARISONS.

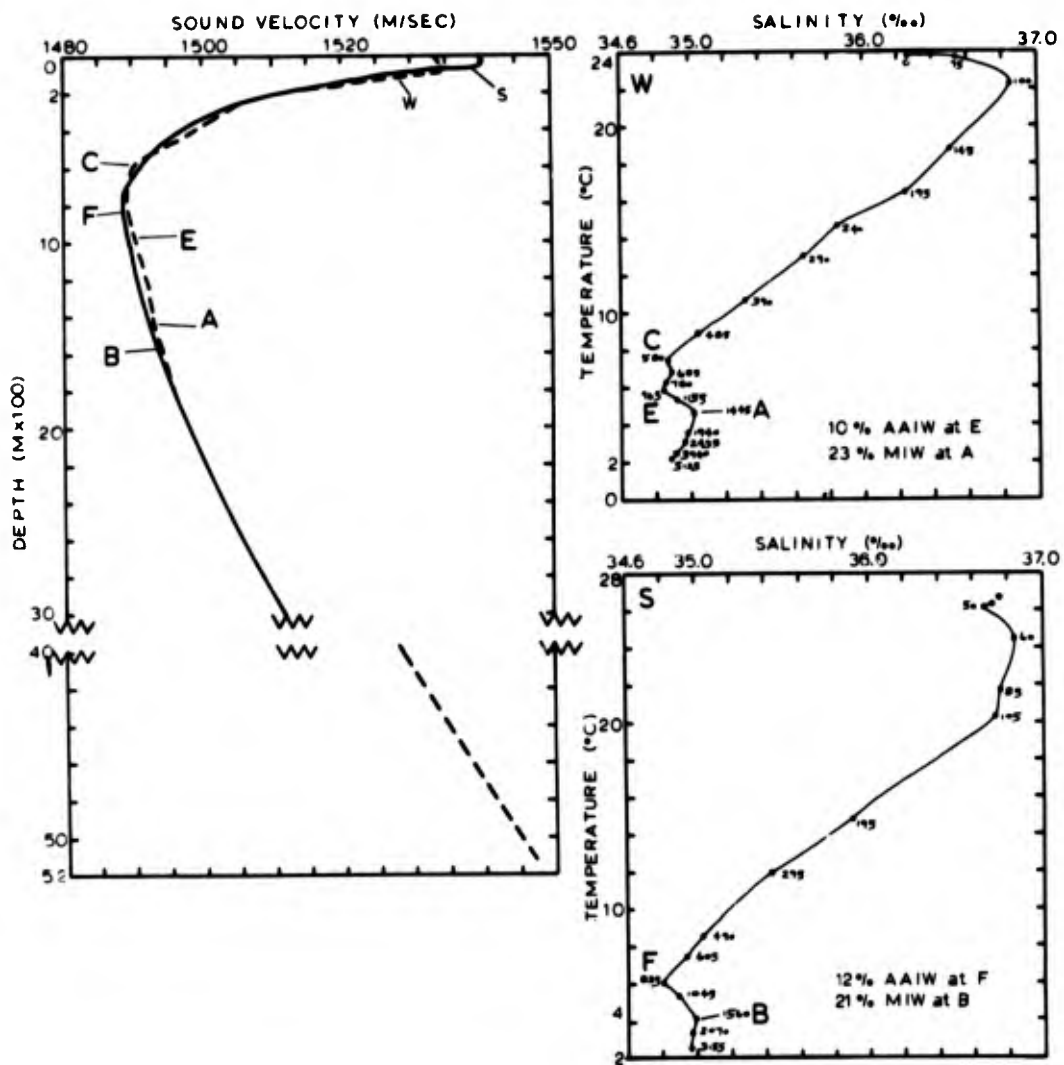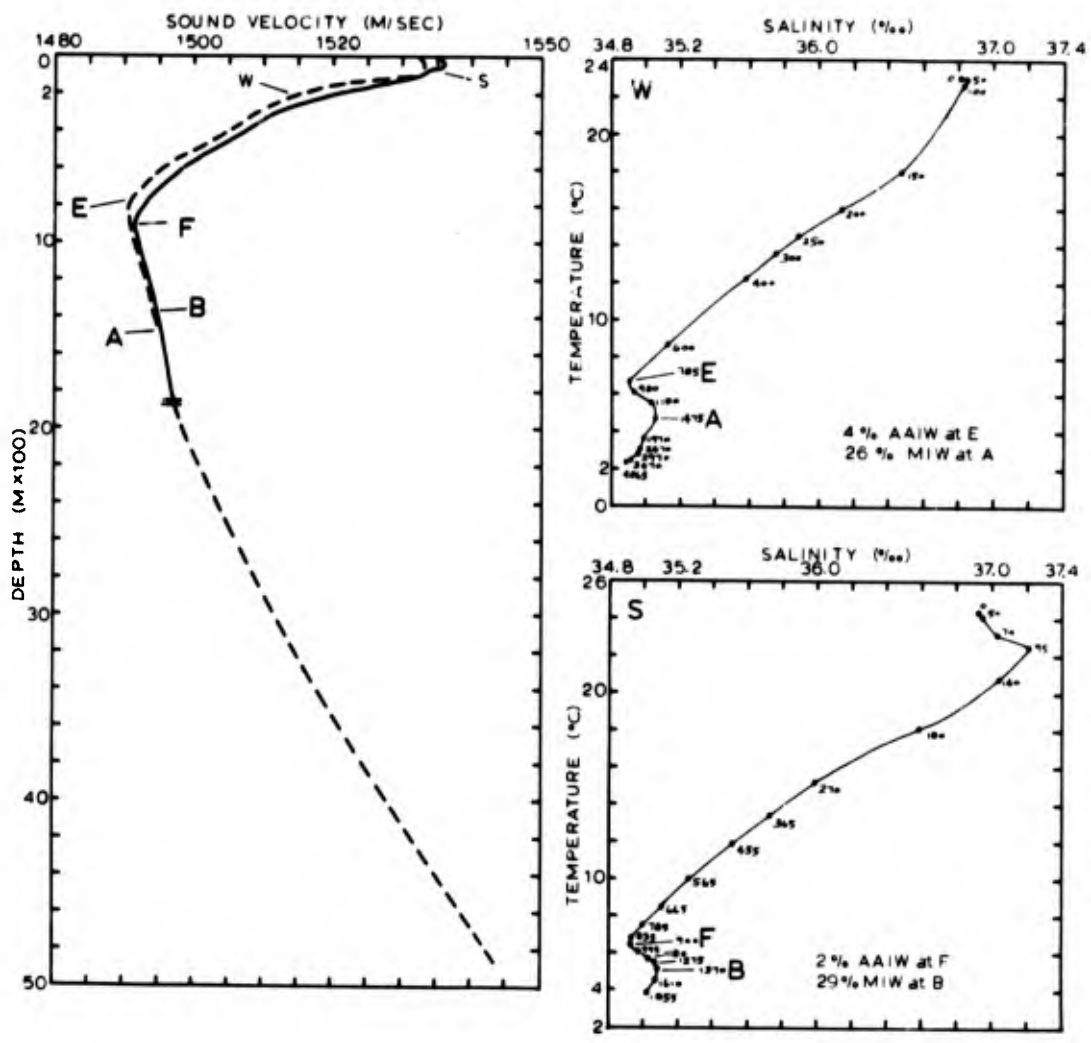FIGURE B-49. SELECTED SOUND VELOCITY/T-S COMPARISONS.

83

FIGURE B-50. SELECTED SOUND VELOCITY/T-S COMPARISONS.
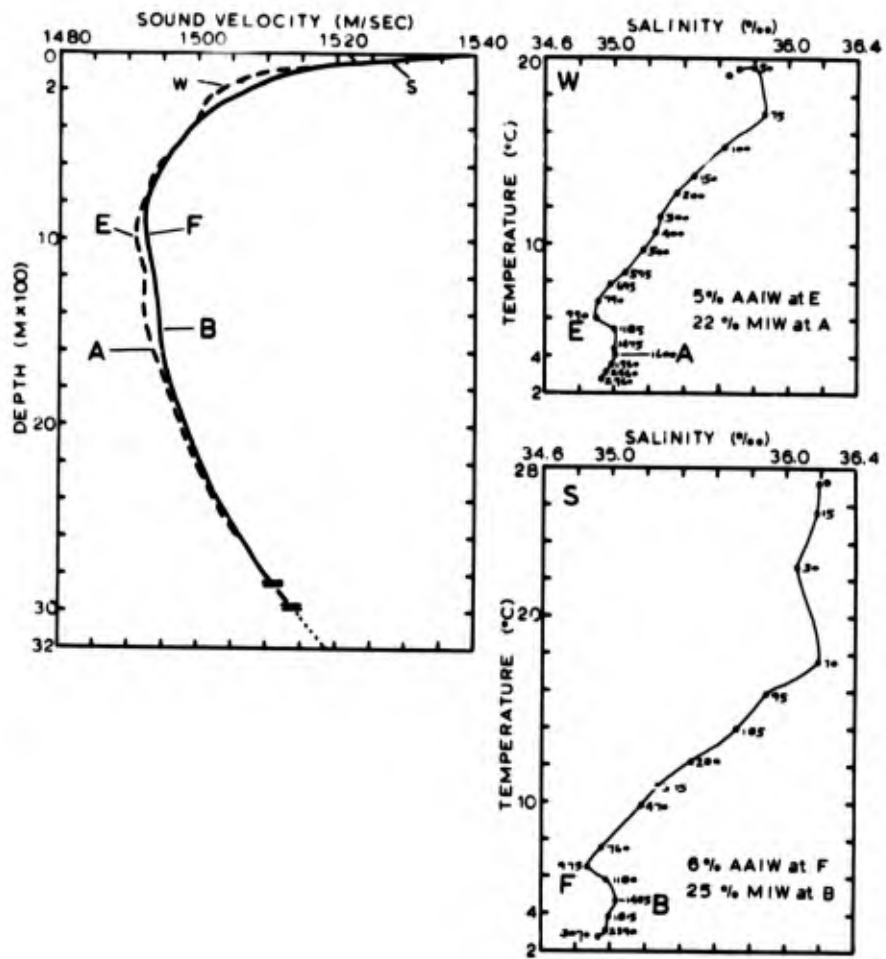
FIGURE B-51. SELECTED SOUND VELOCITY/T-S COMPARISONS.

FIGURE B-52. SELECTED SOUND VELOCITY/T-S COMPARISONS.